Status of the FOOT experiment and first measurements of ^{16}O fragmentation cross sections on C target

FramentatiOn Of Target

Gaia Franciosini,
on behalf of the FOOT collaboration

SAPIENZA UNIVERSITÀ DI ROMA
INFN
CENTRO RICERCHE ENRICO FERMI

Particle Therapy

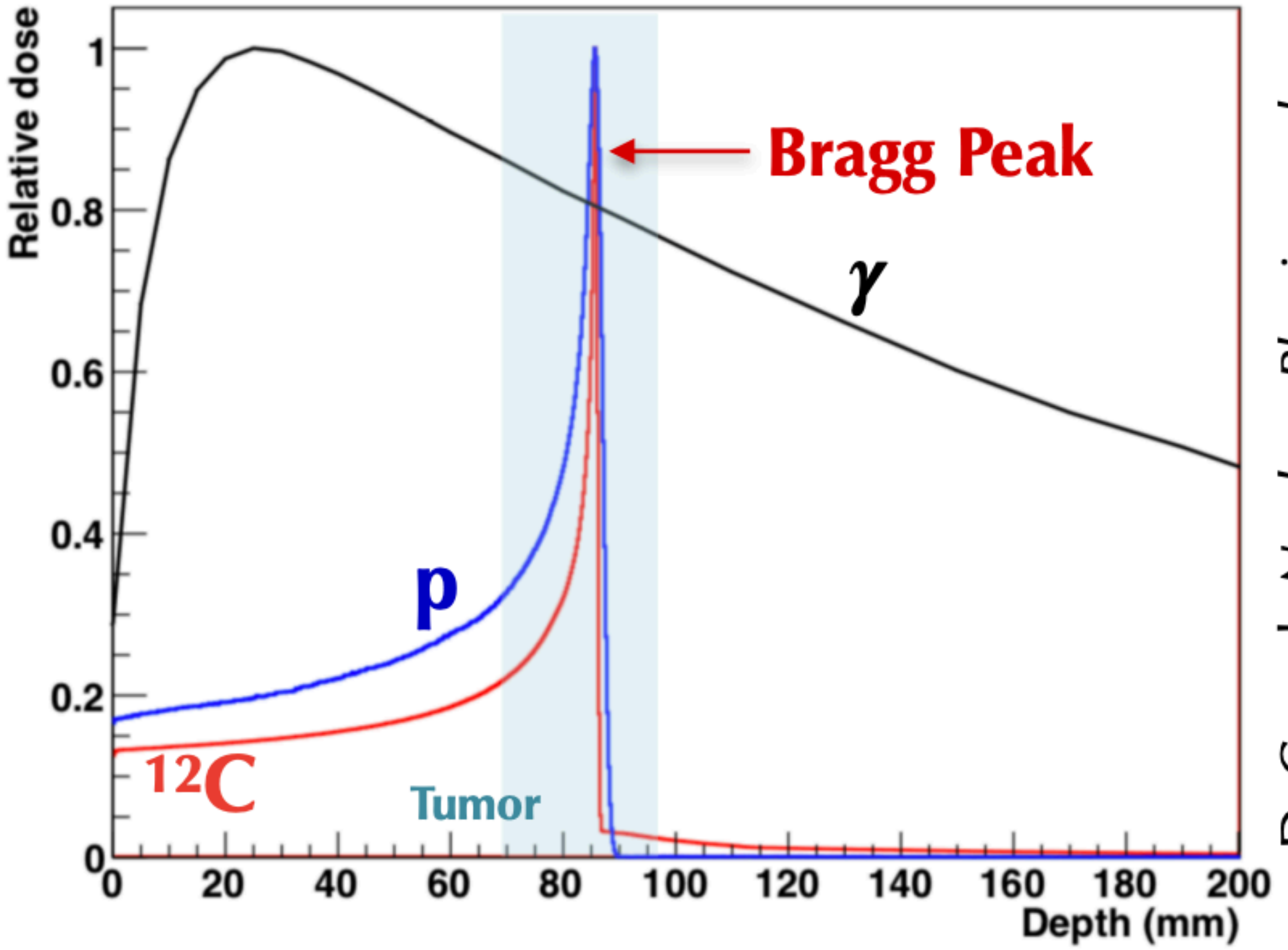

D. Cussol, *Nuclear Physics and Hadrontherapy* (2000)

- Particle Therapy (**PT**) uses **proton or light ions (He, C, O)** beams to treat **deep-seated solid tumors**.

- Advantages wrt conventional radiotherapy:

1. Maximum dose released inside the tumor: **Bragg Peak**
2. High **RBE**

$$\mathrm{RBE} = \frac{D_\gamma}{D_{part}}$$

- Disadvantages: **fragmentation** of **projectile** and **target** nuclei

Particle Therapy

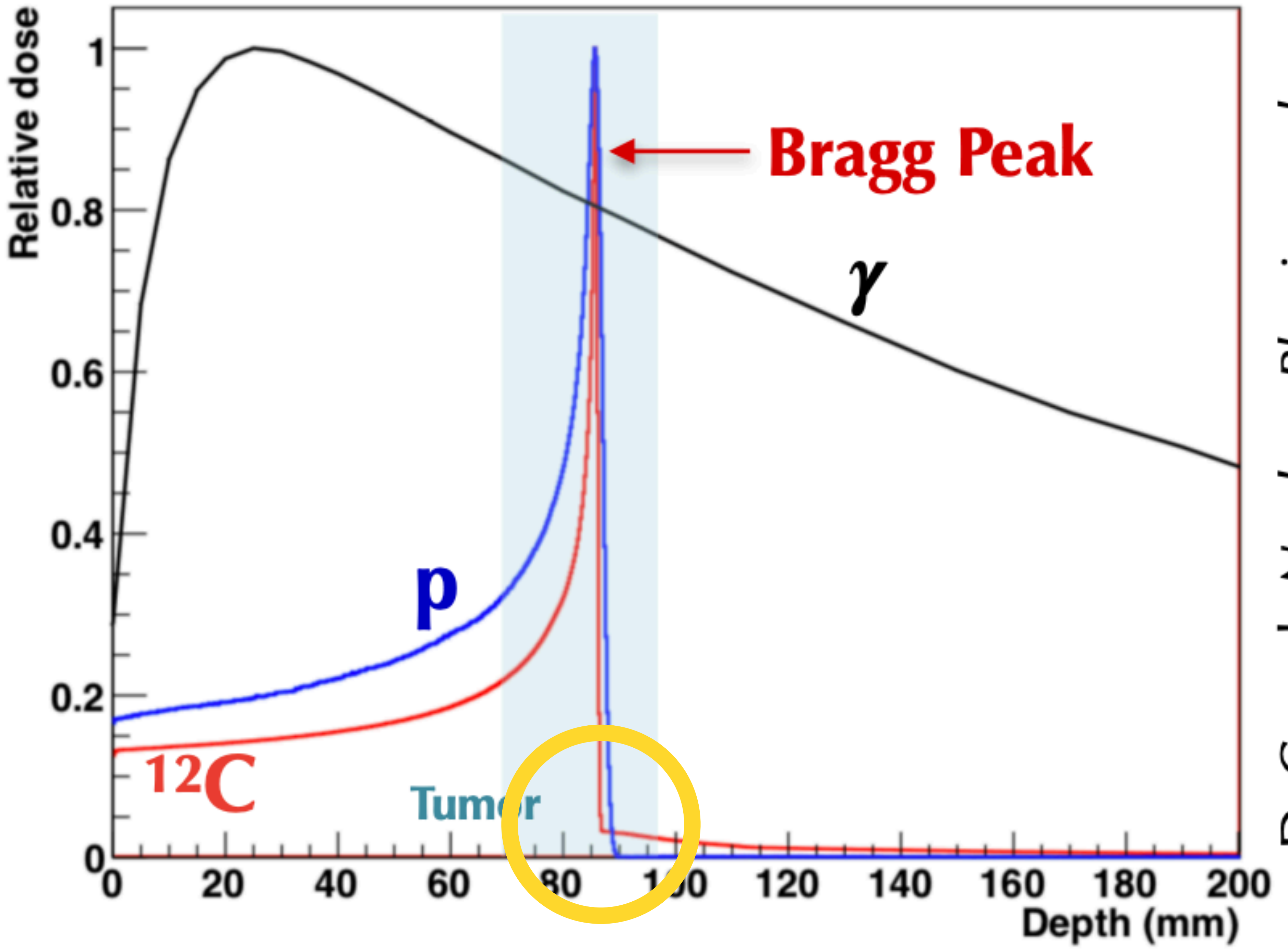

D. Cussol, Nuclear Physics and Hadrontherapy (2000)

- Particle Therapy (**PT**) uses **proton or light ions (He, C, O)** beams to treat **deep-seated solid tumors.**

- Advantages wrt conventional radiotherapy:

1. Maximum dose released inside the tumor: **Bragg Peak**
2. High **RBE**

$$\mathrm{RBE} = \frac{D_\gamma}{D_{part}}$$

- Disadvantages: **fragmentation** of **projectile** and **target** nuclei

Projectile fragments:

lower Z and higher range ($\beta_{frag} \sim \beta_{beam}$)

FRAGMENTATION TAIL

Particle Therapy

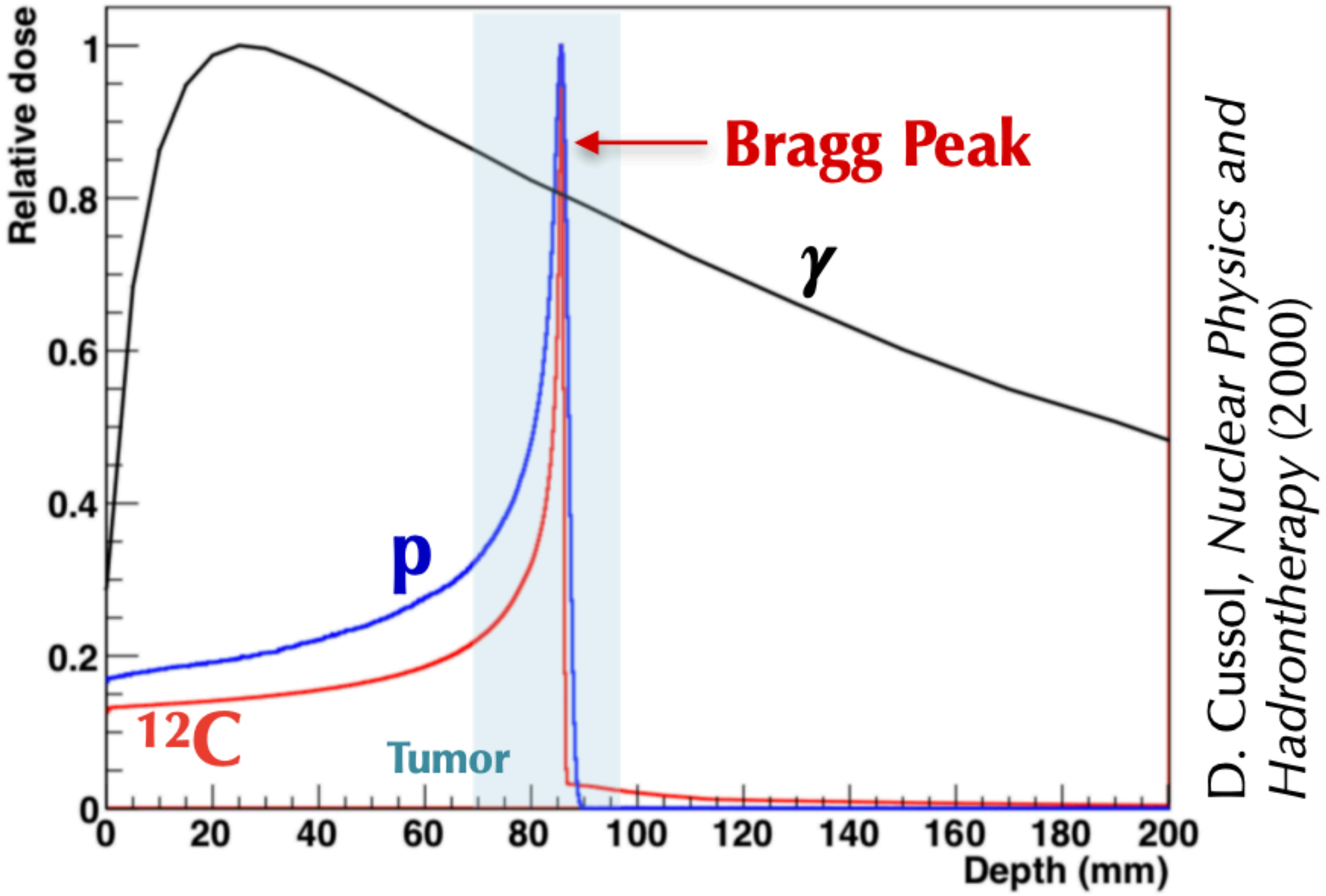

- Particle Therapy (**PT**) uses **proton or light ions (He, C, O)** beams to treat **deep-seated solid tumors.**
- Advantages wrt conventional radiotherapy:

1. Maximum dose released inside the tumor: **Bragg Peak**
2. High **RBE**

$$\text{RBE} = \frac{D_\gamma}{D_{part}}$$

- Disadvantages: **fragmentation** of **projectile** and **target** nuclei

Projectile fragments:
lower Z and higher range ($\beta_{frag} \sim \beta_{beam}$)

FRAGMENTATION TAIL

Target fragments:
Low kinetic energy and low range

LOCAL REALSE

Projectile fragmentation consequences

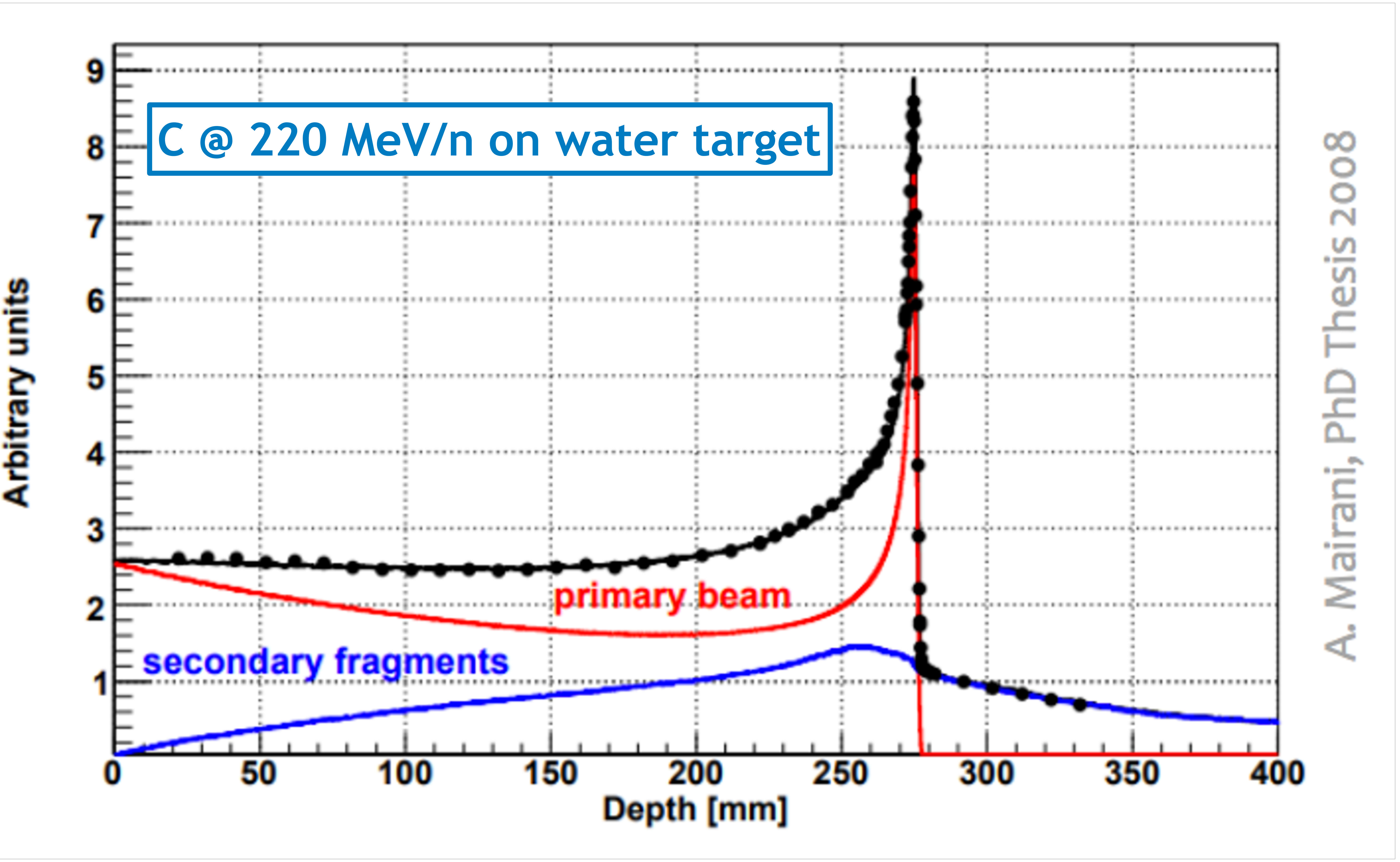

- Fragmentation processes modify the delivered dose map

- This effect strongly depends on the **mass** and the **energy** of the ion beam and on the **target** involved in the interaction

Very few experimental data available

Treatment plans for PT are not yet able to include the fragmentation contribution with the accuracy (3%) required for radiotherapy

Target fragmentation contribution

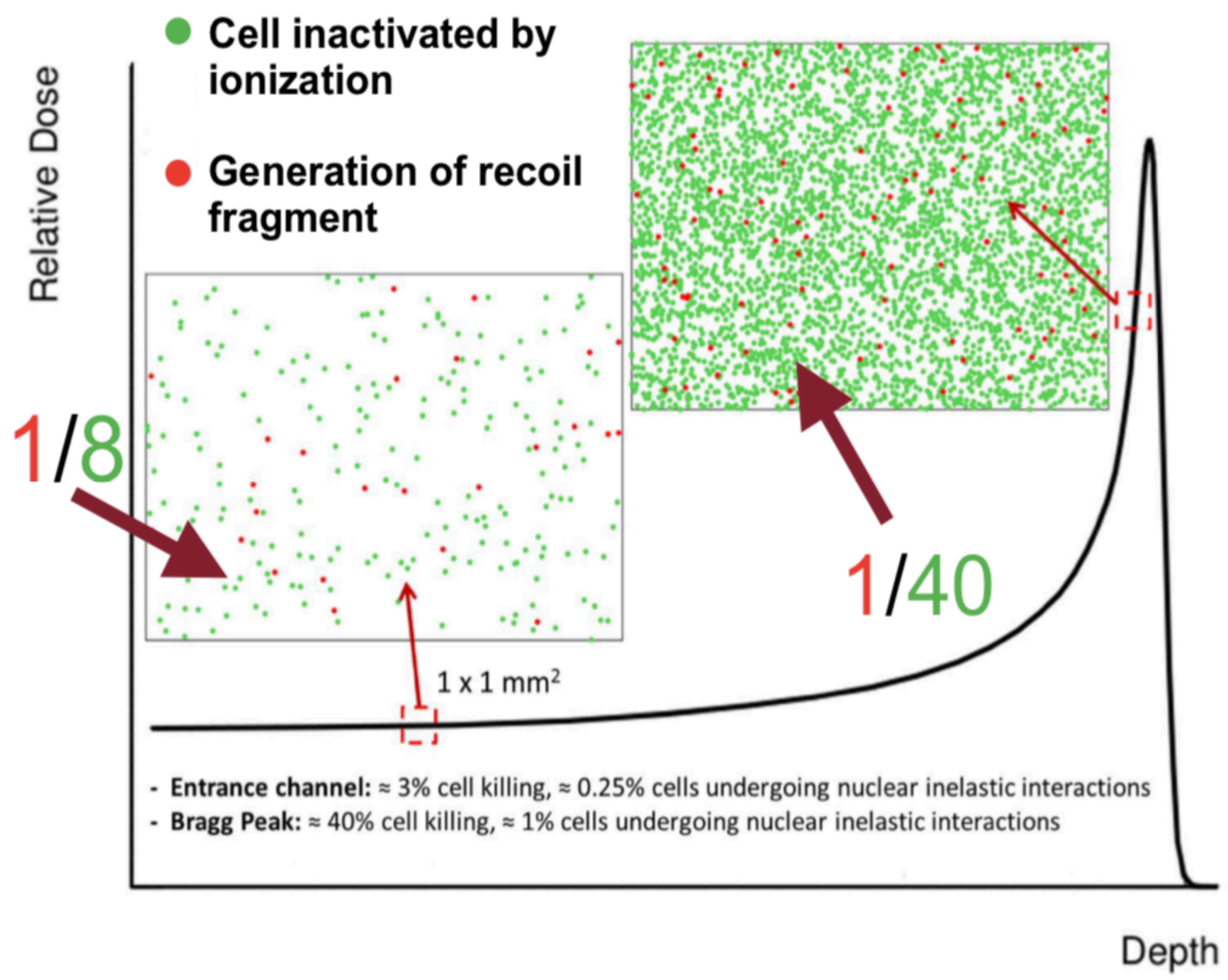

Tommasino Durante.
Cancers 2015, 7, 353-381; doi:10.3390/cancers7010353

- The particles produced in target fragmentation are one of the causes contributing (~10%) to the increase of proton RBE

Clinical practice protons RBE = 1.1

$$p + x \rightarrow p + \sum_i x_i$$

$$T_{x_i} << T_p$$

$$\left(\frac{dE}{dx}\right)_x >> \left(\frac{dE}{dx}\right)_p$$

Target fragments have **high RBE** values

The particles produced in target fragmentation, especially the heavier fragments, are one of the causes contributing to the increase of proton RBE

FragmentatiOn Of Target (FOOT) experiment

Measurements of target and projectile fragmentation cross section relevant for PT and for Radio Protection in Space applications.

TPS in Particle Therapy

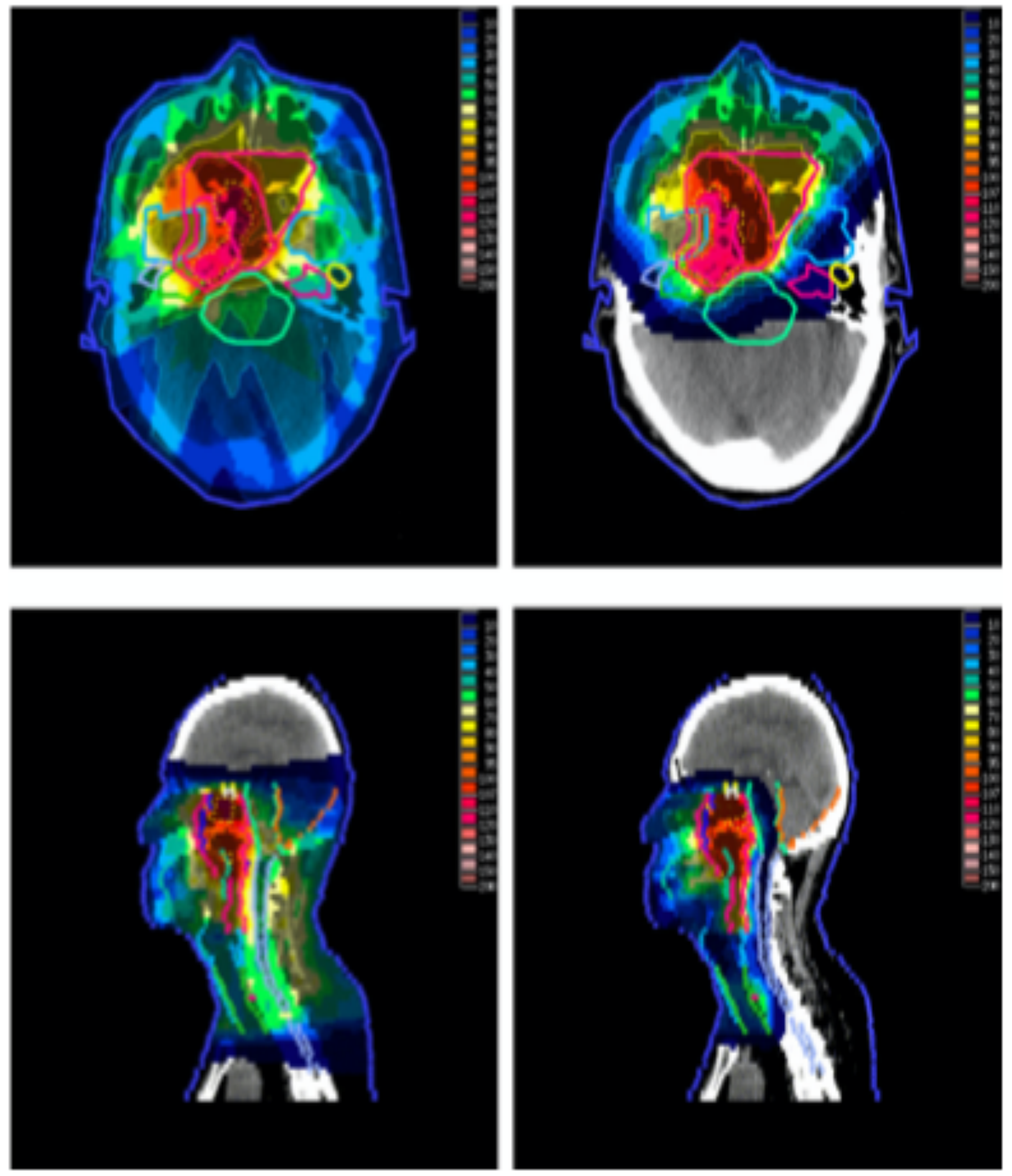

- Projectile fragmentation of ^{4}He, ^{12}C, ^{16}O beams in the energy range 100÷500 MeV/u interaction with the main constituents of human body (H, C, O, Ca)
- ^{12}C and ^{16}O target fragmentation induced by 50÷250 MeV proton beams

Radio-protection in space

- Same PT ions (plus ions up to ^{56}Fe) interacting with hydrogen-rich targets, of interest for **shielding**, at the increased energy range of 100÷800 MeV/u

Strategy for target fragmentation measurement

Direct kinematic

Target fragments have a very **low energy** and so a very **low range** that make the detection really difficult.

Inverse kinematic

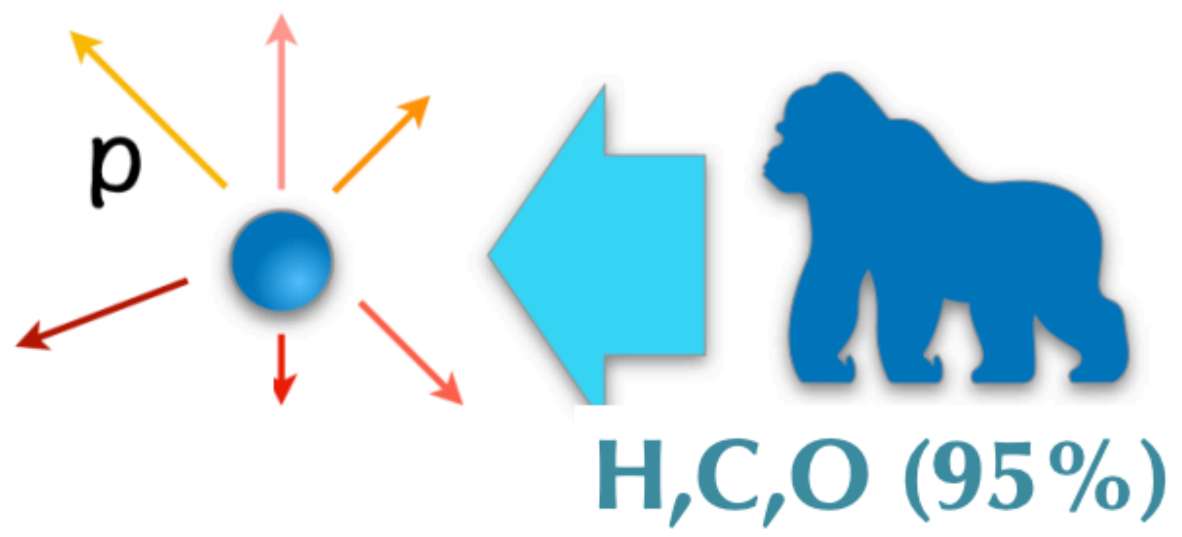

In this case the fragments have a **longer range** and a **mean kinetic energy comparable to the projectile one.**

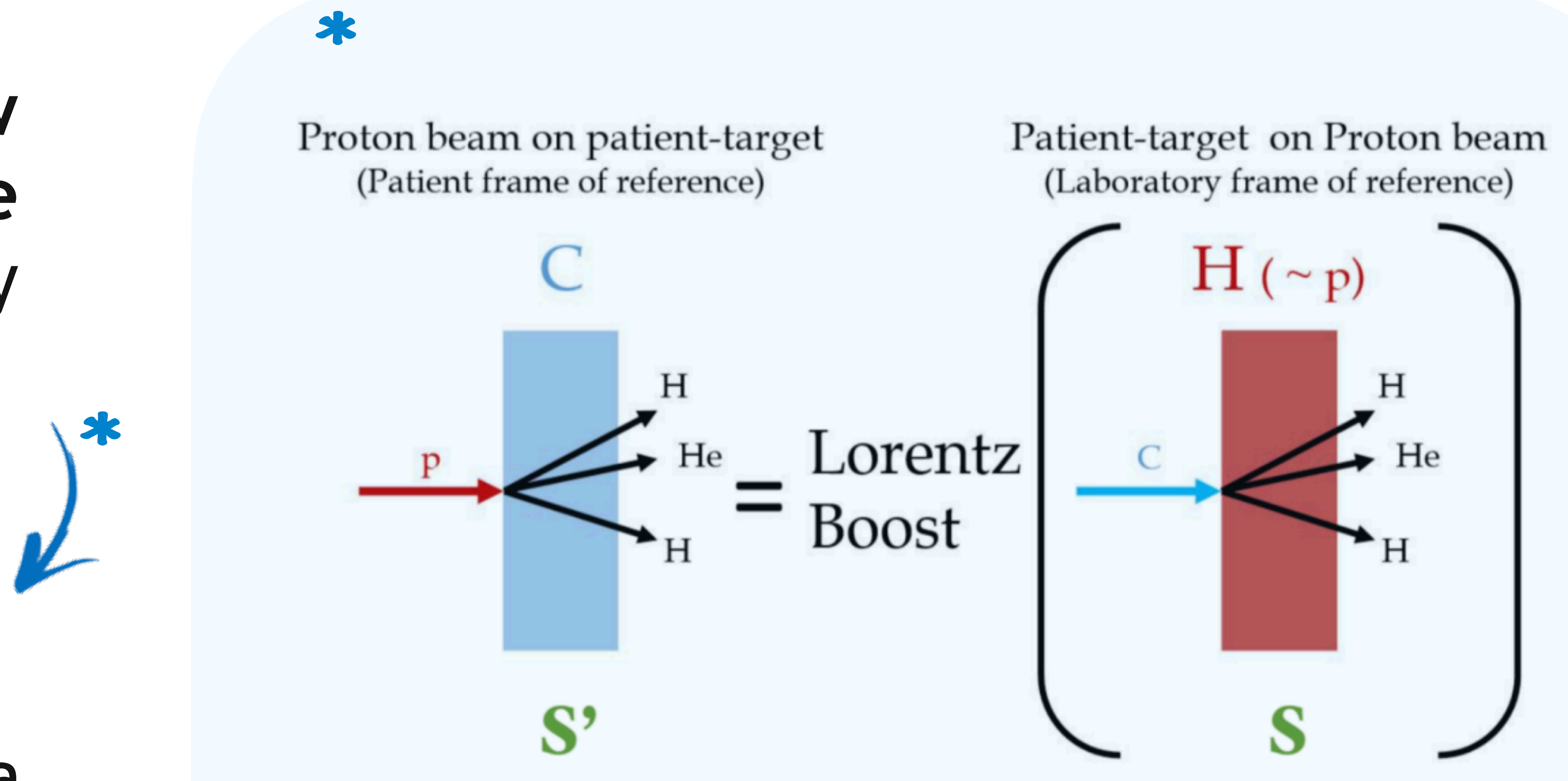

By applying a Lorentz boost it is possible to switch from the laboratory frame to the "patient frame"

With this strategy the fragmentation of **tissue-like ion beams** (mainly C and O) impinging on a **hydrogen enriched target** are studied moving from the challenging measurement of target fragmentation to the easier case of projectile fragmentation

FOOT detector

The FOOT detector is a movable set-up to fit the experimental rooms dimensions of different PT treatment centers / experimental facility (CNAO, HIT, GSI) with ions beams.

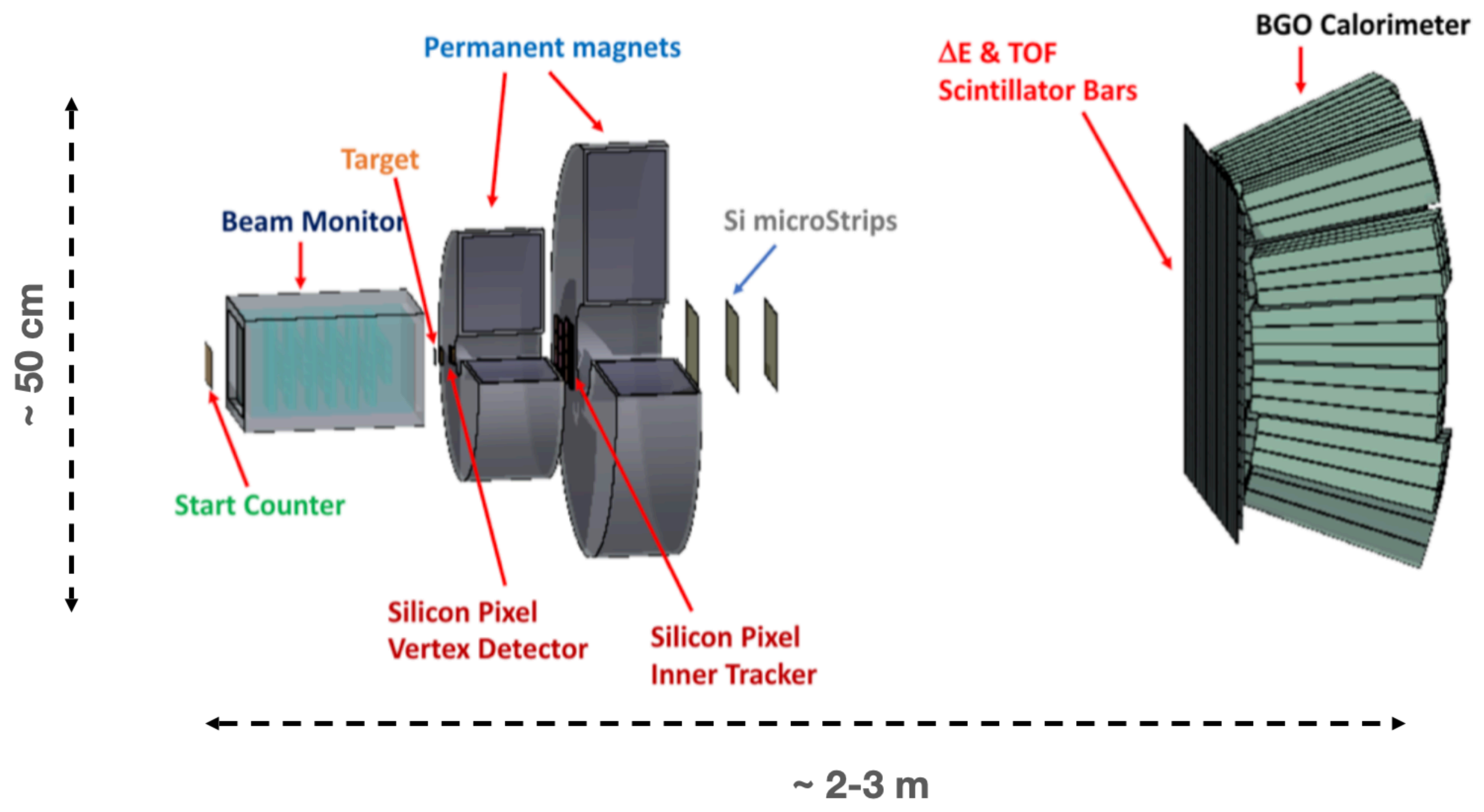

- Fixed target experiments with magnetic spectrometer for the isotopic (charge and mass) identification of fragments
- Thin beam detectors to minimize fragmentation out-of-targets
- Redundancy in mass measurement from (p,ToF), (E_{kin},ToF) and (E_{kin},p)

Radiobiological accuracy needed in PT:

- ✓ $d\sigma/dE$ for target fragm. in PT ~ 10%
- ✓ $d^2\sigma/d\Omega dE$ for projectile fragm. in PT ~ 5%
- ✓ ΔZ ~ 2-3% ; ΔA ~ 5%

Required FOOT performances:

- ✓ $\sigma(p)/p < 5\%$
- ✓ $\sigma(E_{kin})/E_{kin} < 3\%$
- ✓ $\sigma(\Delta E)/\Delta E < 5\%$
- ✓ $\sigma(TOF) < 100$ ps

FOOT detector

The FOOT detector is a movable set-up to fit the experimental rooms dimensions of different PT treatment centers / experimental facility (CNAO, HIT, GSI) with ions beams.

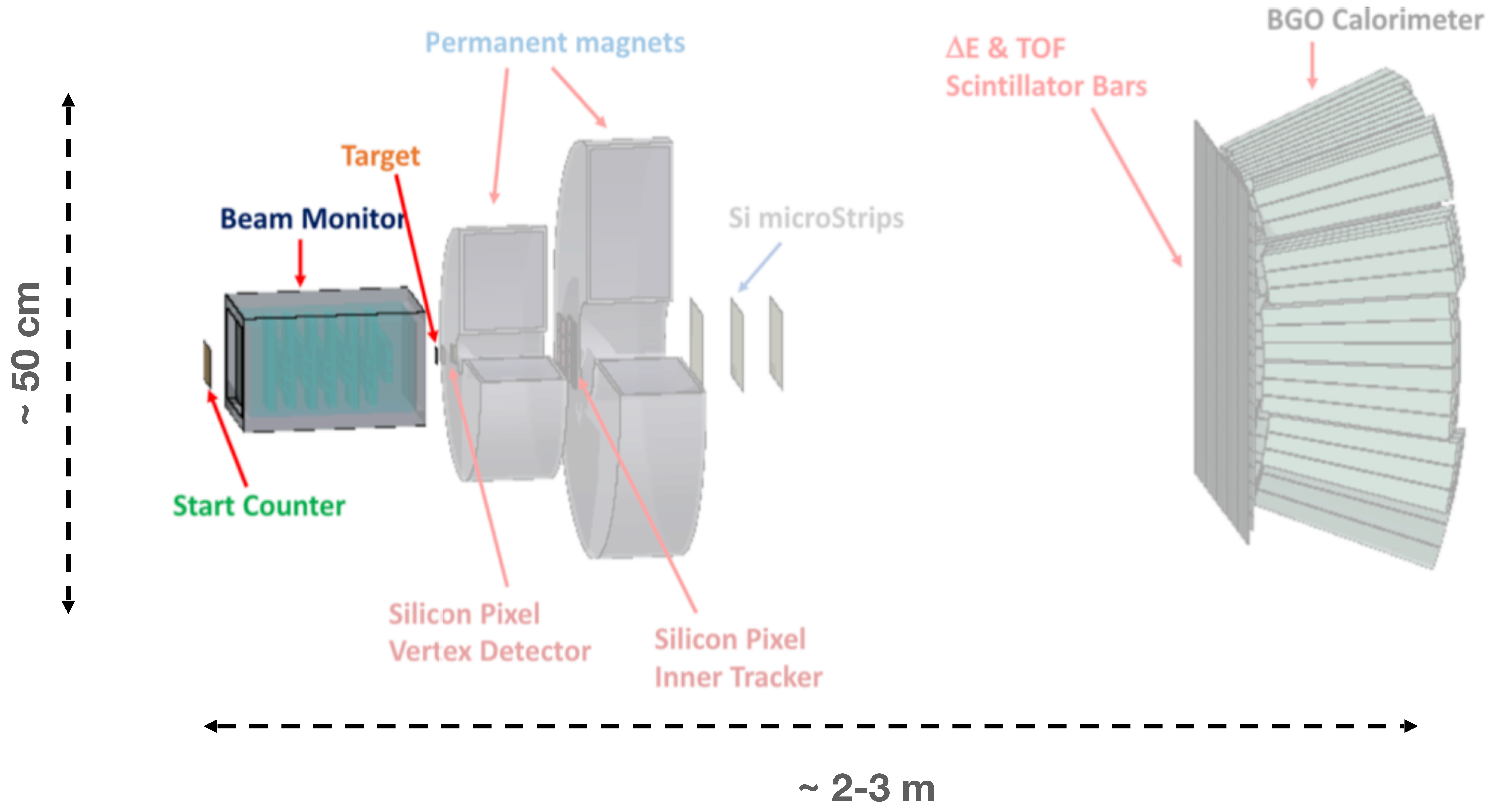

Pre-target region

- Very thin plastic scintillator (250 μm) for TOF measurement and trigger
- Drift chamber (12 xy wire layers) for the beam direction and position measurement

FOOT detector

The FOOT detector is a movable set-up to fit the experimental rooms dimensions of different PT treatment centers / experimental facility (CNAO, HIT, GSI) with ions beams.

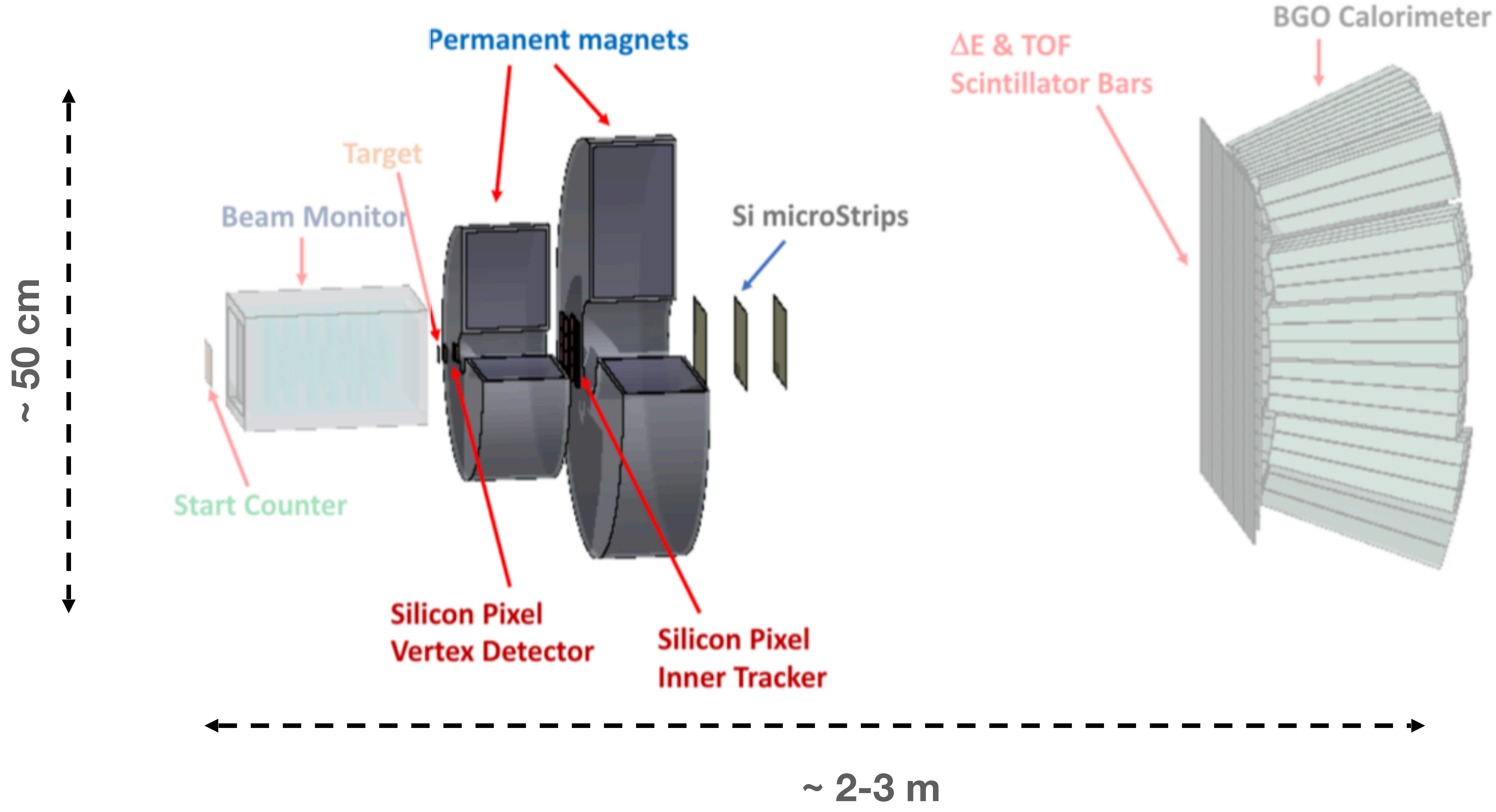

Tracking and magnetic region

- Permanent magnet in Halbach configuration B_{MAX}~ 1.4 T
- MAPS (M-28) and micro strip silicon detector (MSD) for tracking and momenum reconstruction

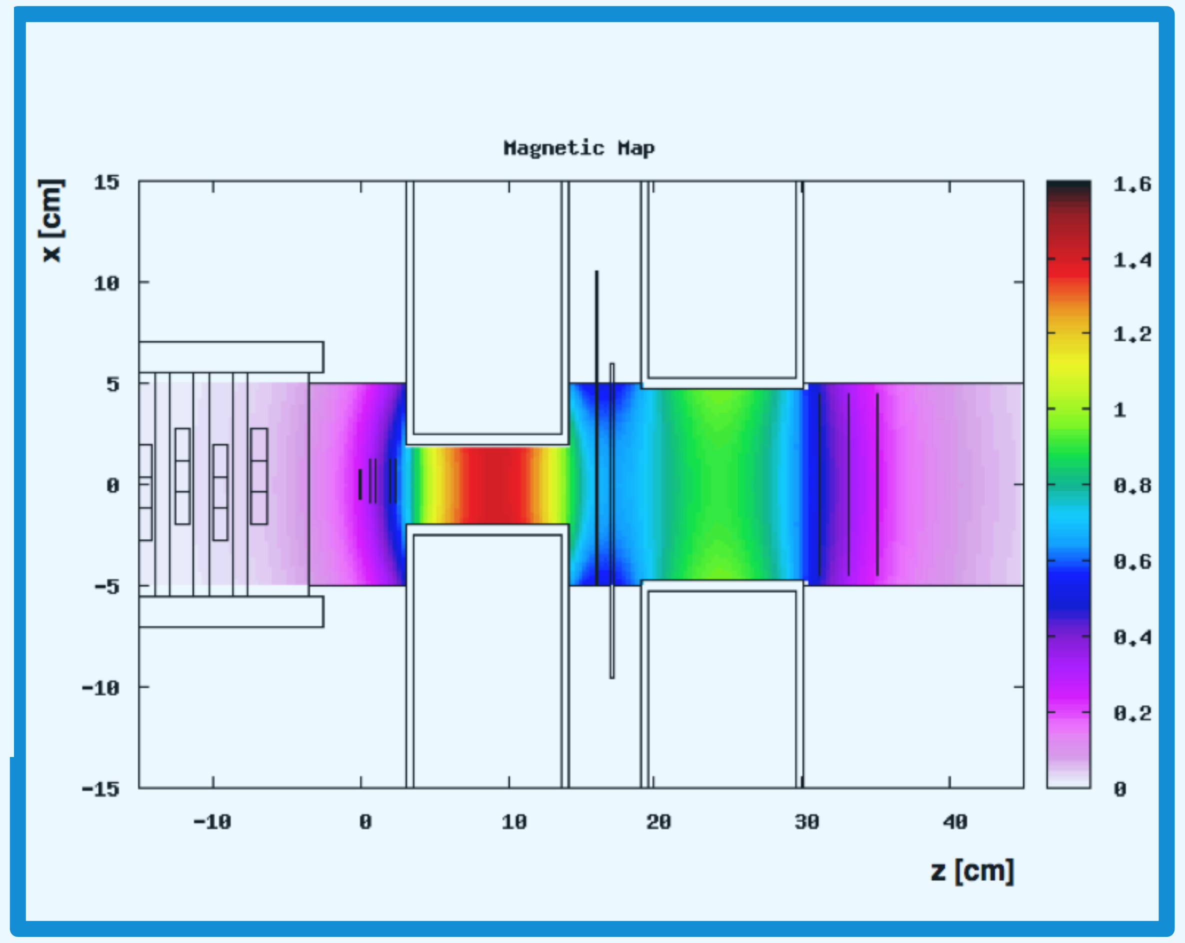

FOOT detector

The FOOT detector is a movable set-up to fit the experimental rooms dimensions of different PT treatment centers / experimental facility (CNAO, HIT, GSI) with ions beams.

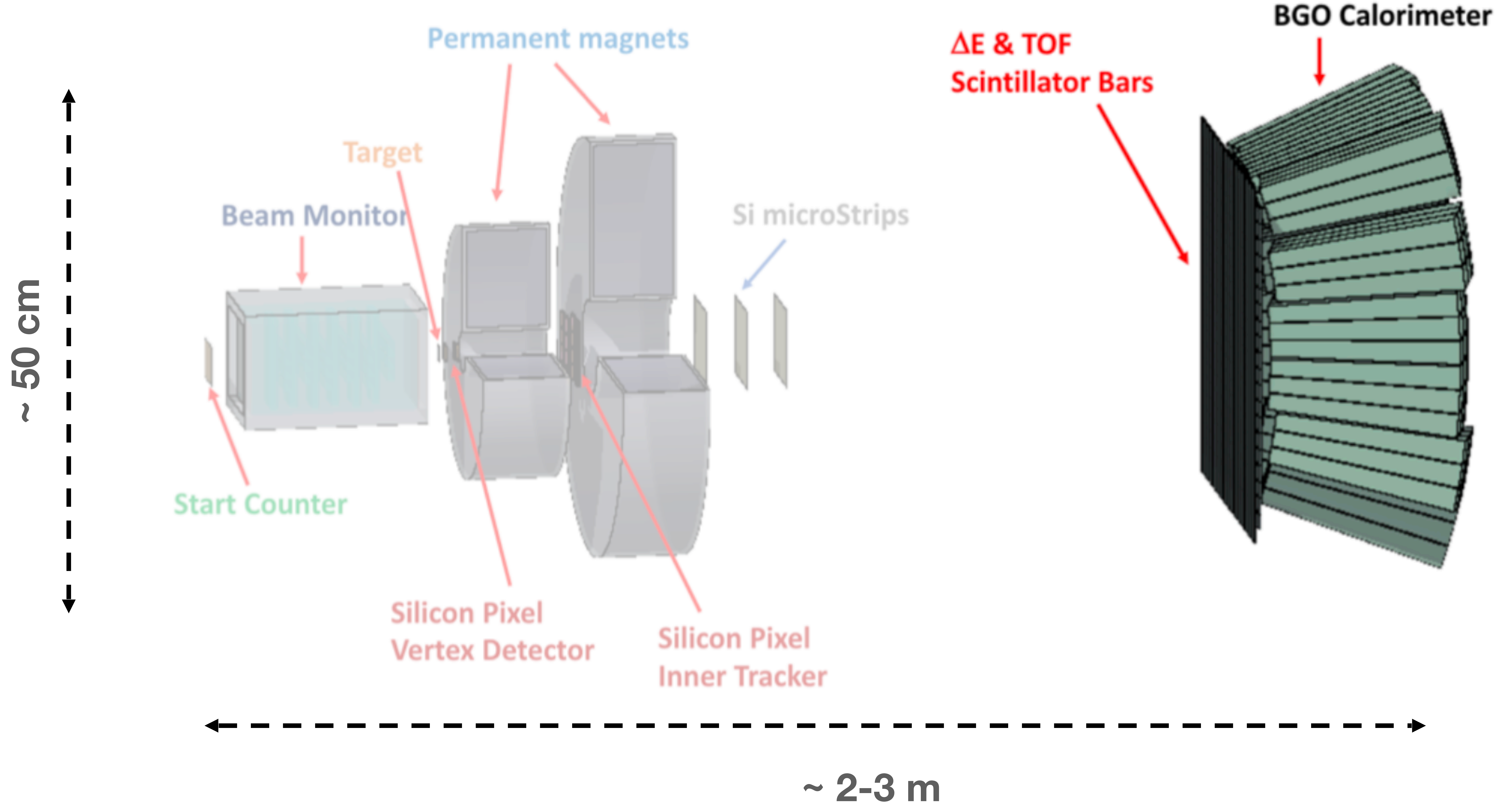

Mass and charge identification

- Two layers xy of plastic scintillator bars for Z identification through dE/dx and TOF
- BGO calorimeter for the E_{kin} measurement

FOOT … “a table top experiment”, “a movable setup”

FOOT … "a table top experiment", "a movable setup"

2019

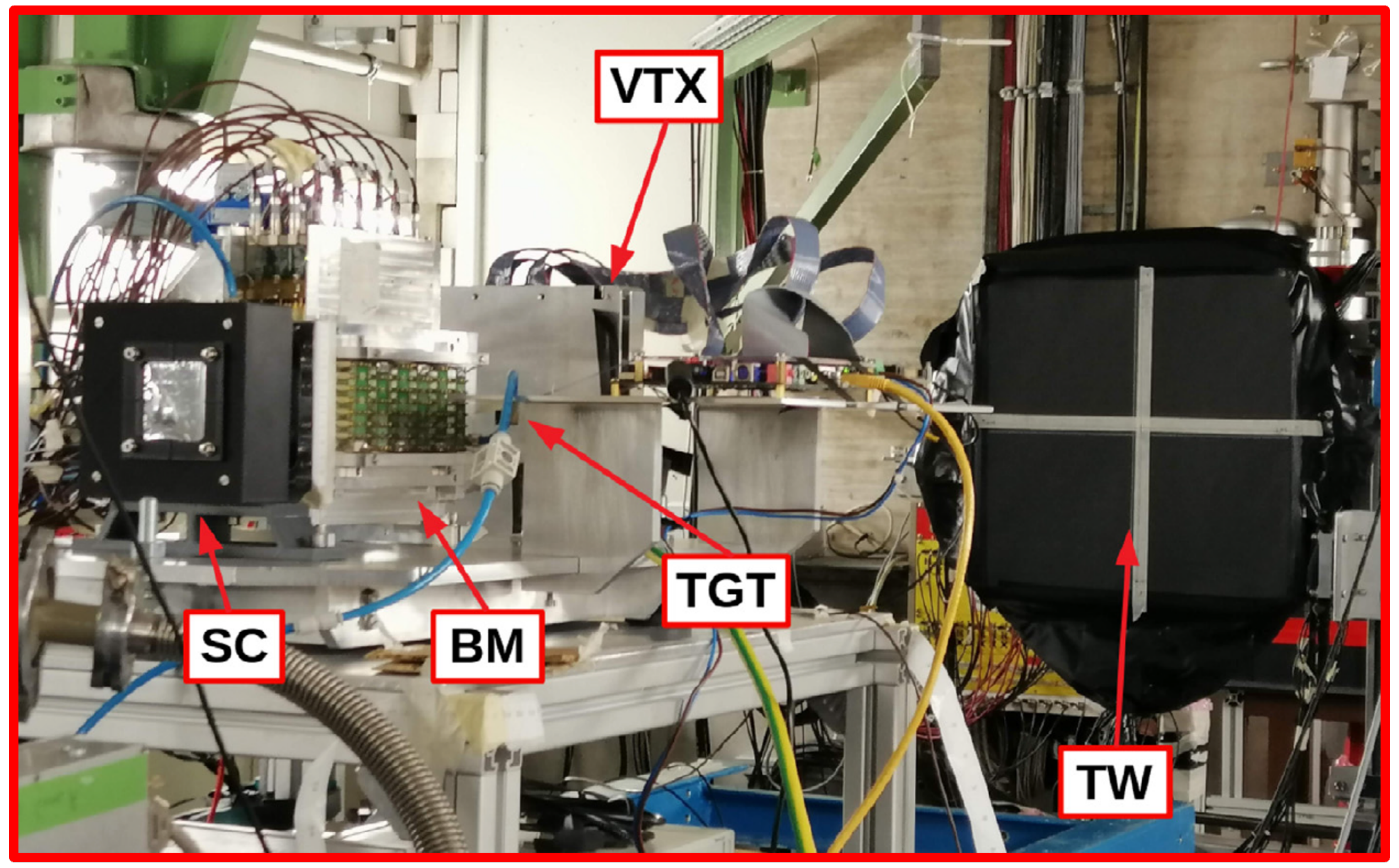

FOOT set up at GSI

FOOT … “a table top experiment”, “a movable setup”

2019

2021

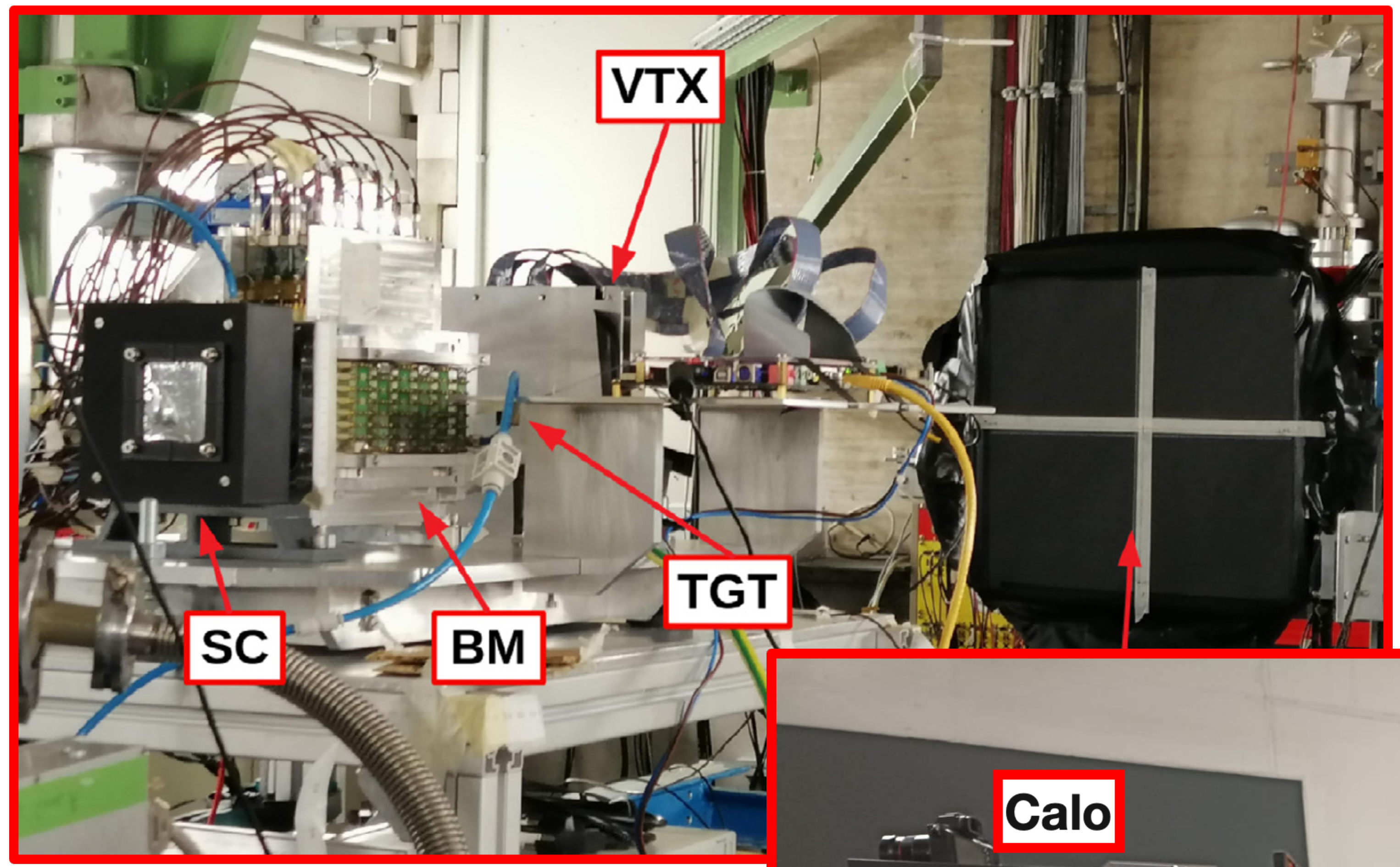

FOOT set up a

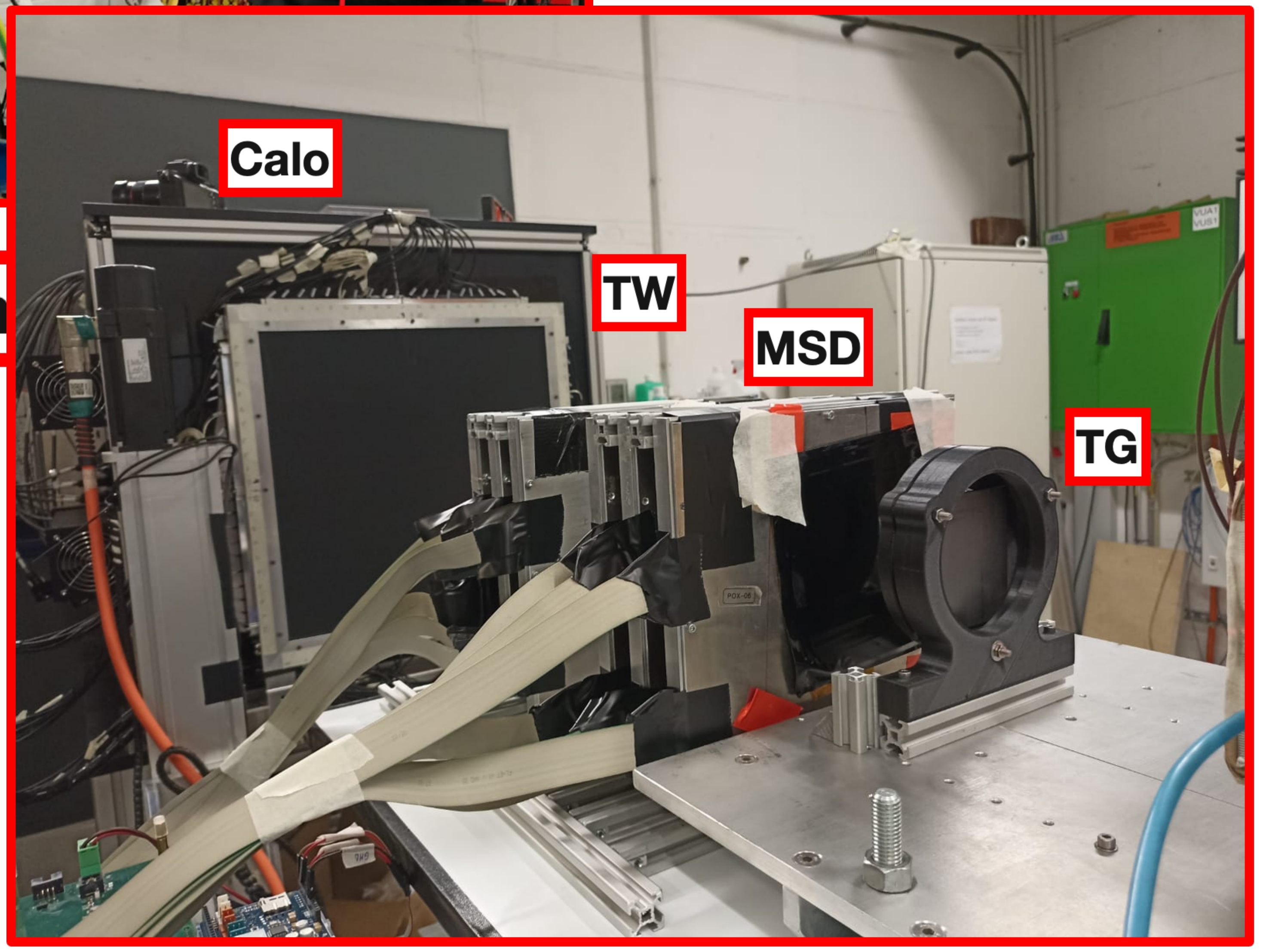

FOOT set up at HIT

FOOT … “a table top experiment”, “a movable setup”

2019 — 2021 — 2022

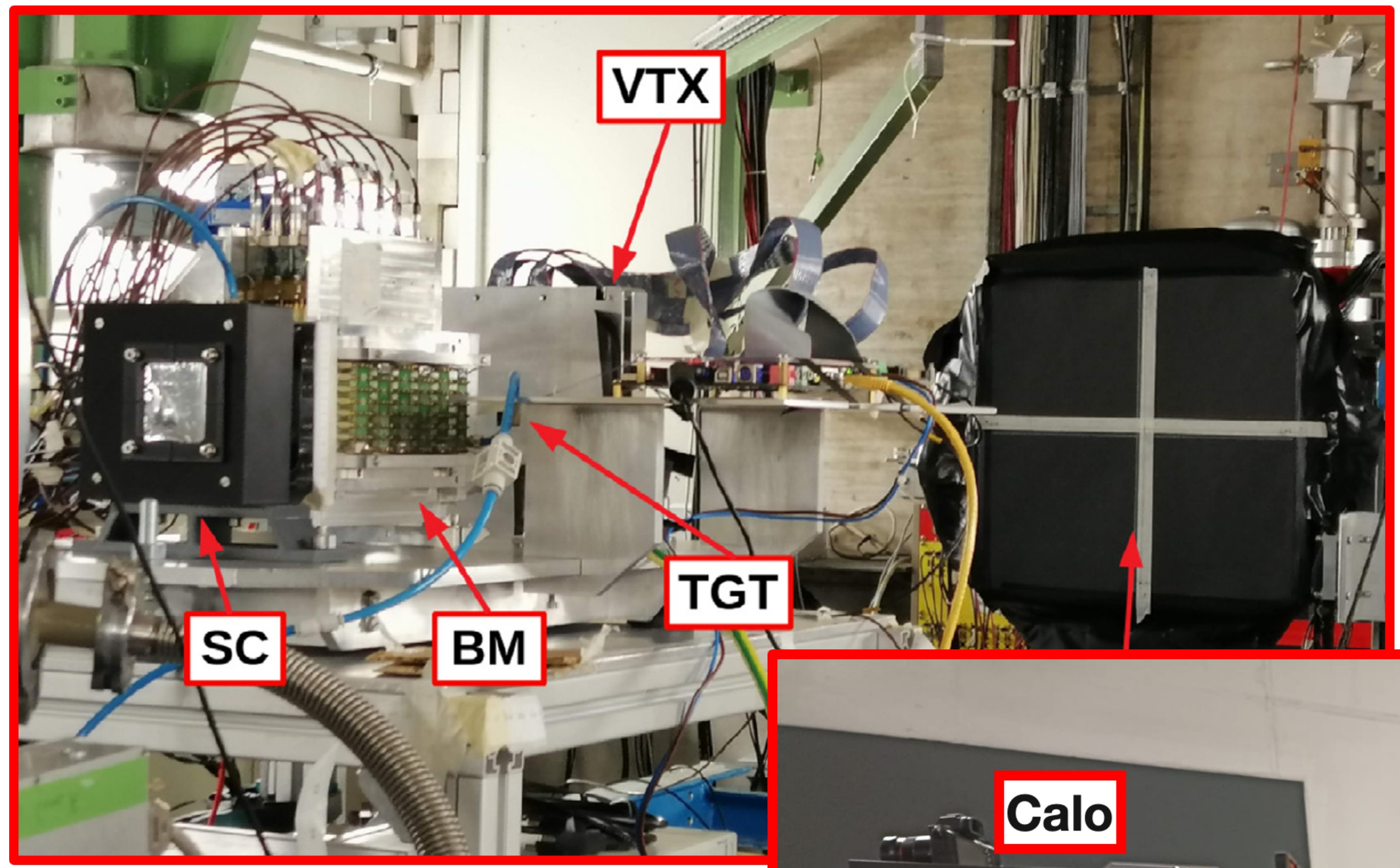

FOOT set up a

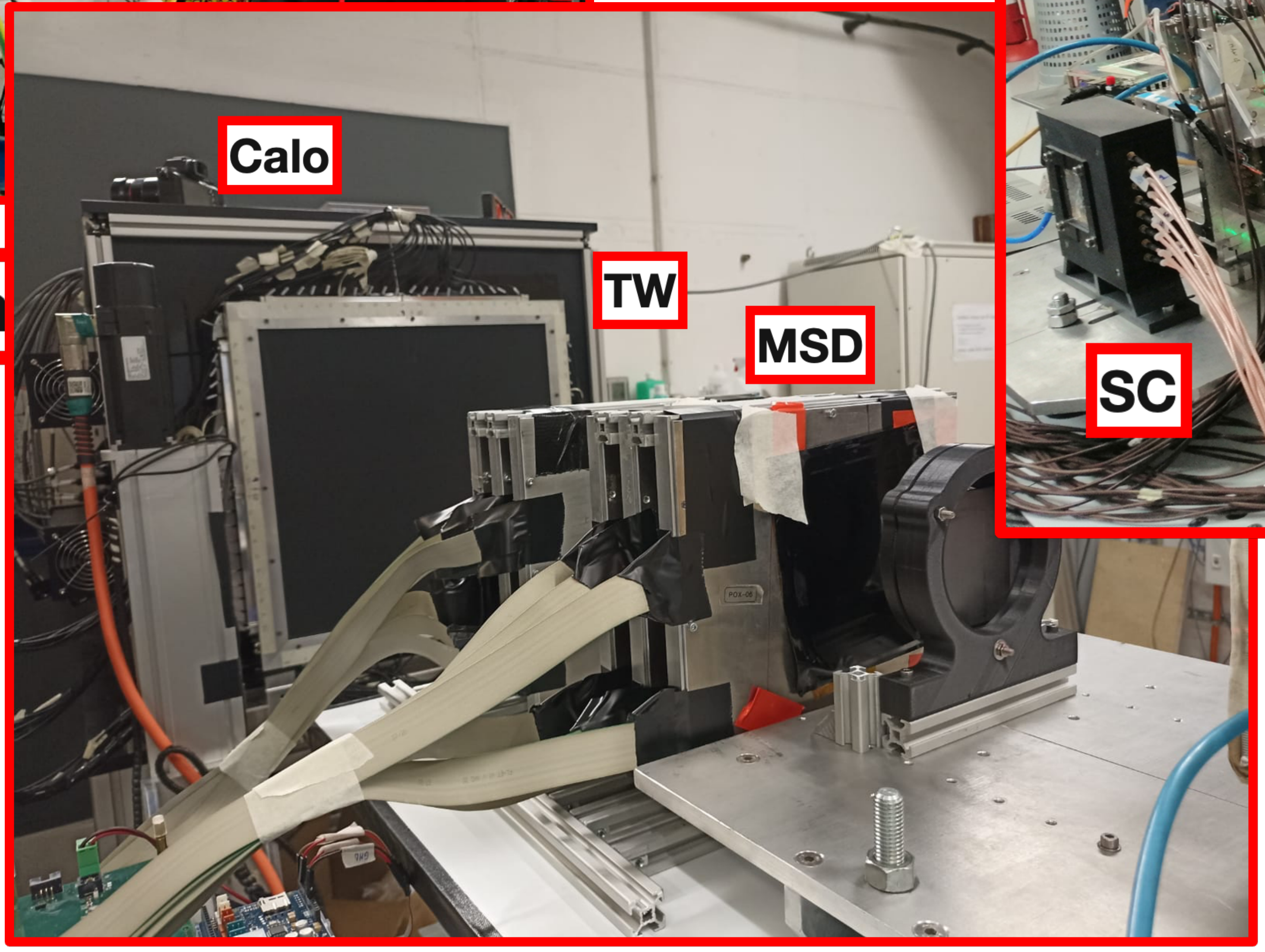

FOOT set up at HIT

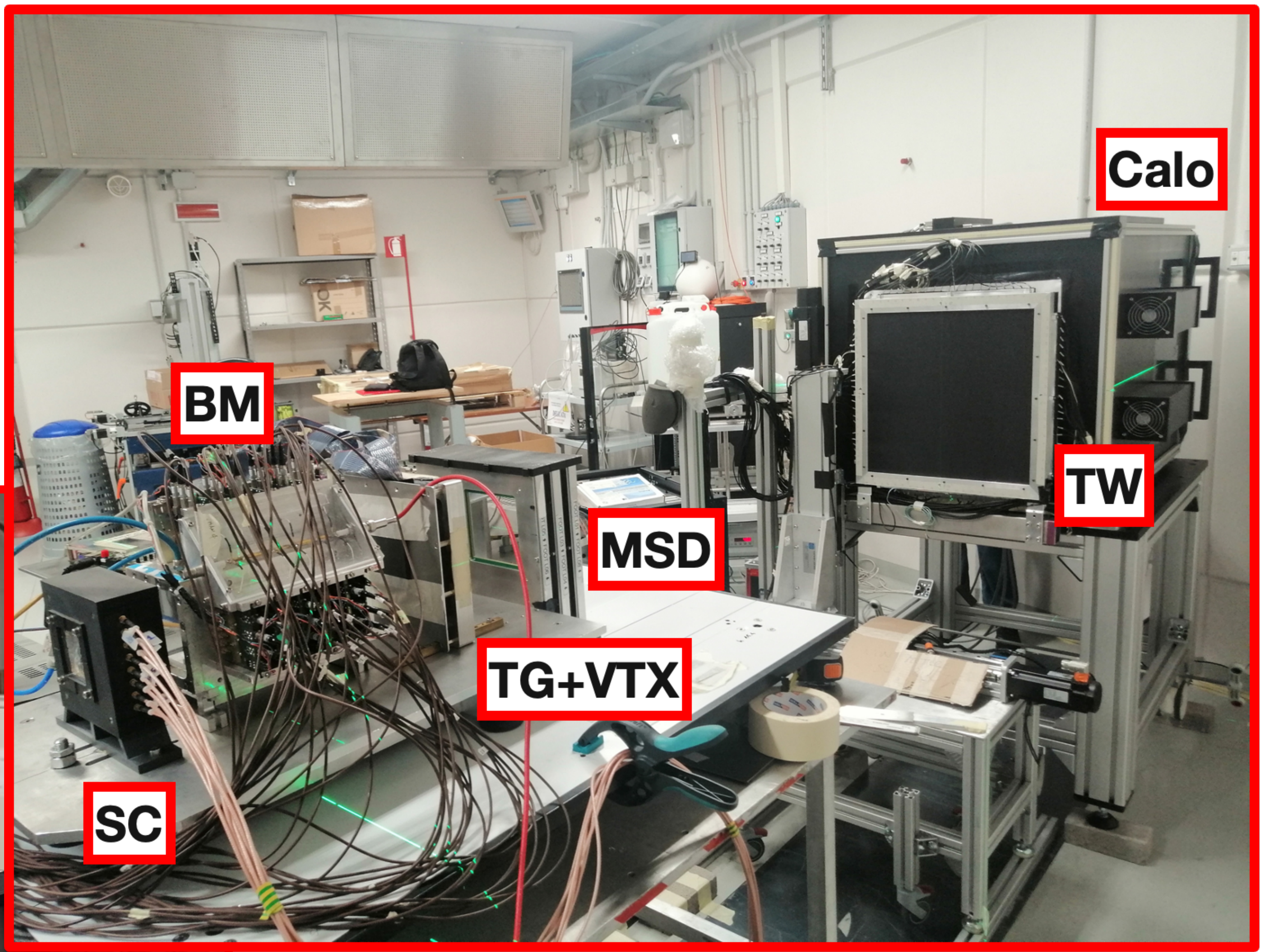

FOOT set up at CNAO

FOOT … “a table top experiment”, “a movable setup”

2019 | 2021 | 2022 | 2023

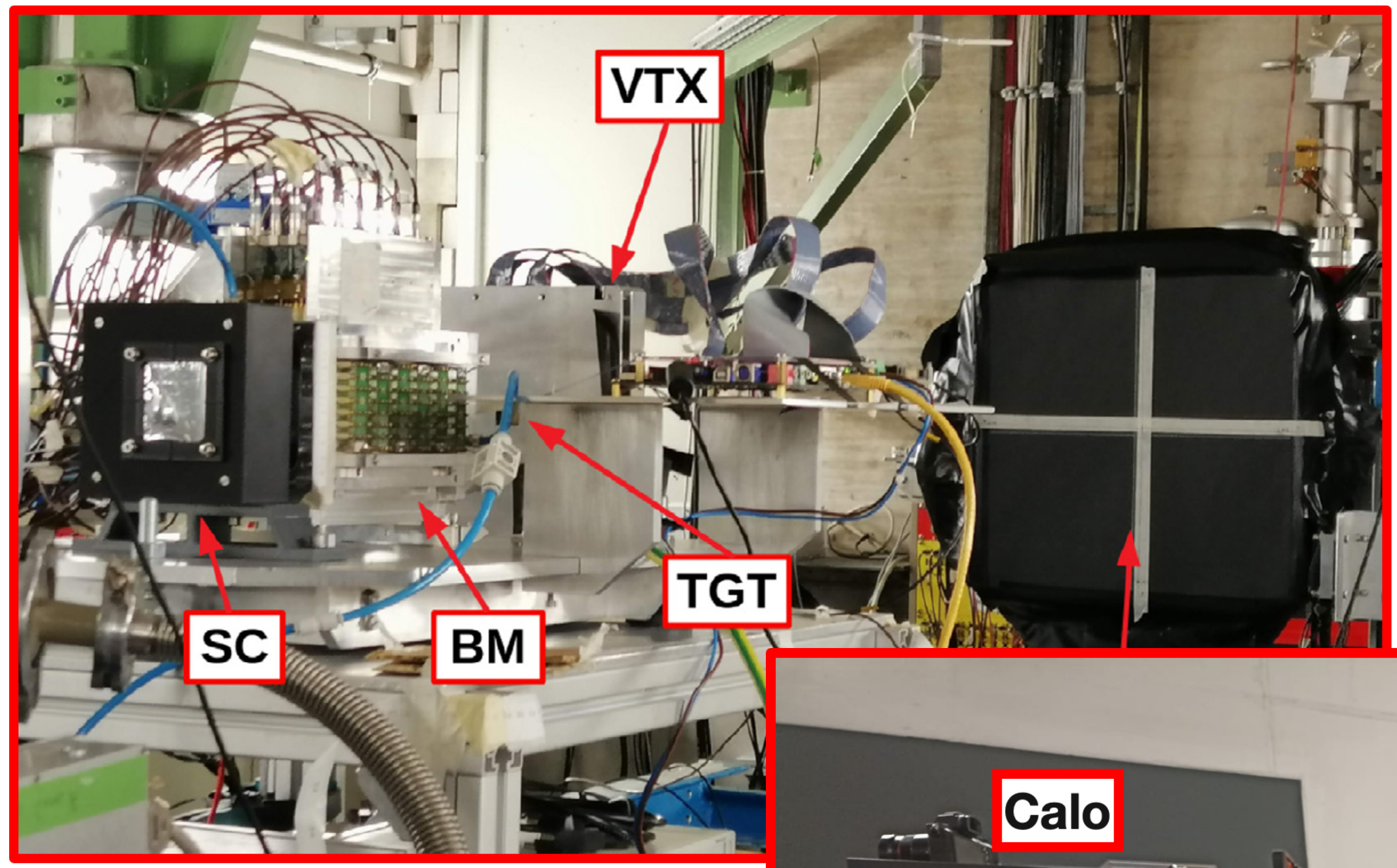

FOOT set up a

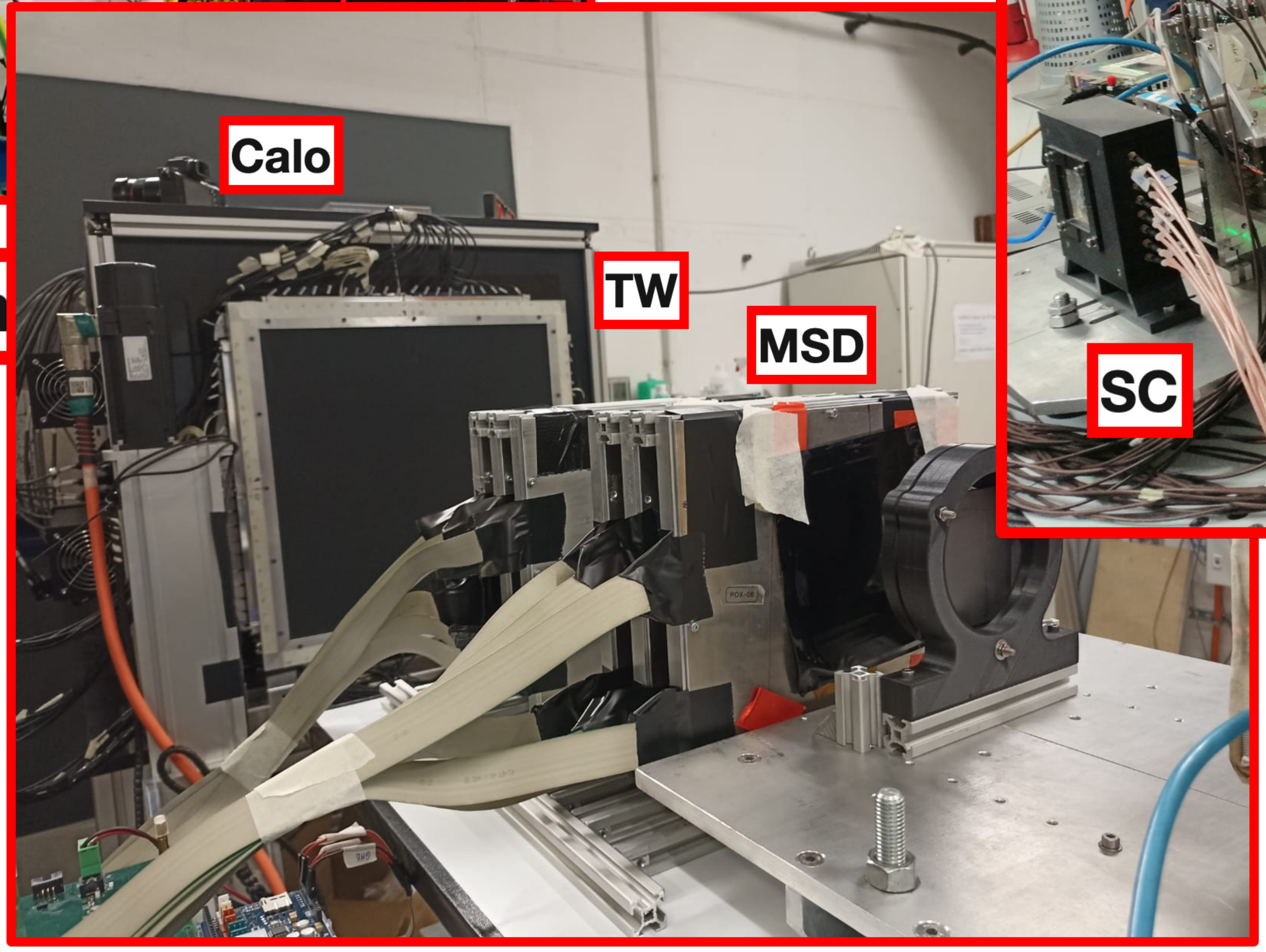

FOOT set up at HIT

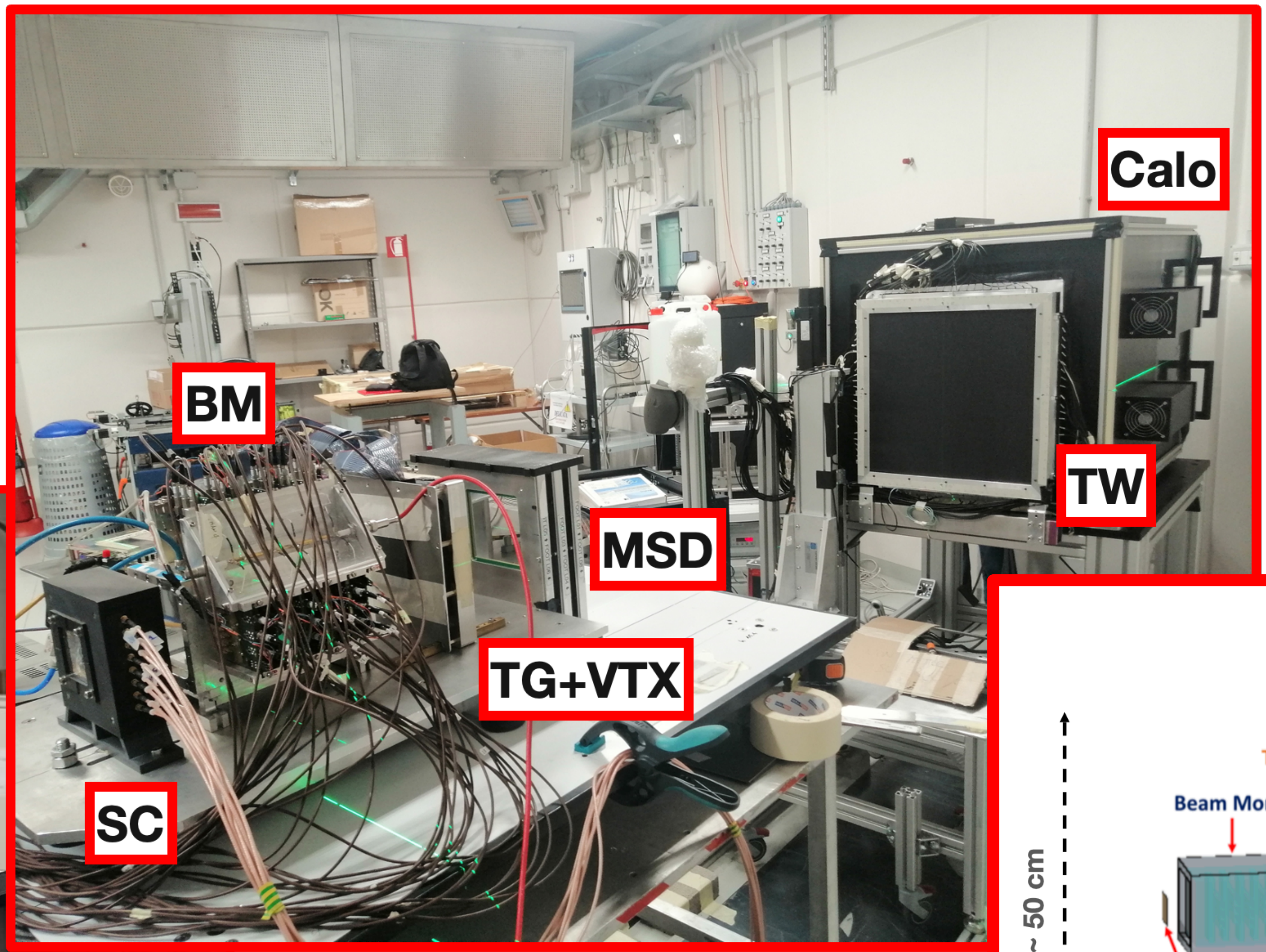

FOOT set up at CN

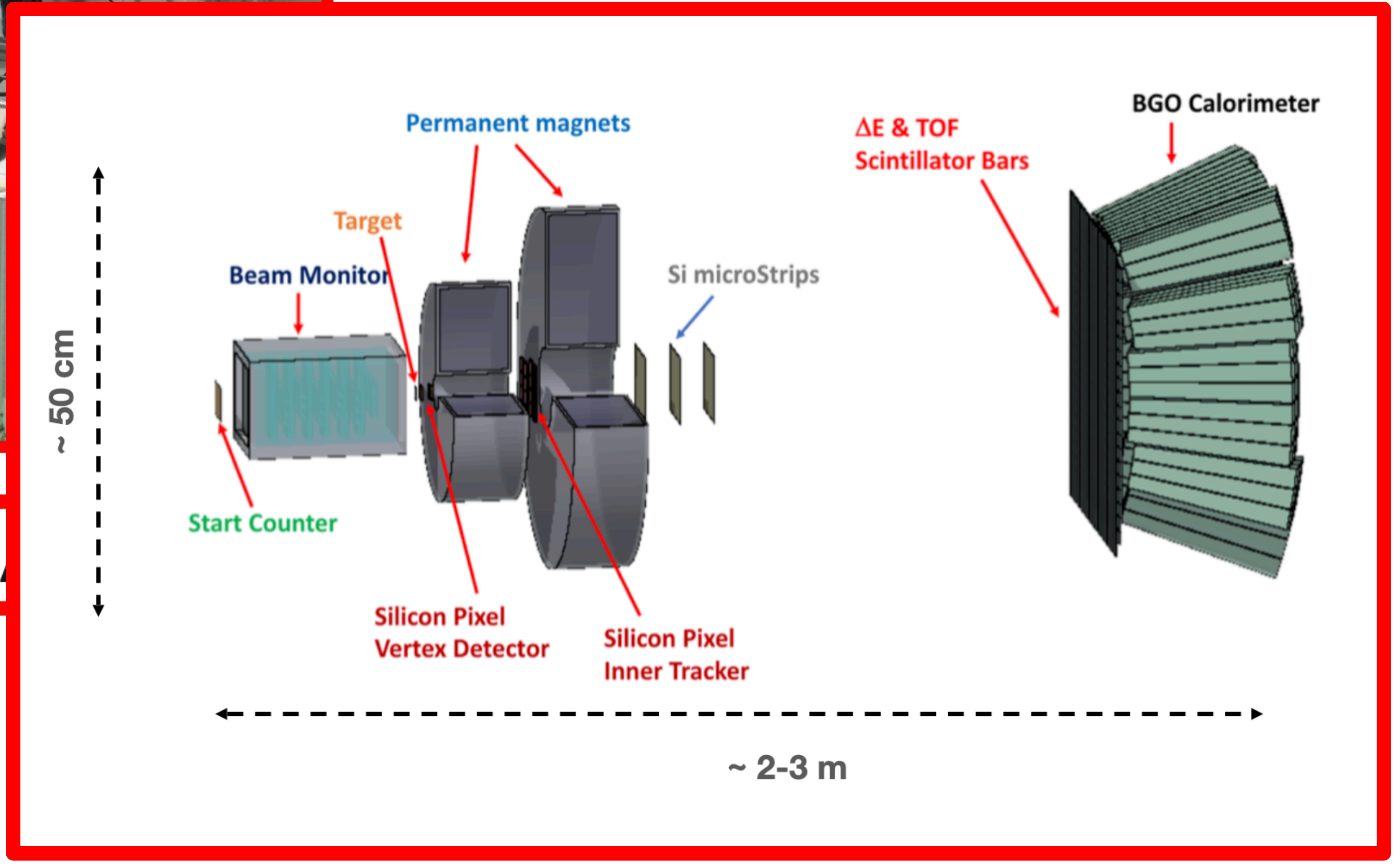

COMPLETE FOOT DETECTOR

FOOT performances and status

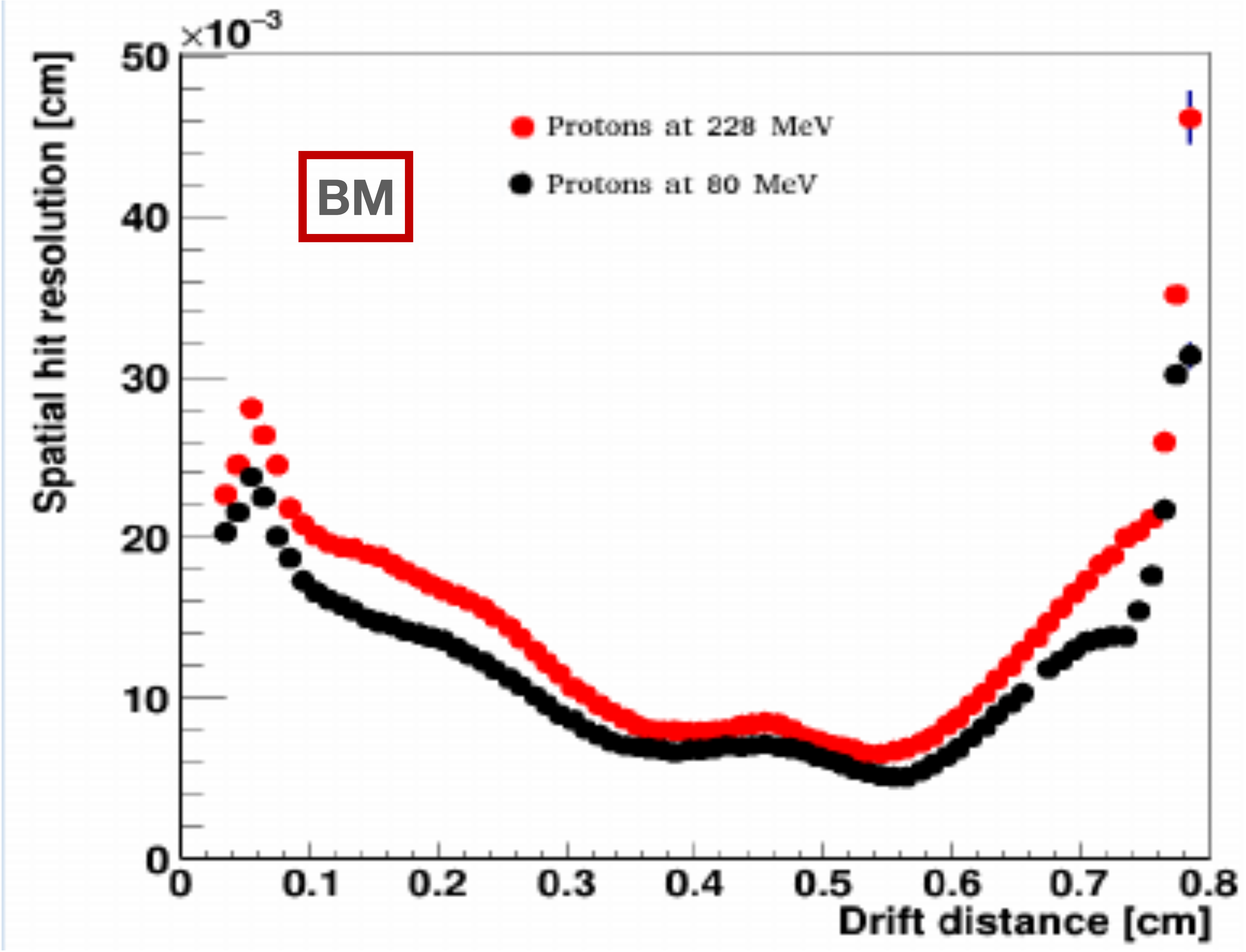

FOOT performances:

- ✓ $\sigma(E_{kin})/E_{kin} < 3\%$
- ✓ $\sigma(\Delta E)/ \Delta E \sim 4\text{-}5\%$
- ✓ $\sigma(TOF) > 50$ ps
- ✓ $\sigma(p)/p < 5\%$

FOOT performances and status

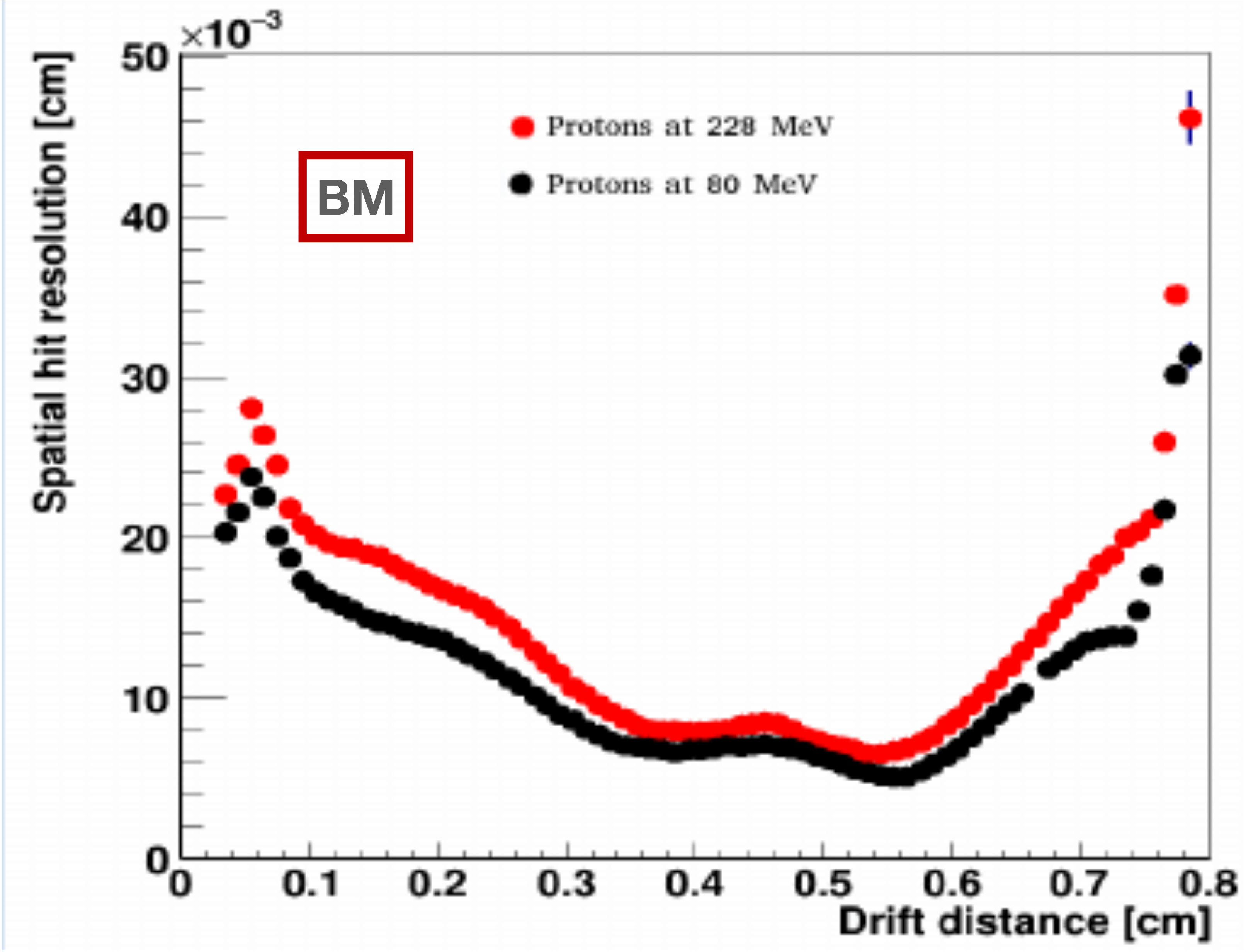

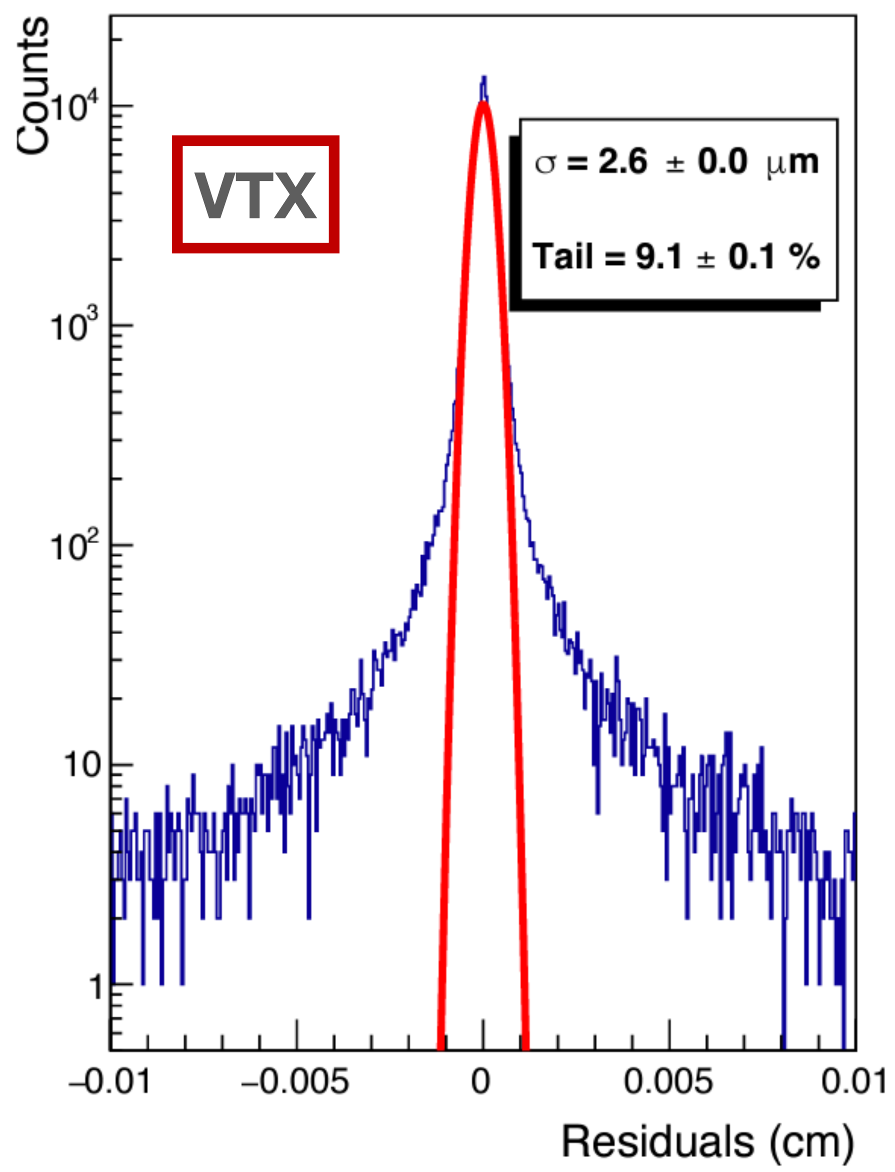

FOOT performances:

- ✓ $\sigma(E_{kin})/E_{kin} < 3\%$
- ✓ $\sigma(\Delta E)/\Delta E \sim 4\text{-}5\%$
- ✓ $\sigma(TOF) > 50$ ps
- ✓ $\sigma(p)/p < 5\%$

FOOT performances and status

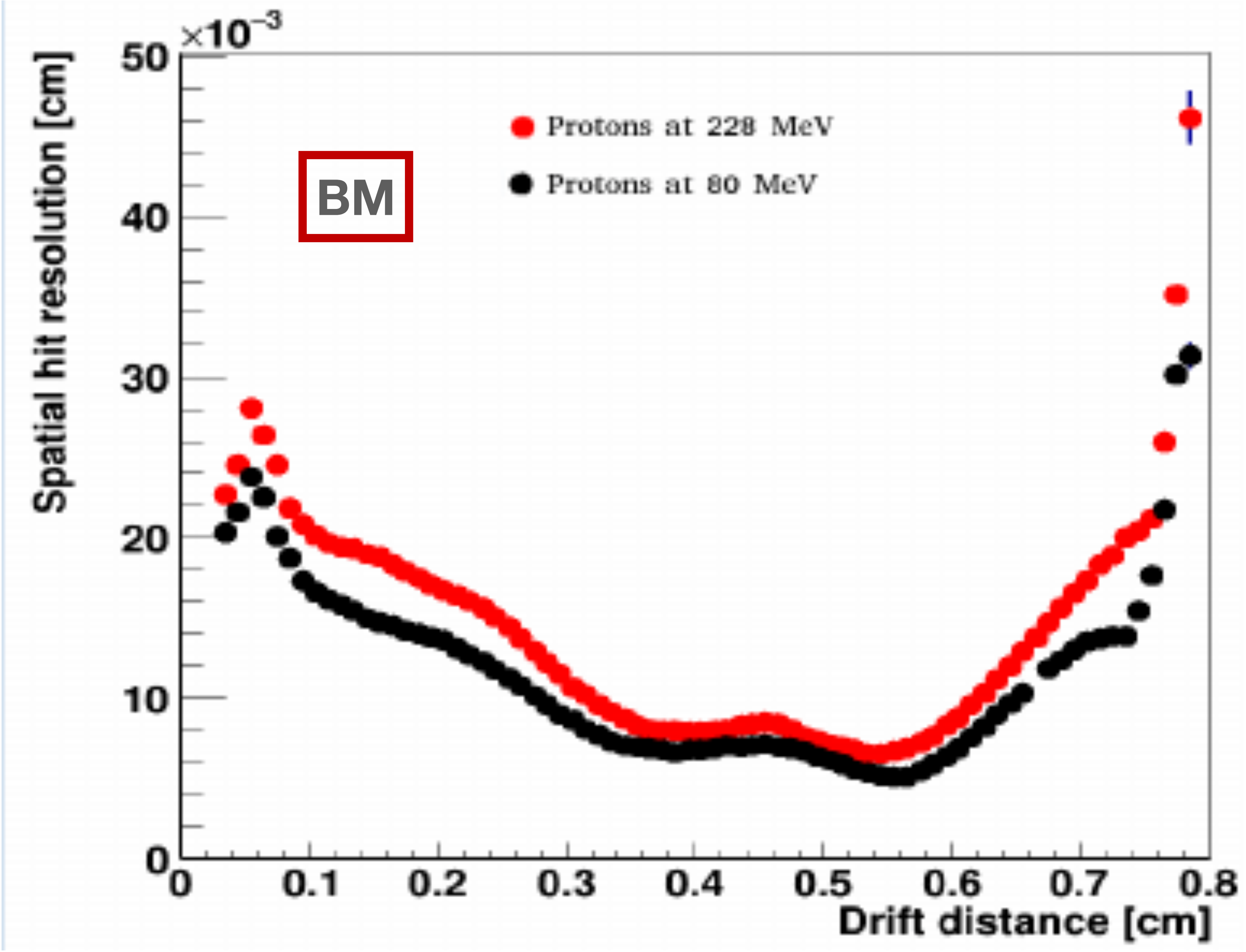

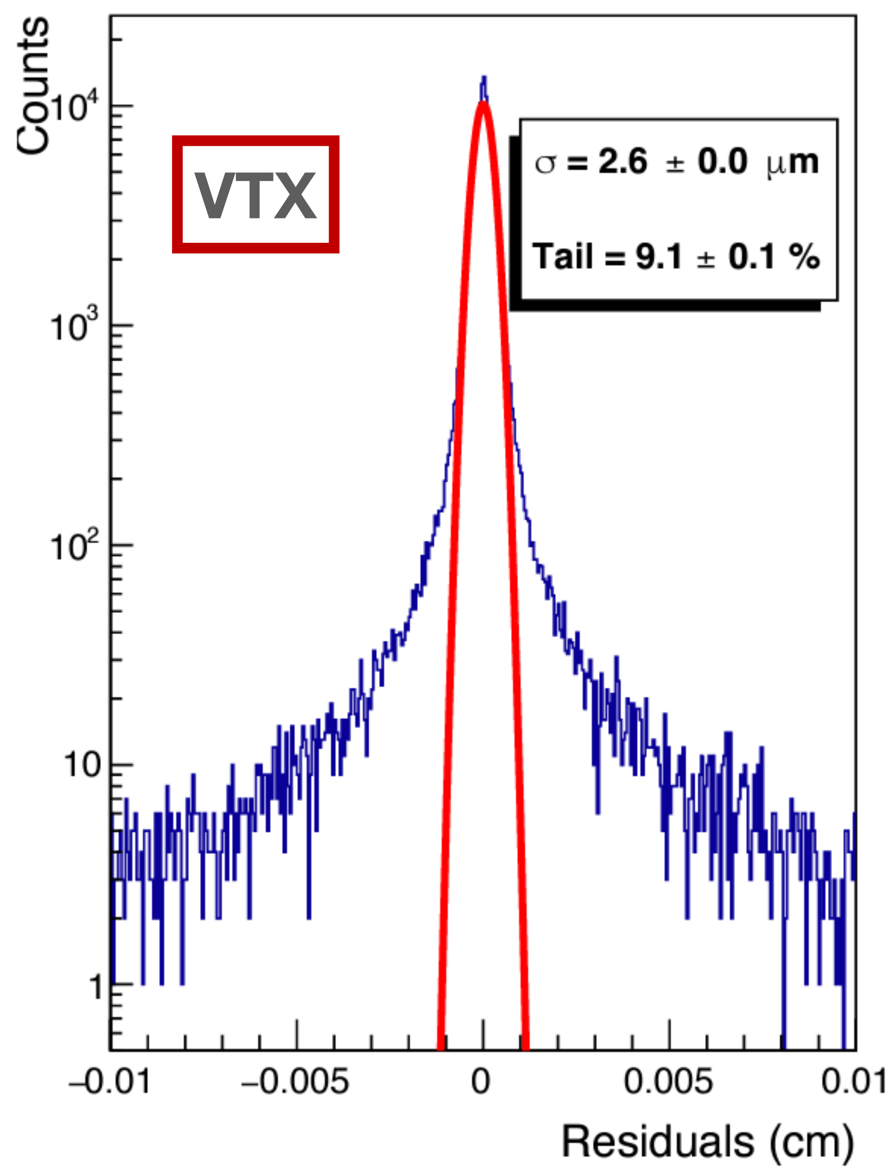

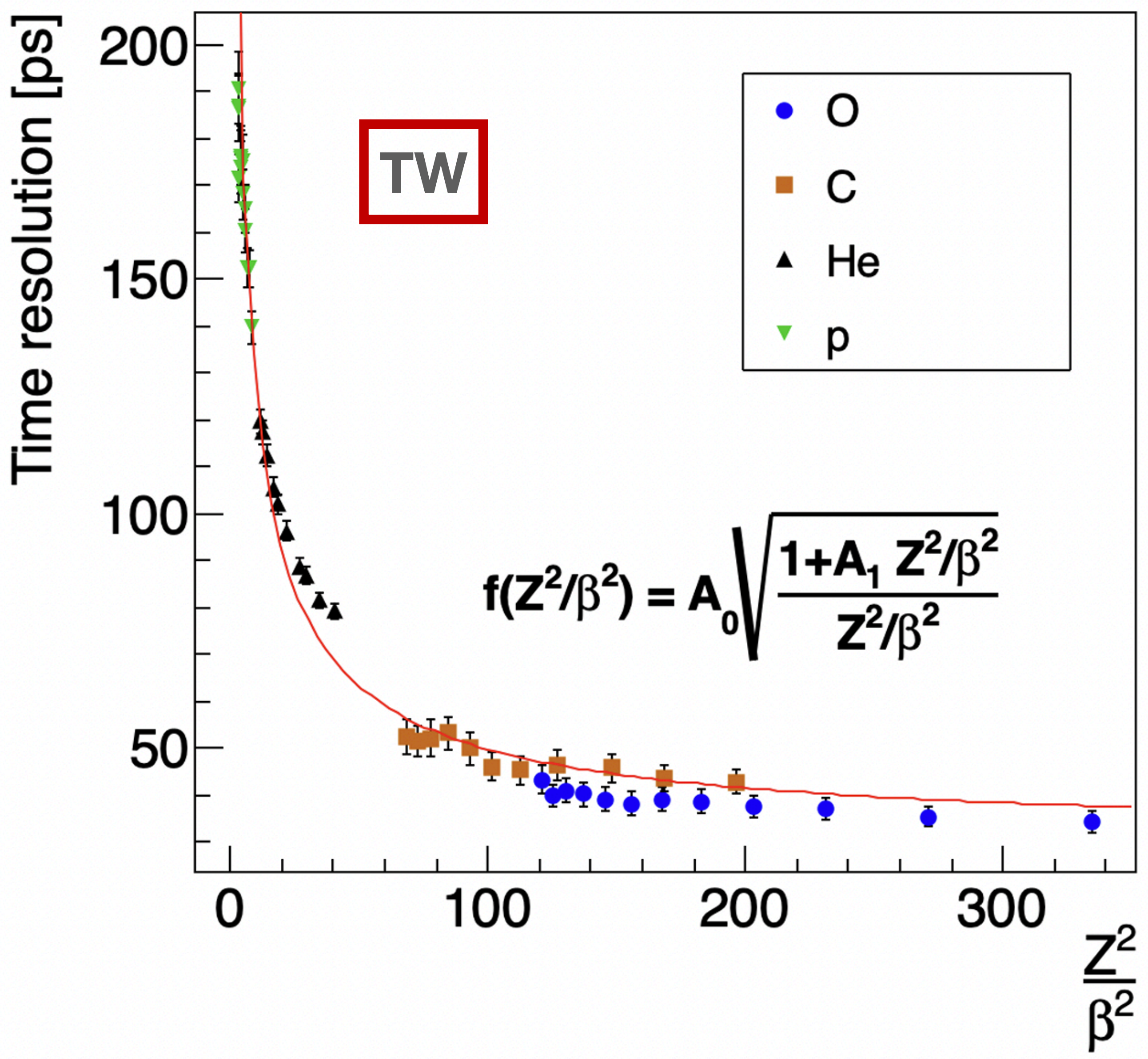

FOOT performances:

- ✓ $\sigma(E_{kin})/E_{kin} < 3\%$
- ✓ $\sigma(\Delta E)/\Delta E \sim 4\text{-}5\%$
- ✓ $\sigma(TOF) > 50$ ps
- ✓ $\sigma(p)/p < 5\%$

FOOT performances and status

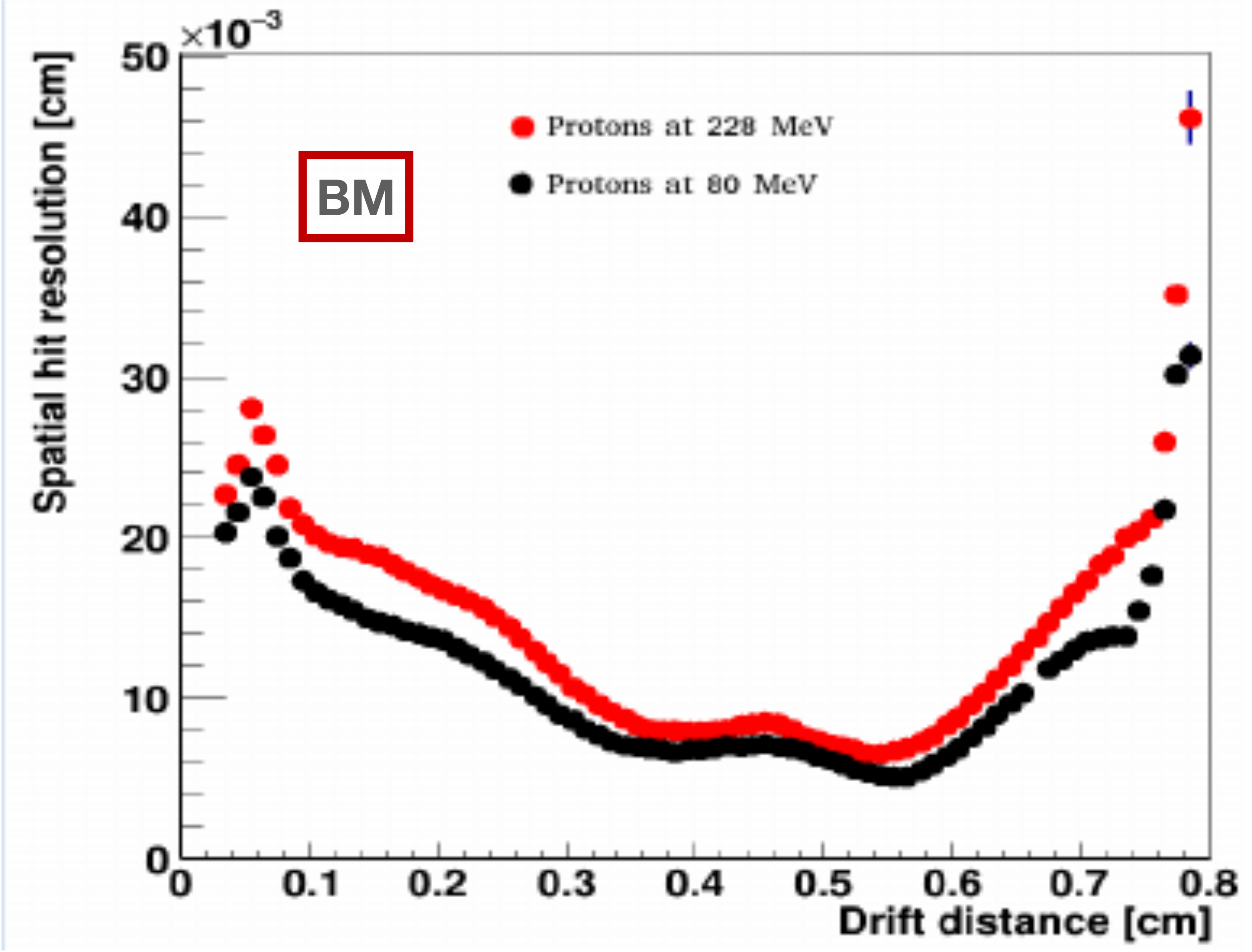

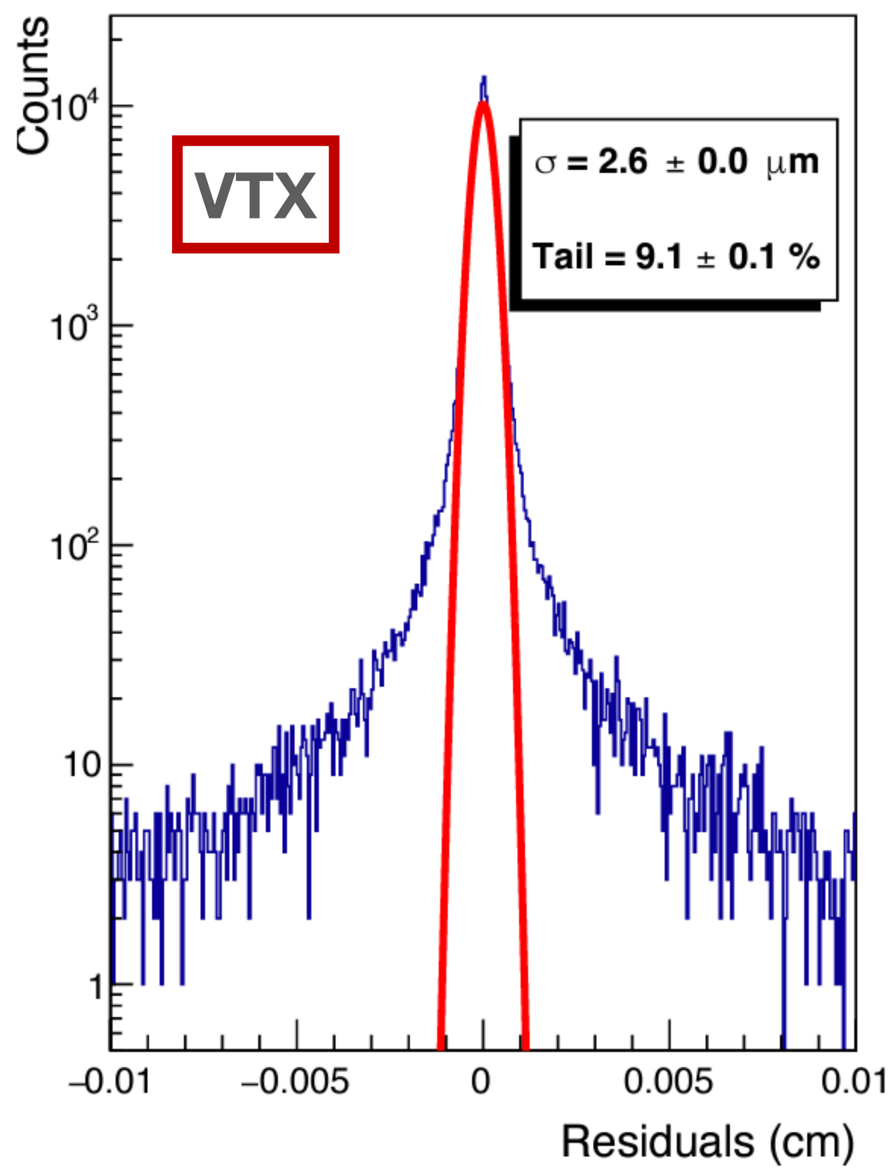

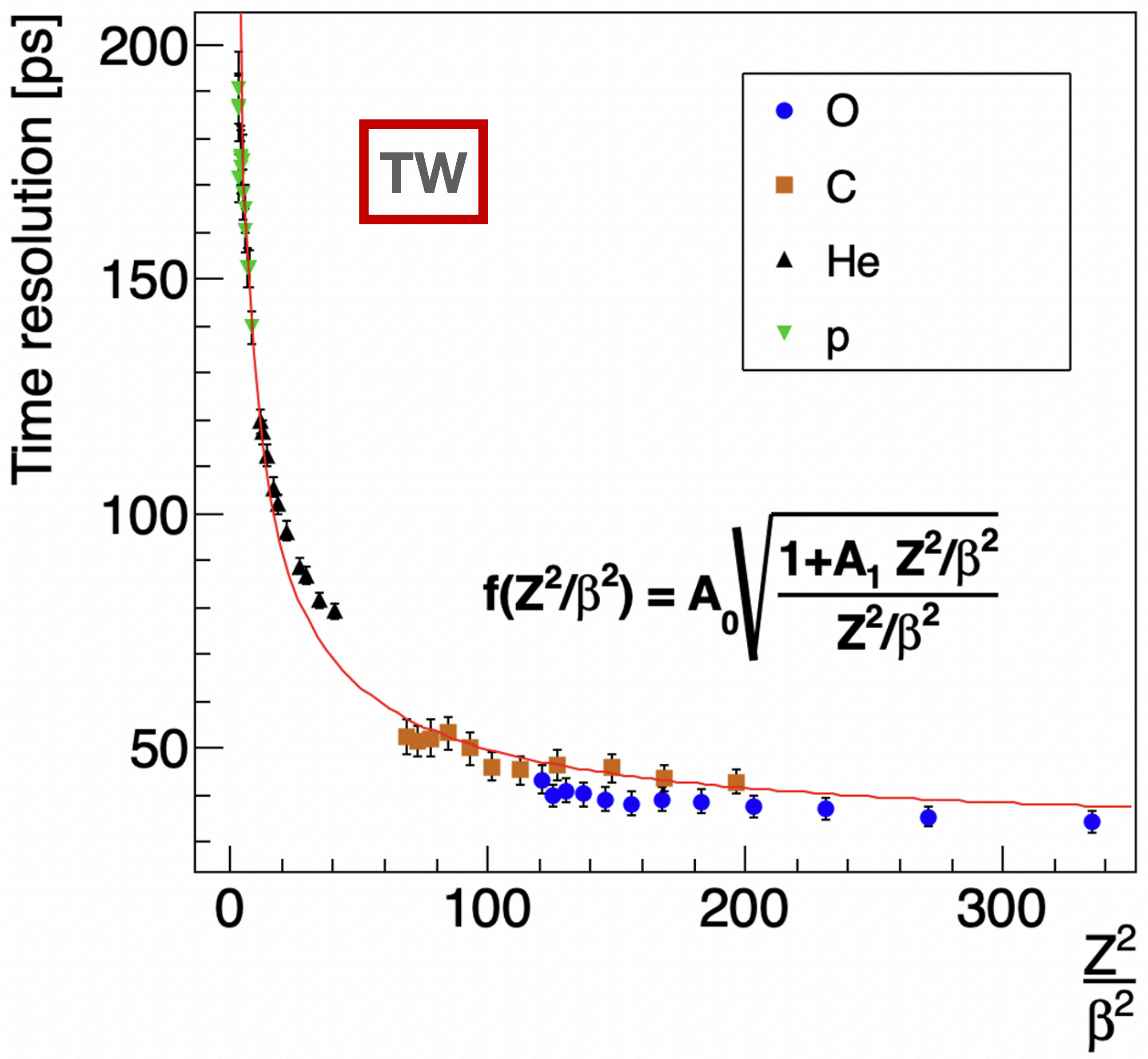

FOOT performances:

- ✓ $\sigma(E_{kin})/E_{kin} < 3\%$
- ✓ $\sigma(\Delta E)/\Delta E \sim 4\text{-}5\%$
- ✓ $\sigma(TOF) > 50$ ps
- ✓ $\sigma(p)/p < 5\%$

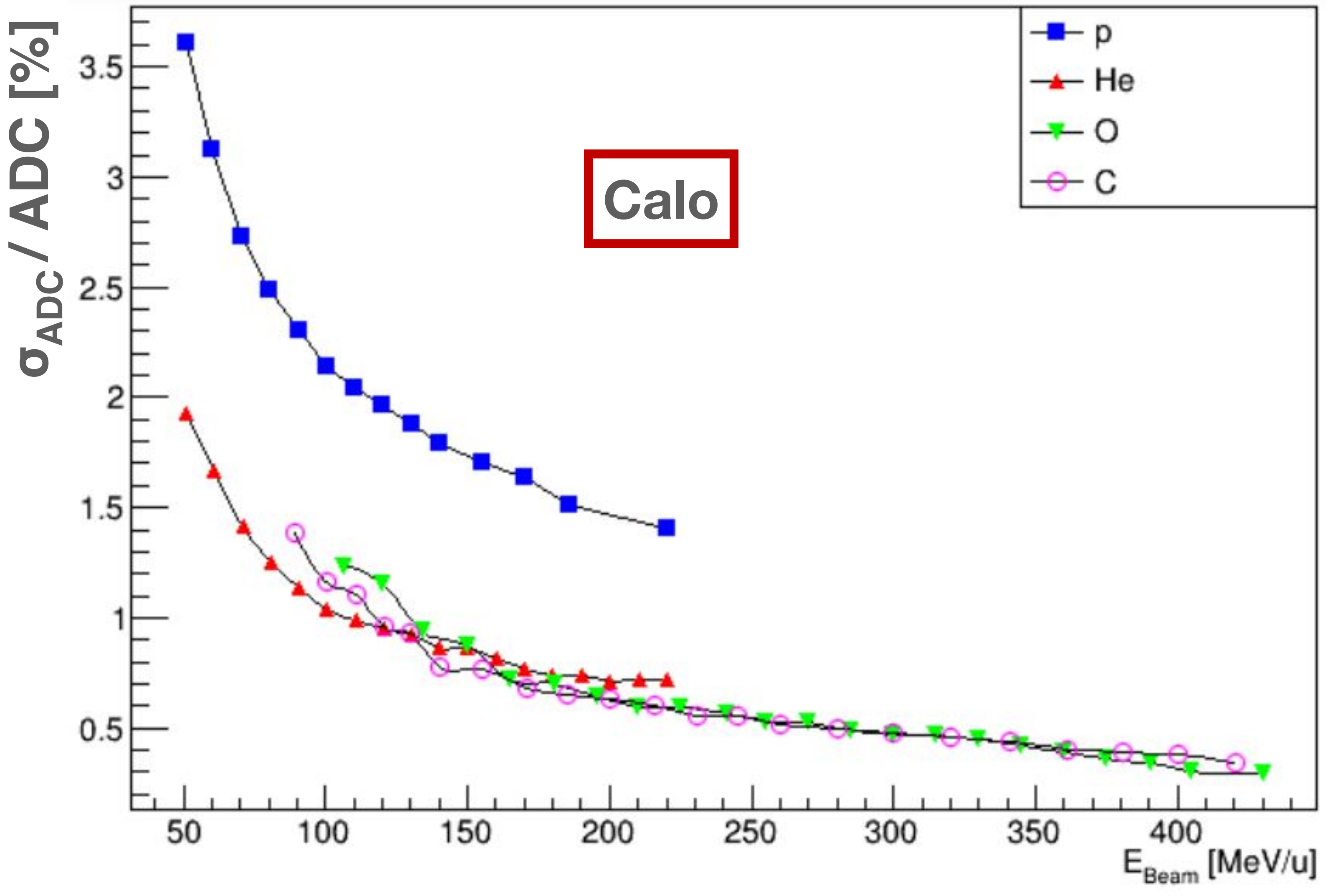

FOOT performances and status

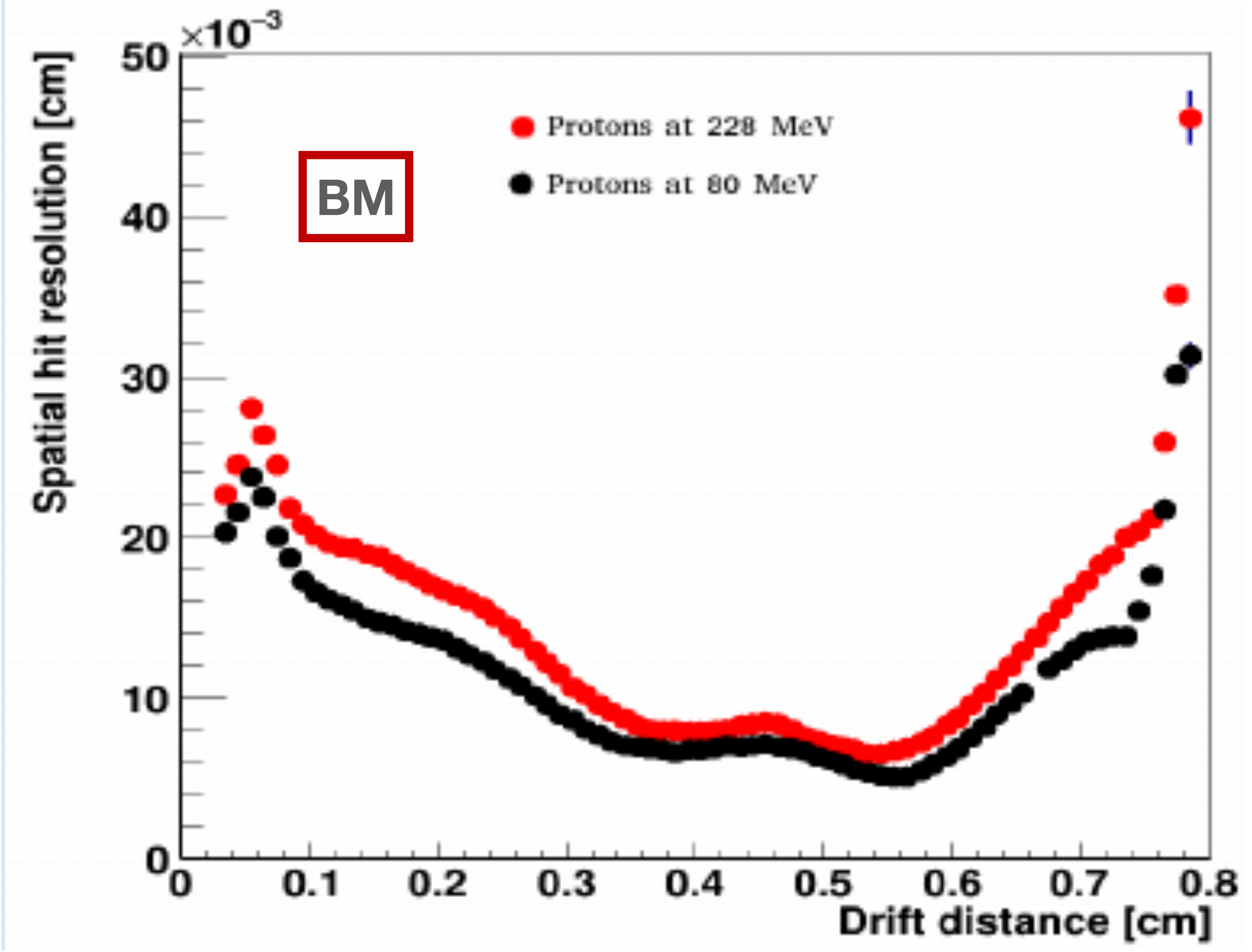

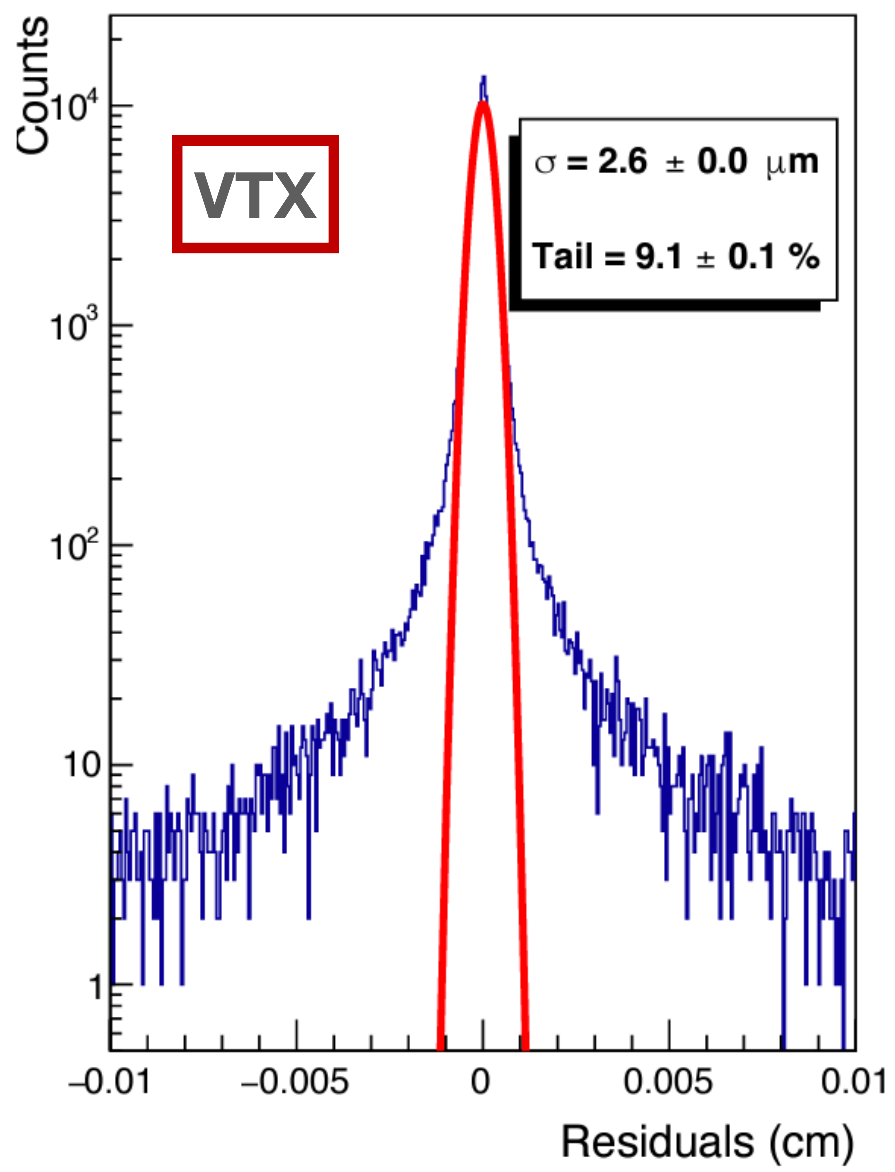

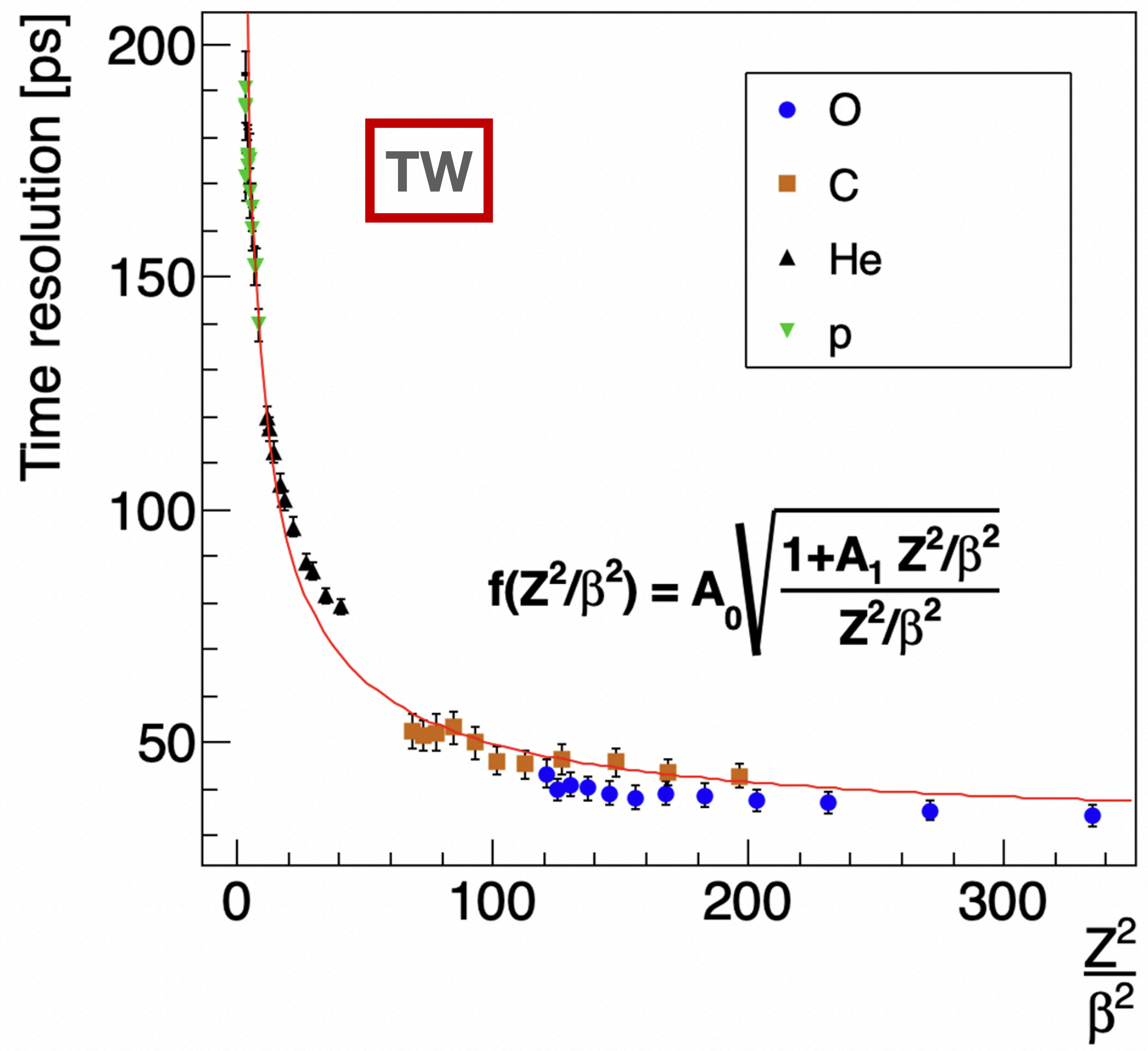

FOOT performances:

- ✓ $\sigma(E_{kin})/E_{kin} < 3\%$
- ✓ $\sigma(\Delta E)/\Delta E \sim 4\text{-}5\%$
- ✓ $\sigma(TOF) > 50$ ps
- ✓ $\sigma(p)/p < 5\%$

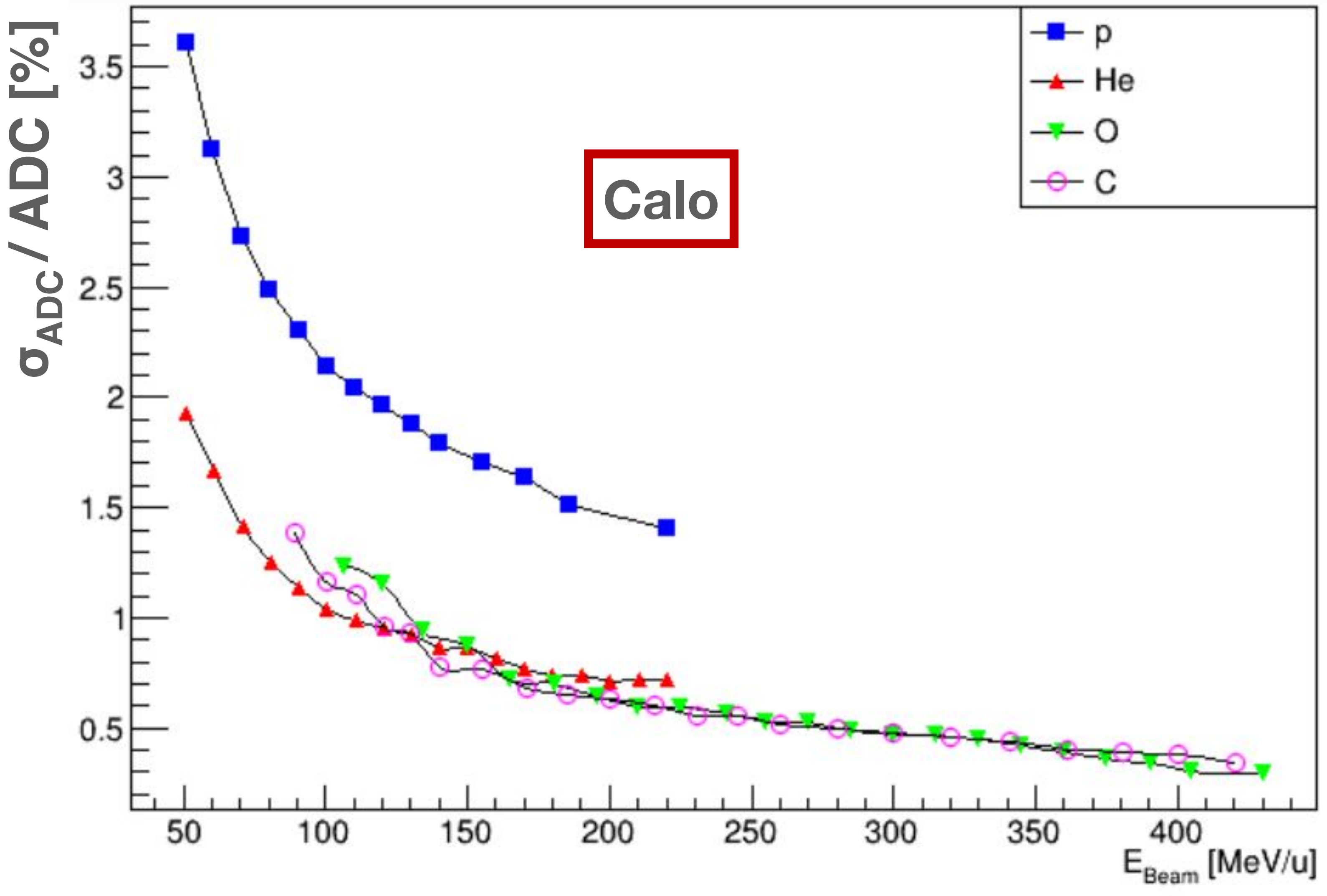

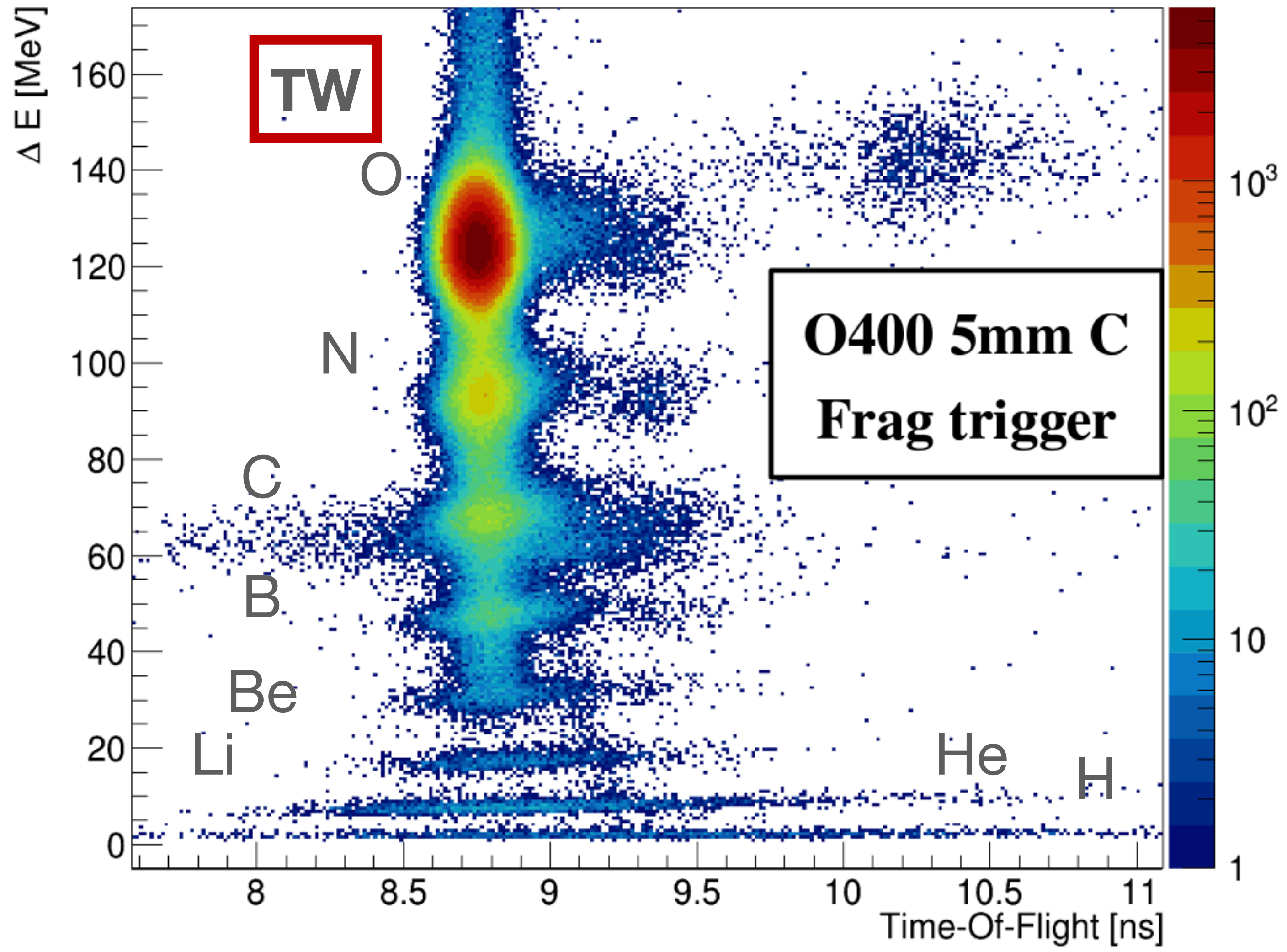

FOOT performances and status

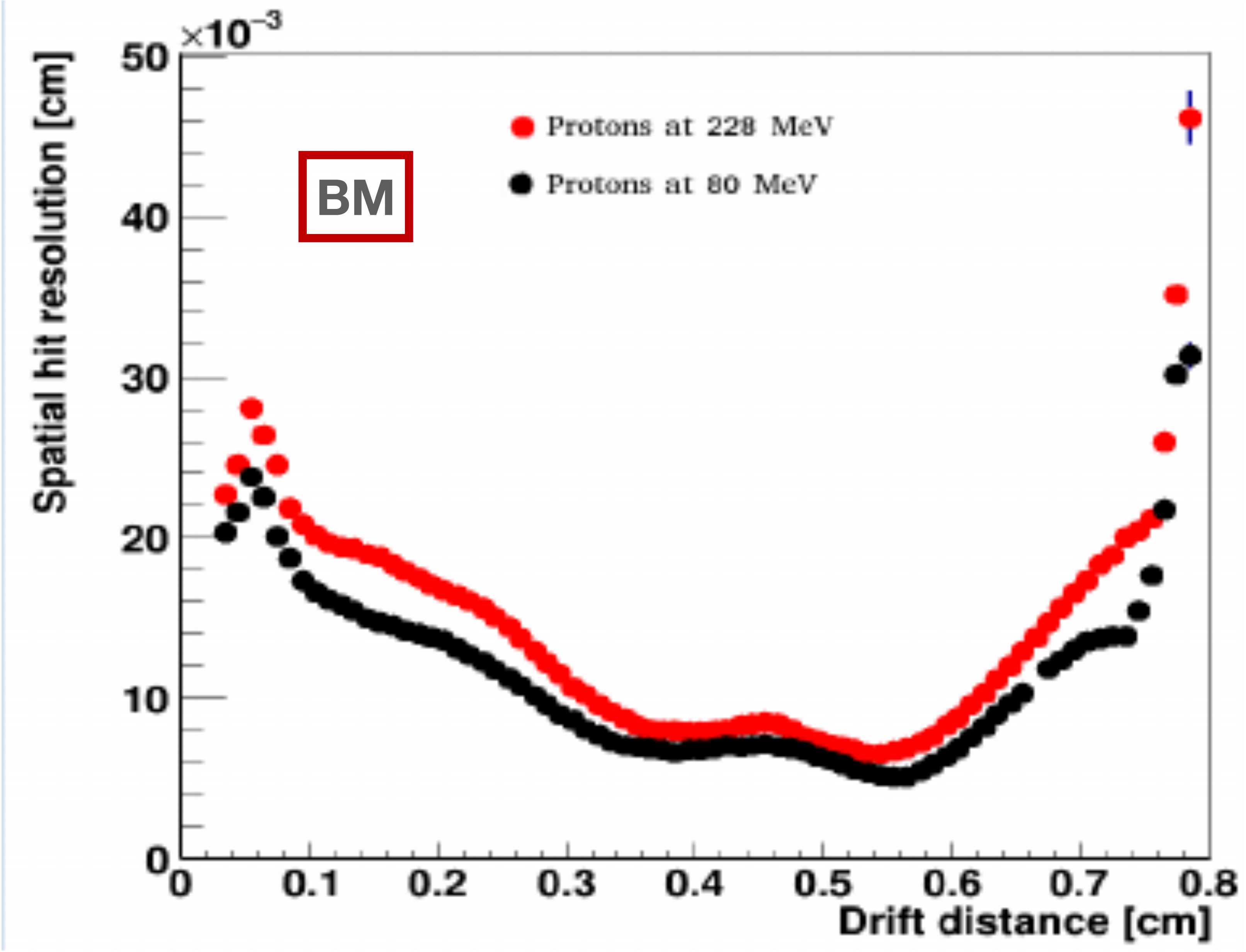

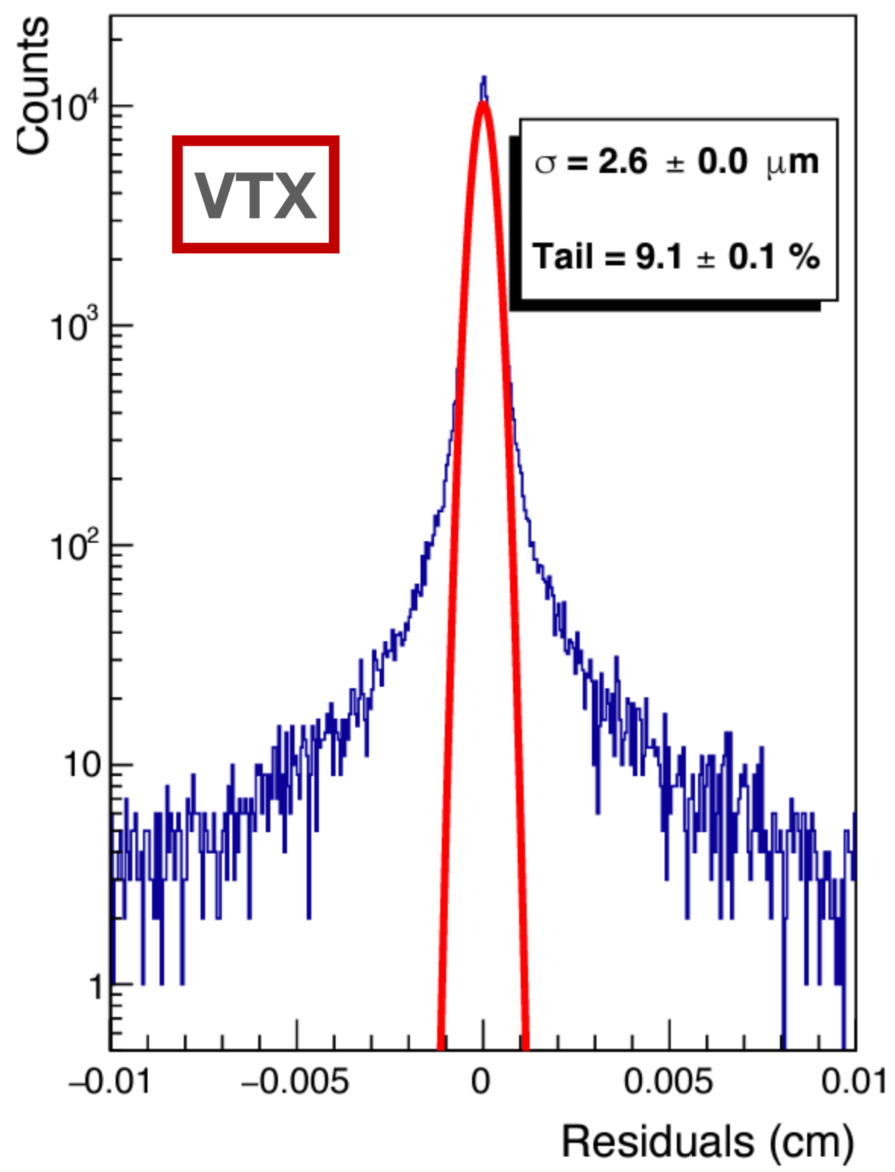

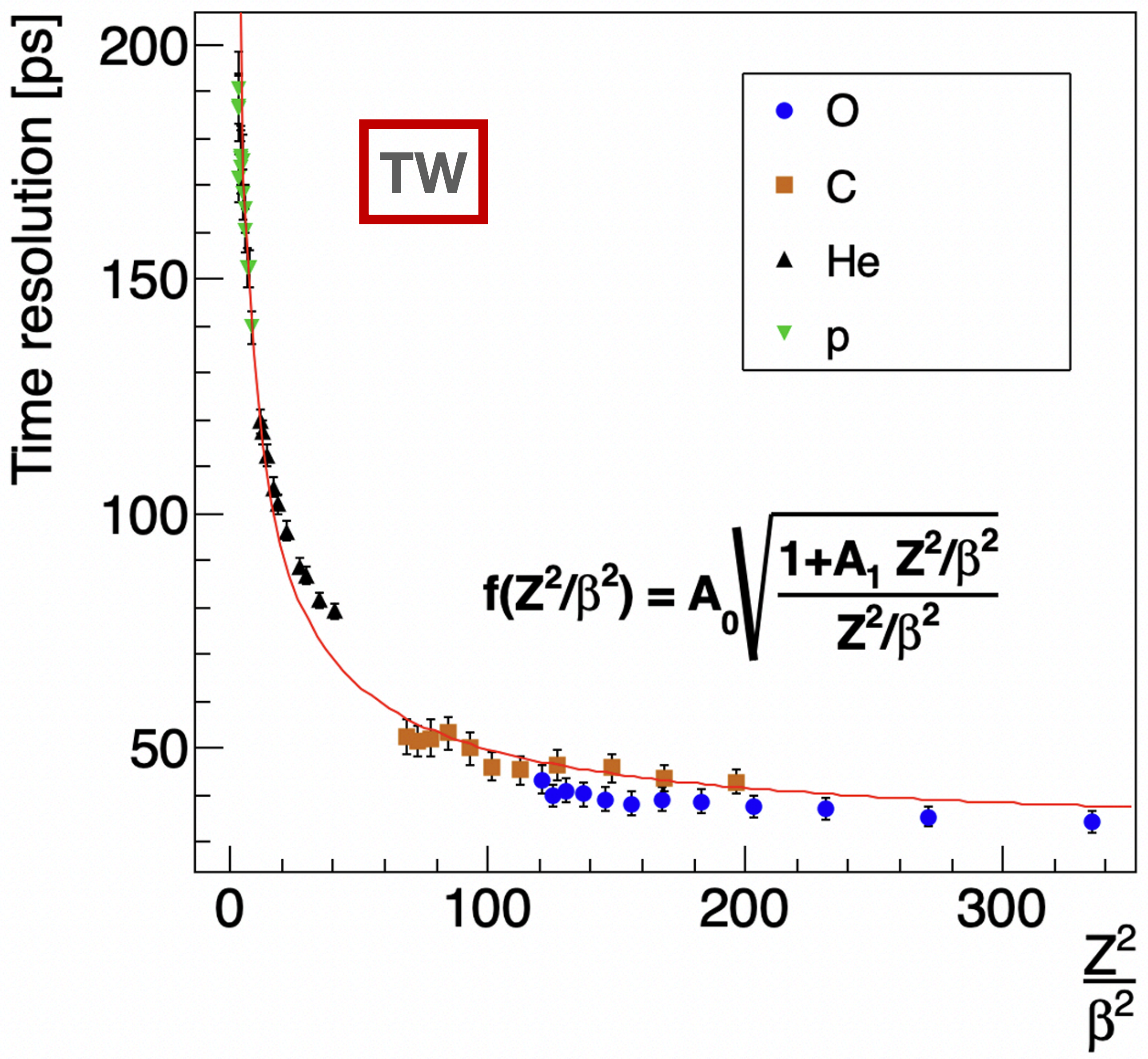

FOOT performances:

- ✓ $\sigma(E_{kin})/E_{kin} < 3\%$
- ✓ $\sigma(\Delta E)/\Delta E \sim$ 4-5%
- ✓ σ(TOF) > 50 ps
- ✓ σ(p)/p < 5%

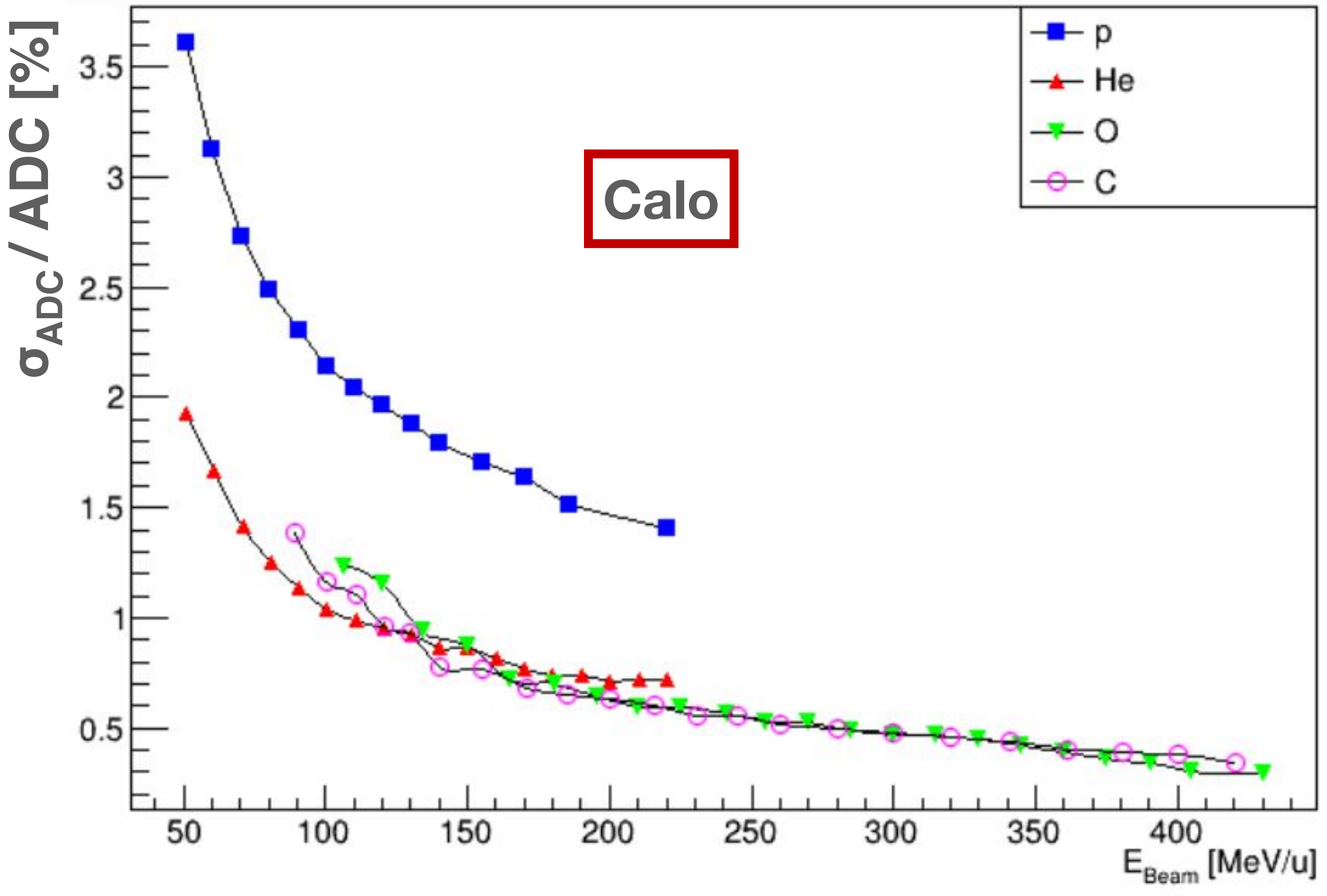

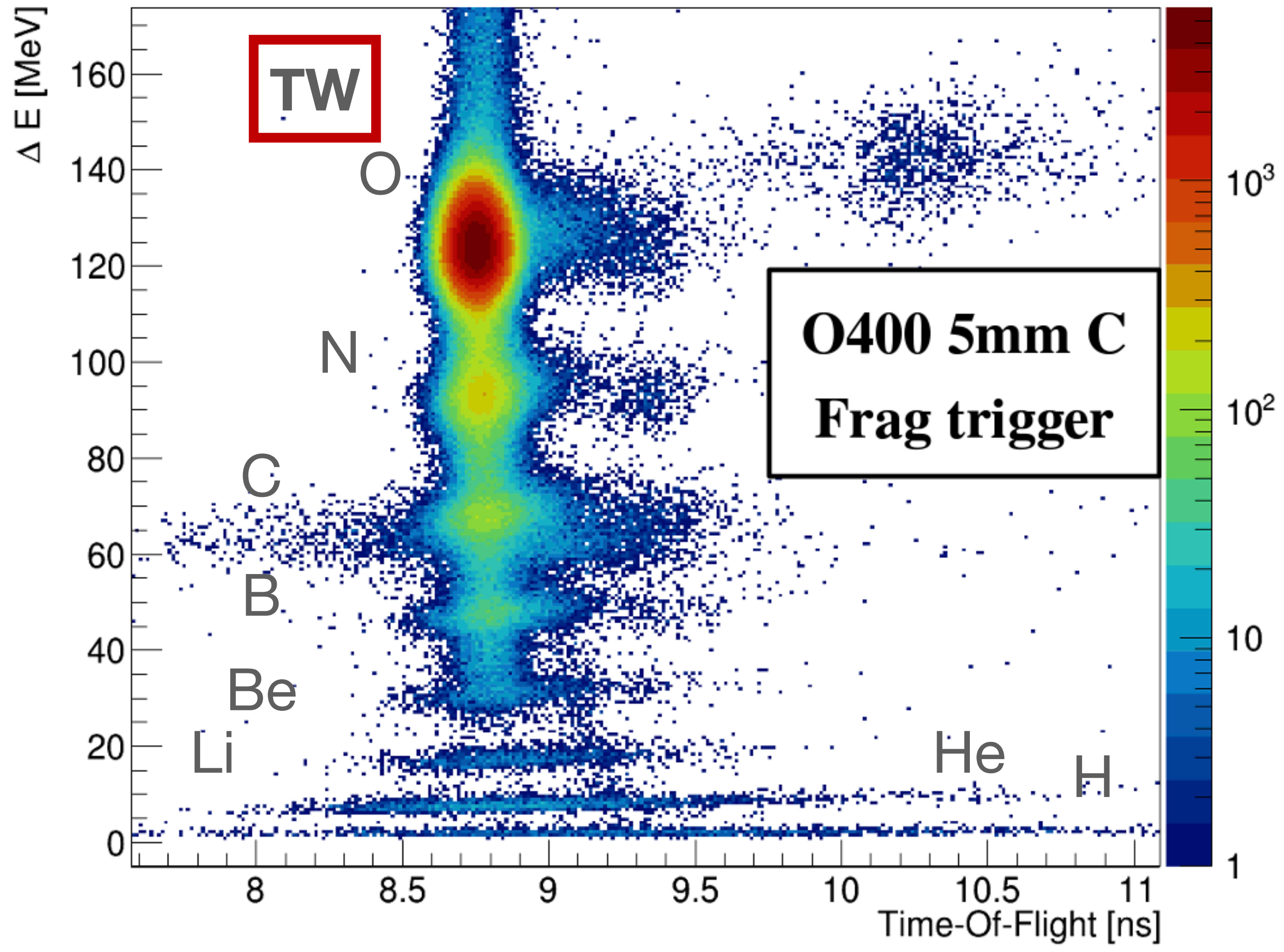

Detectors status:

- The setup is almost completed (No magnets yet)
- Different detectors already characterized and calibrated: TOF system, Drift chamber, Vertex
- Characterization of trackers (IT and MSD) and calorimeter ongoing

Fragmentation of ^{16}O beam [400 MeV/u] on C target

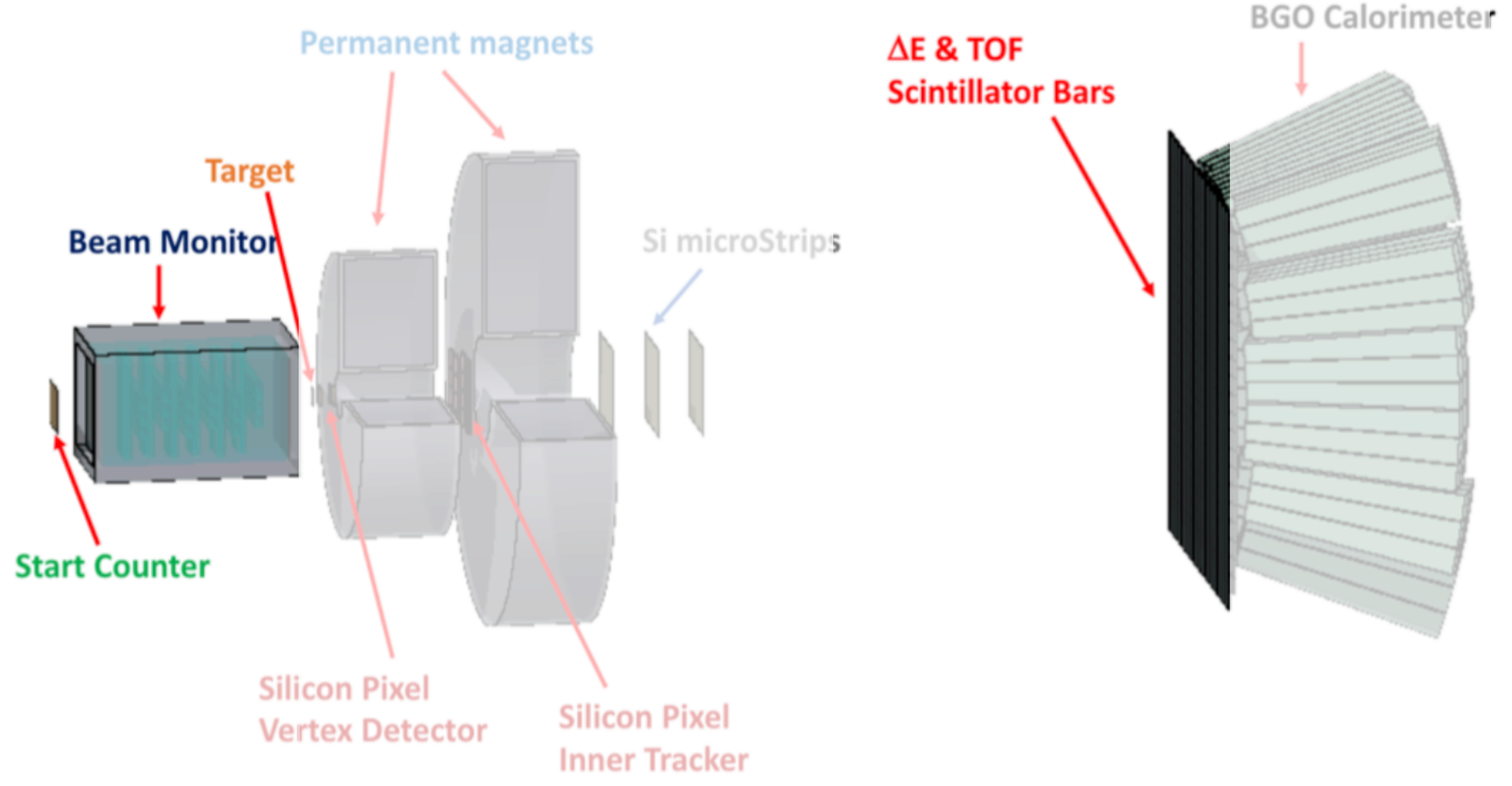

^{16}O at 400 MeV/u on graphite target at GSI cave A: partial FOOT setup

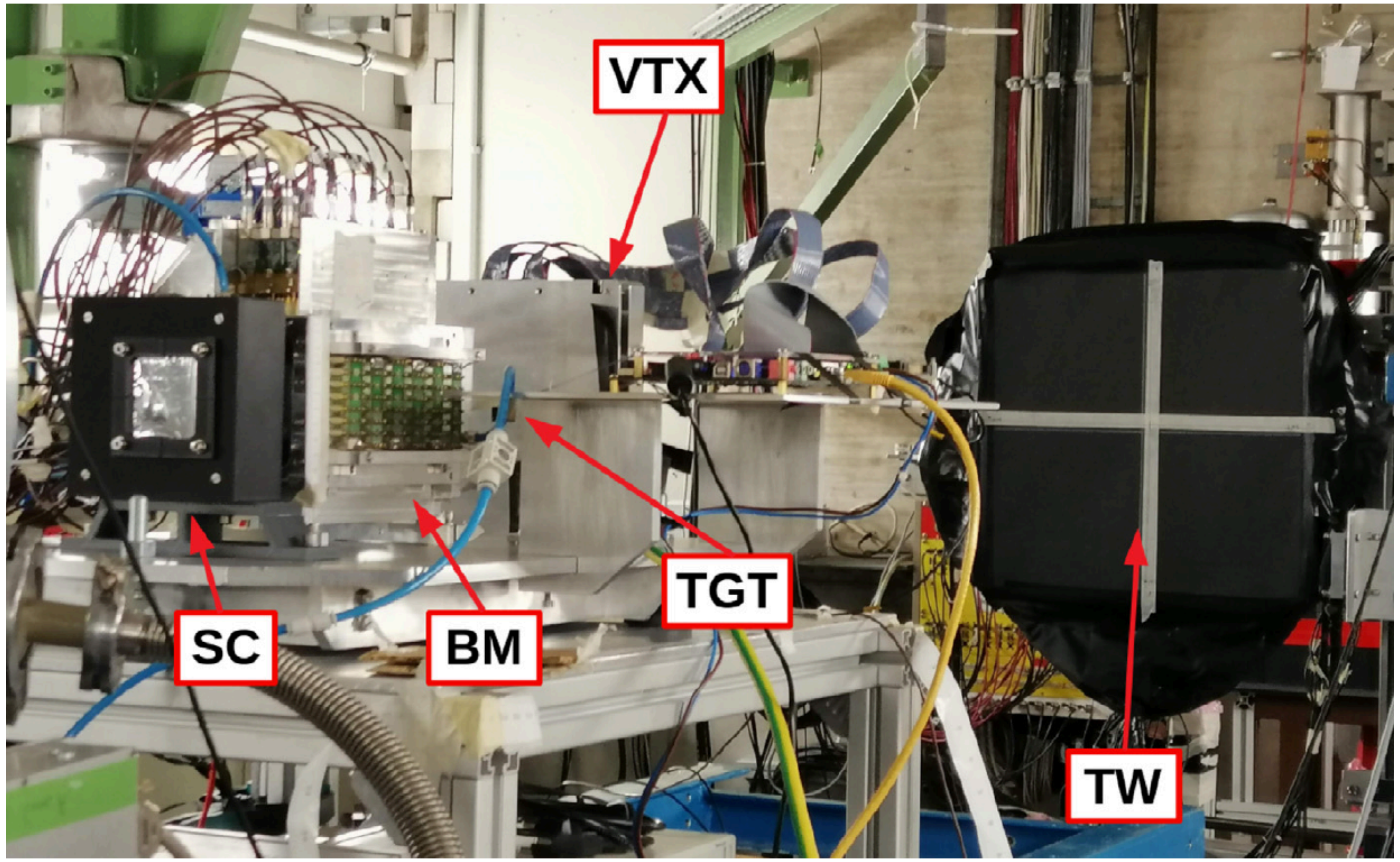

- Only SC, BM, and TW detector (scintillating bars)
- ΔE-TOF system for nuclear charge identification
- Elemental fragmentation cross sections of 16O at 400 MeV/u on C target

[Limited acquisition time and available space ("table top experiment")]

Fragmentation of ^{16}O beam [400 MeV/u] on C target

Fragments charge identifications with the ΔE-ToF system

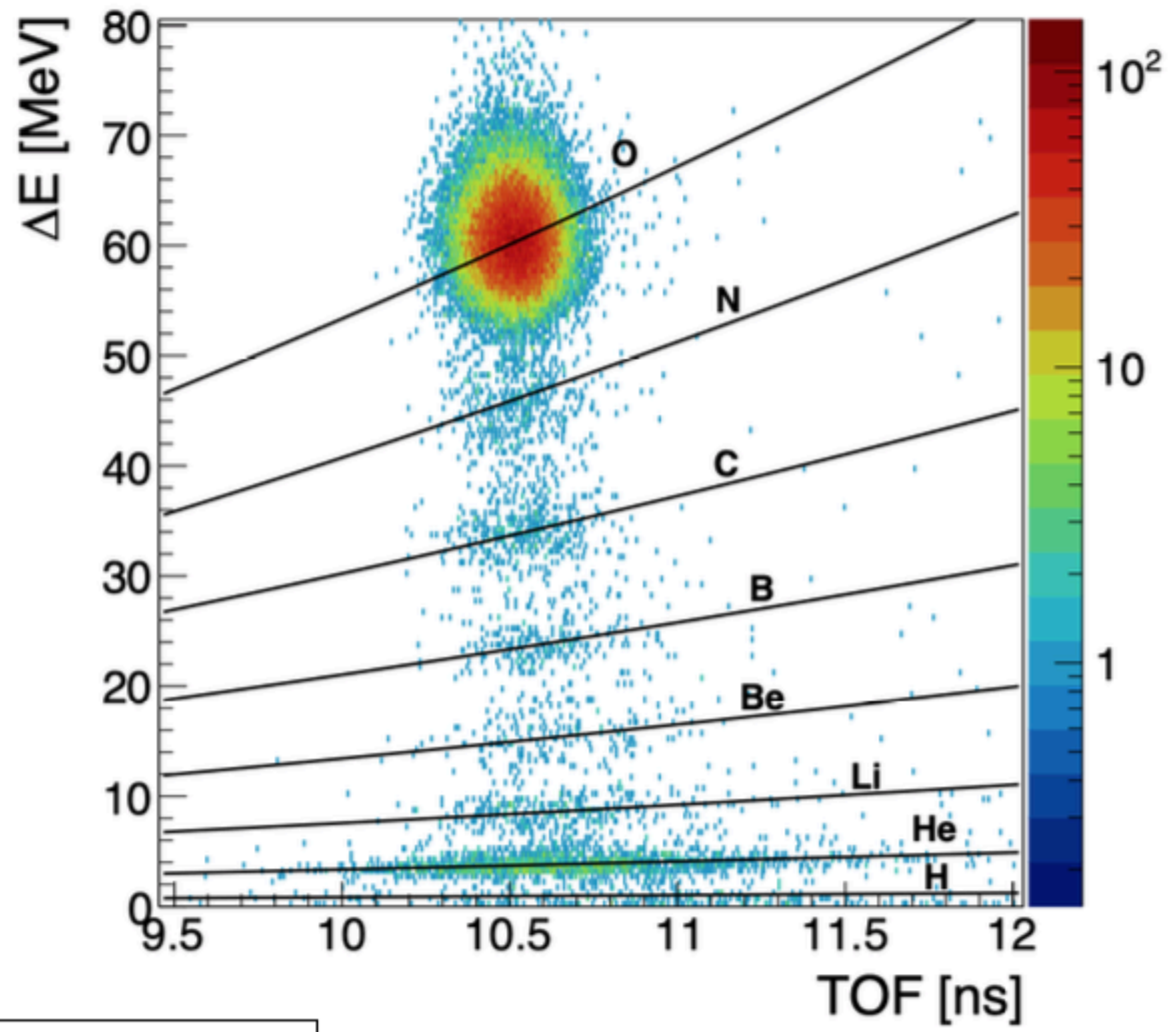

After reconstruction

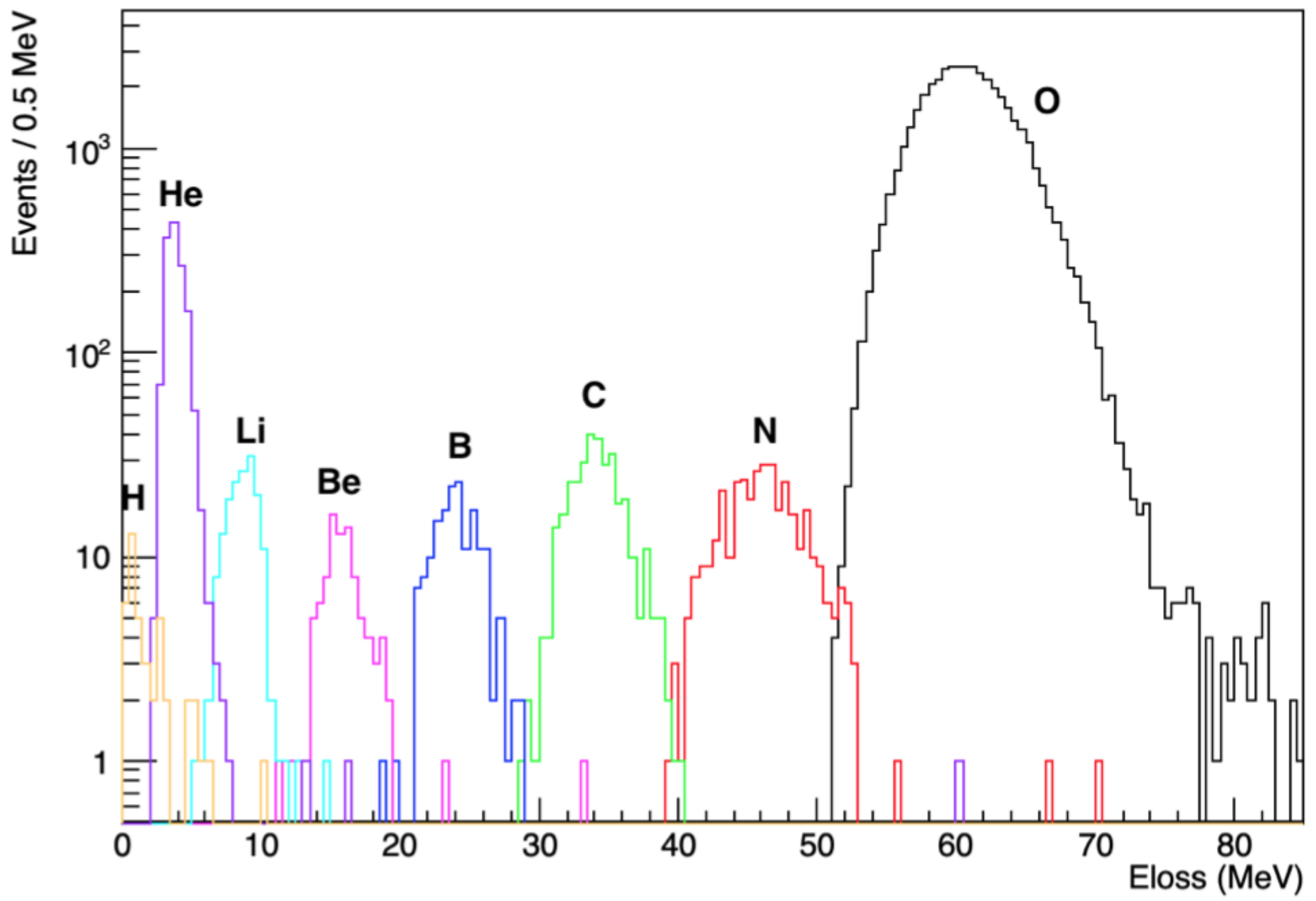

^{16}O at 400 MeV/u on graphite target at GSI cave A: partial FOOT setup

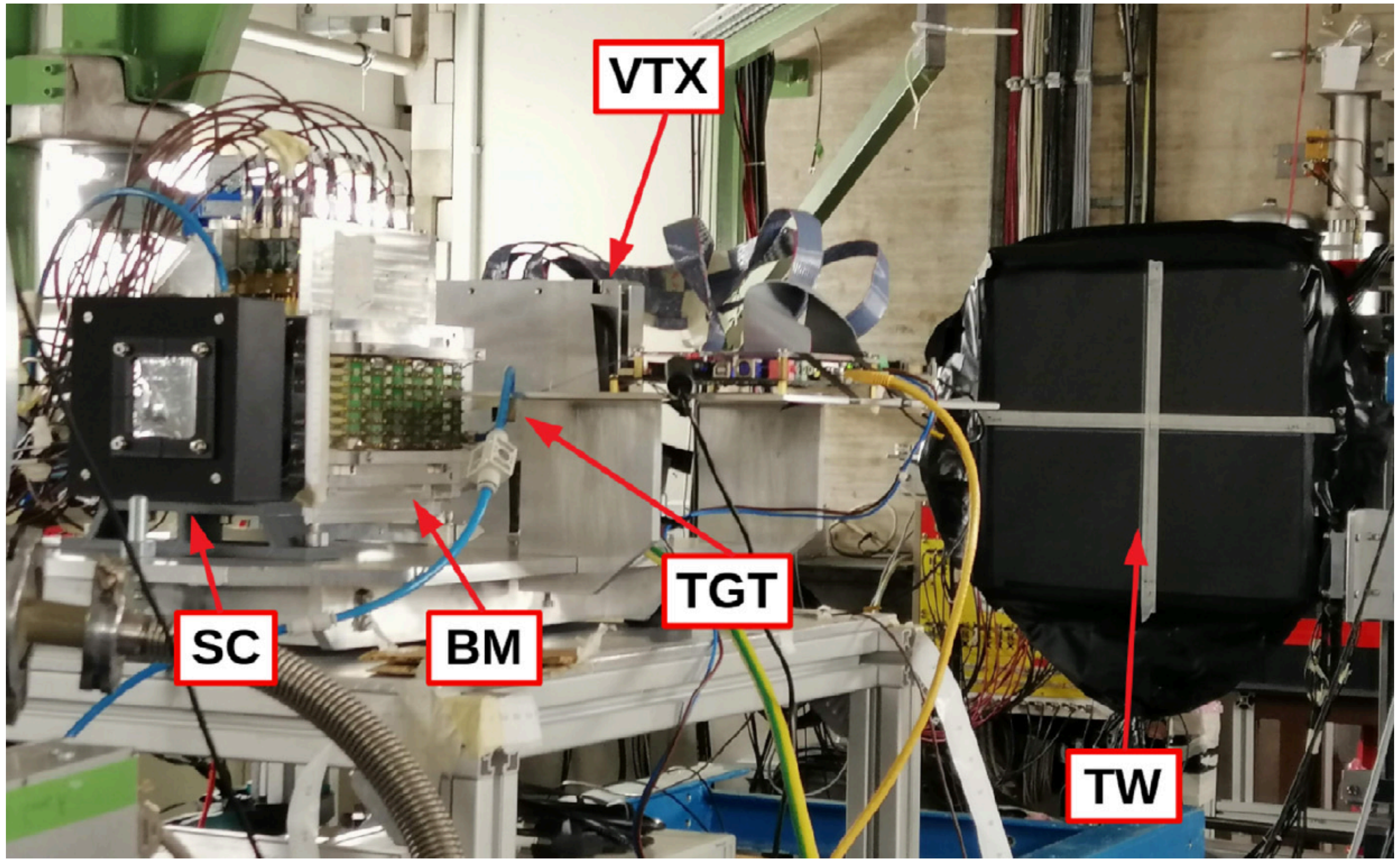

Elemental fragmentation cross section for 1<Z<8

Element	$\sigma_{frag} \pm \Delta_{stat} \pm \Delta_{sys}$ [mbarn]	$\Delta_{stat}/\sigma_{frag}$	$\Delta_{sys}/\sigma_{frag}$	σ_{MC} [mbarn]
He	$789 \pm 35 \pm 67$	4.4 %	8.5 %	705 ± 2
Li	$101 \pm 13 \pm 10$	12.5 %	10.4 %	74.9 ± 0.6
Be	$33 \pm 9 \pm 3$	26 %	10.3 %	37.5 ± 0.4
B	$78 \pm 11 \pm 6$	14 %	8.5 %	41.8 ± 0.4
C	$131 \pm 14 \pm 4$	11 %	2.8 %	87.7 ± 0.6
N	$117 \pm 14 \pm 6$	12 %	4.8 %	110.3 ± 0.7

Toppi M. et al, Front. Phys. 10:979229. doi: 10.3389/fphy.2022.979229

Conclusions

- The FOOT experiment is designed for the measurement of the fragmentation differential cross sections of interest in Particle Therapy and radio protection in space with an accuracy better than 10%
- The final set up is almost completed (Inner Tracker (IT) + Calo still in development, Magnet not present yet). Characterization of trackers (IT and MSD) and calorimeter ongoing
- Data takings performed at GSI, HIT and CNAO with an increasing set-up provided many data for study FOOT performances/calibration and improve our detector knowledge (trigger, rate capability, DAQ, on-line monitoring and reconstruction) and beam characteristics (CNAO)
- First elemental fragmentation cross section measurement of a ^{16}O beam at 400 MeV/u with a partial setup, integrated in the detector acceptance
- **At the end of the 2023 the first data taking with magnet is expected at CNAO**

Thanks for your attention!

Spare Slides

Fragments angular and energetic distributions

- Z>2 fragments ~ same velocity of the ^{16}O ions. Emitted in forward direction
- Protons & neutrons are the most abundant fragments: wide kinetic energy and angular distributions

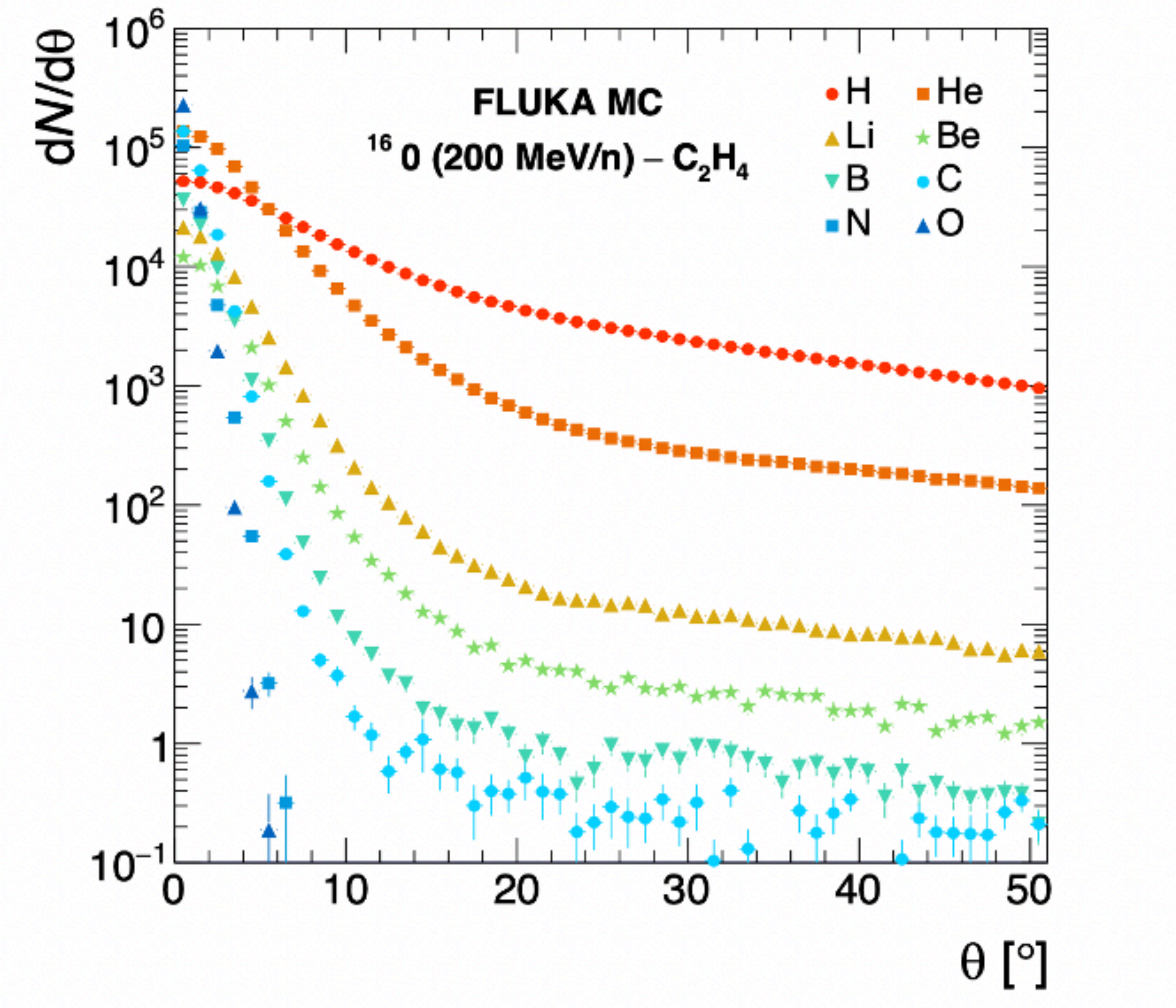

G.Battistoni et al., Front. Phys. 8:568242. doi: 10.3389/fphy.2020.568242

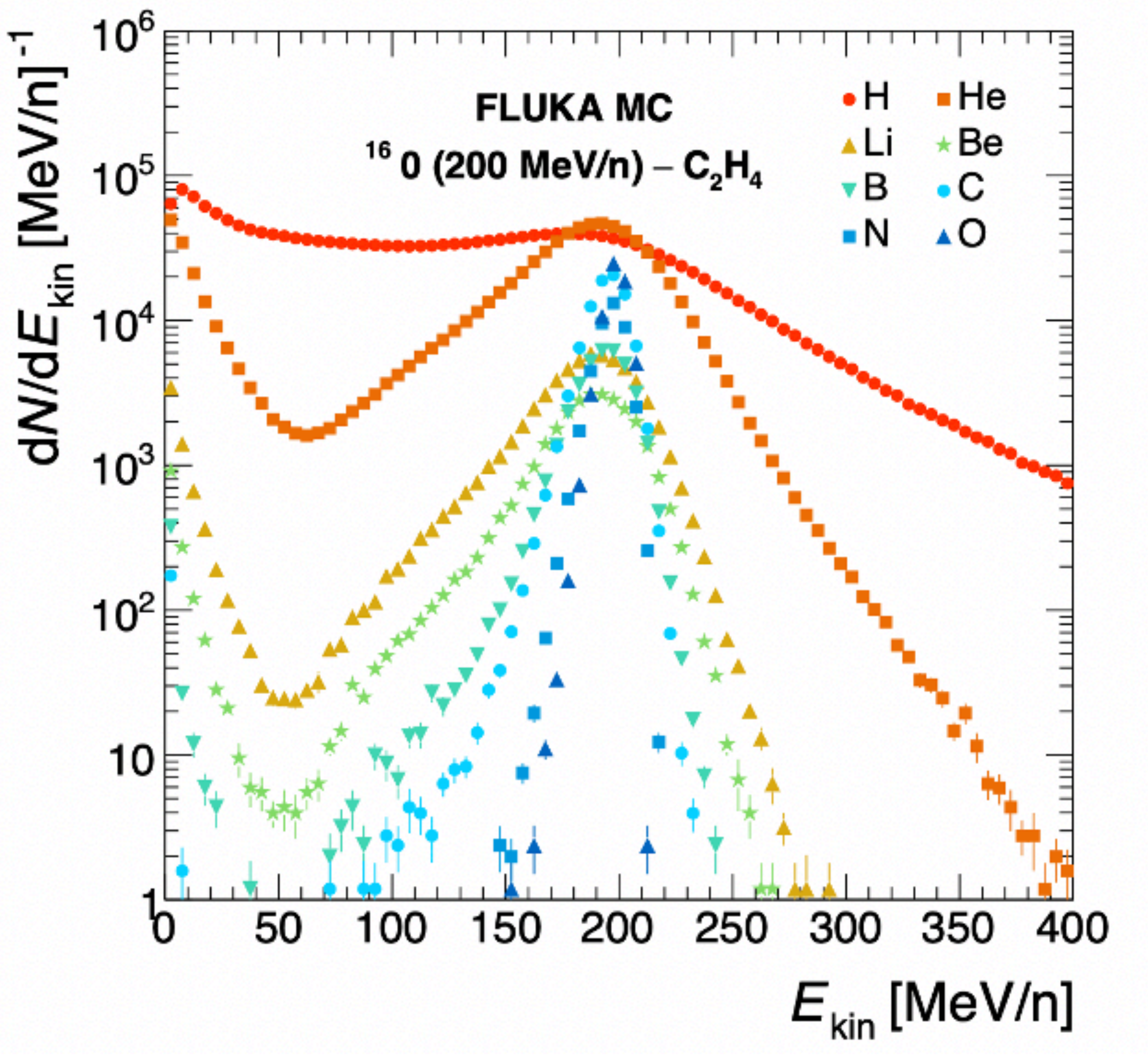

G.Battistoni et al., Front. Phys. 8:568242. doi: 10.3389/fphy.2020.568242

Target fragmentation contribution

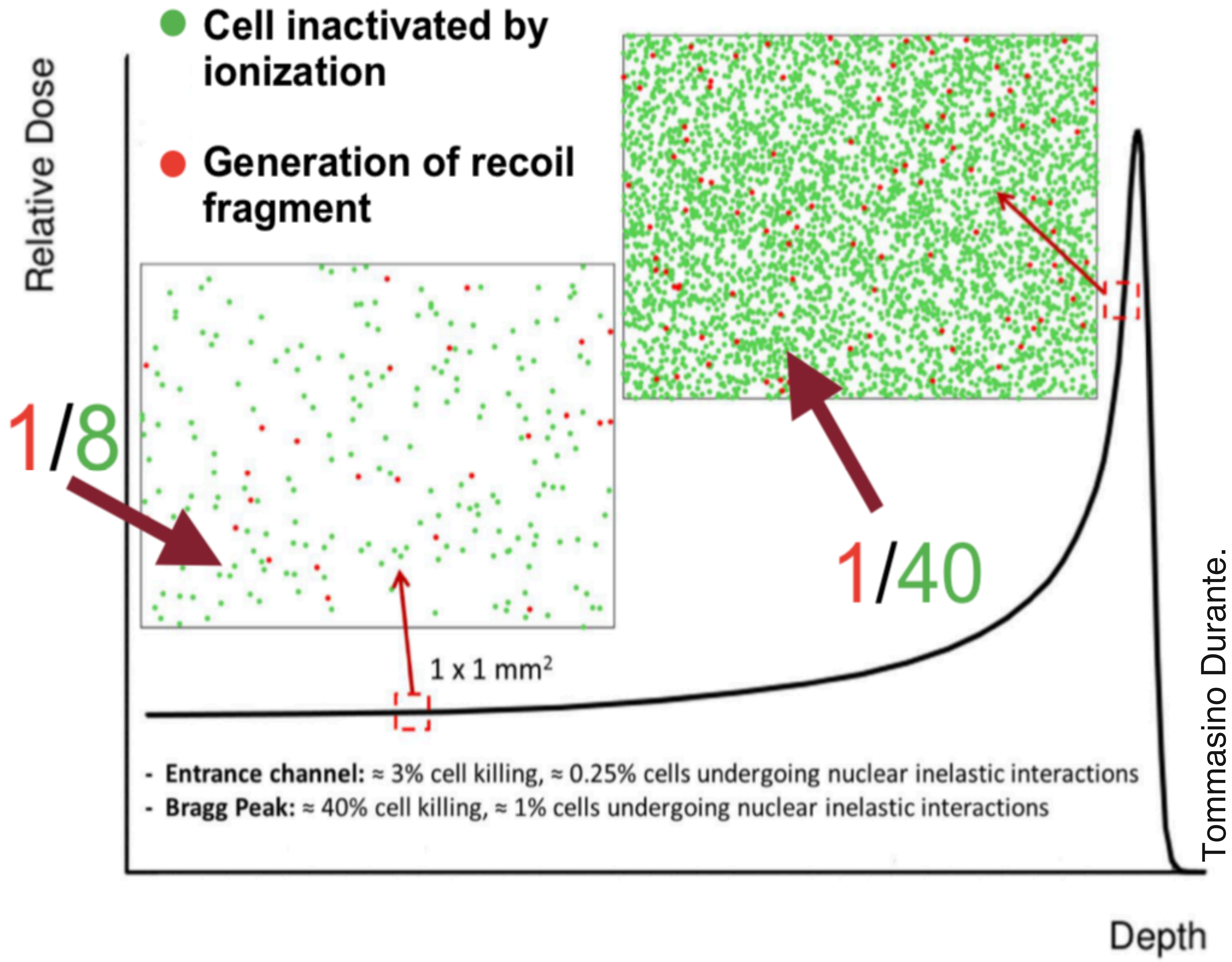

Tommasino Durante.
Cancers 2015, 7, 353-381; doi:10.3390/cancers7010353

Expected average physical parameters for target fragments produced in water by a 180 MeV proton beam

Fragment	E (MeV)	LET (keV/μm)	Range (μm)
^{15}O	1.0	983	2.3
^{15}N	1.0	925	2.5
^{14}N	2.0	1137	3.6
^{13}C	3.0	951	5.4
^{12}C	3.8	912	6.2
^{11}C	4.6	878	7.0
^{10}B	5.4	643	9.9
^{8}Be	6.4	400	15.7
^{6}Li	6.8	215	26.7
^{4}He	6.0	77	48.5
^{3}He	4.7	89	38.8
^{2}H	2.5	14	68.9

GoodHead D.T., Radiation protection dosimetry, 122, 2006

➢ The particles produced in target **fragmentation**, expecially the heavier fragments, are one of the causes contributing to the increase of proton RBE

Isotopic identification

When incident proton beams undergo fragmentation, they produce hydrogen, carbon or helium isotopes which, for a given kinetic energy per nucleon, have different ranges and so they produce different biological damages.

Therefore it is essential to achieve a high accuracy on the isotopic identification (5%) and thus on the TOF, bending and kinetic energy measurements.

The FOOT experiment aims to obtain three different estimations of the mass number:

→β is evaluated from the TOF (**<100 ns**) measurements since β = L/(TOF×c) →TOF DETECTORS

→p is derived from the particle deflection inside the magnetic field (**5%**) →TRACKERS

→E_{kin} is the energy measured by the CALORIMETER (**2-3%**)

- $$A_1 = \frac{m}{u} = \frac{1}{u}\frac{p}{\gamma\beta c}$$
- $$A_2 = \frac{m}{u} = \frac{1}{u}\frac{E_{kin}}{(\gamma - 1)c^2}$$
- $$A_3 = \frac{1}{u}\frac{p^2c^2 - E_{kin}^2}{2c^2 E_{kin}}$$

FOOT physics program

Physics (*)	Application field	Beam	Target	Upper Energy (MeV/nucleon)	Kinematic approach	Interaction process
Target fragmentation	PT	^{12}C	C,C_2H_4	200	inverse	p+C
Target fragmentation	PT	^{16}O	C,C_2H_4	200	inverse	p+C
Beam fragmentation	PT	^{4}He	C, C_2H_4, PMMA	250	direct	α+O α+H, α+O
Beam fragmentation	PT	^{12}C	C, C_2H_4, PMMA	400	direct	C+C, C+H, C+O
Beam fragmentation	PT	^{16}O	C, C_2H_4, PMMA	500	direct	O+C, O+H, O+O
Beam fragmentation	Space	^{4}He	C, C_2H_4, PMMA	800	direct	α+C, α+H, α+O
Beam fragmentation	Space	^{12}C	C, C_2H_4, PMMA	800	direct	C+C, C+H, C+O
Beam fragmentation	Space	^{16}O	C, C_2H_4, PMMA	800	direct	O+C, O+H, O+O

Cross section of H and O targets will be got by subtraction from cross section on C target and composite targets:

- polyethylene (C_2H_4)
- polymethyl methacrylate (PMMA, $C_5O_2H_8$)

(*) Extension of the FOOT experiment to measure neutrons

Strategy for fragmentation measurement

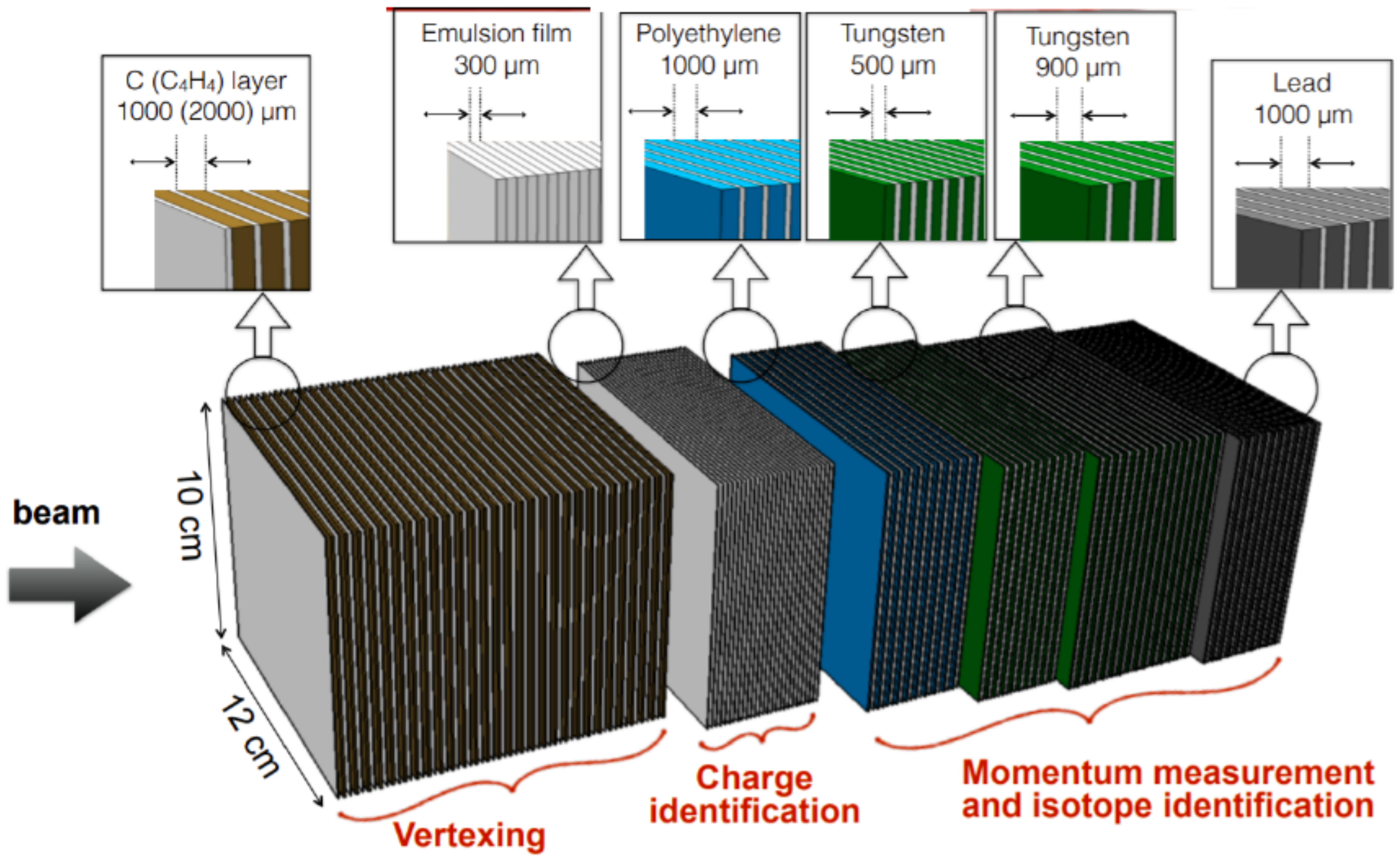

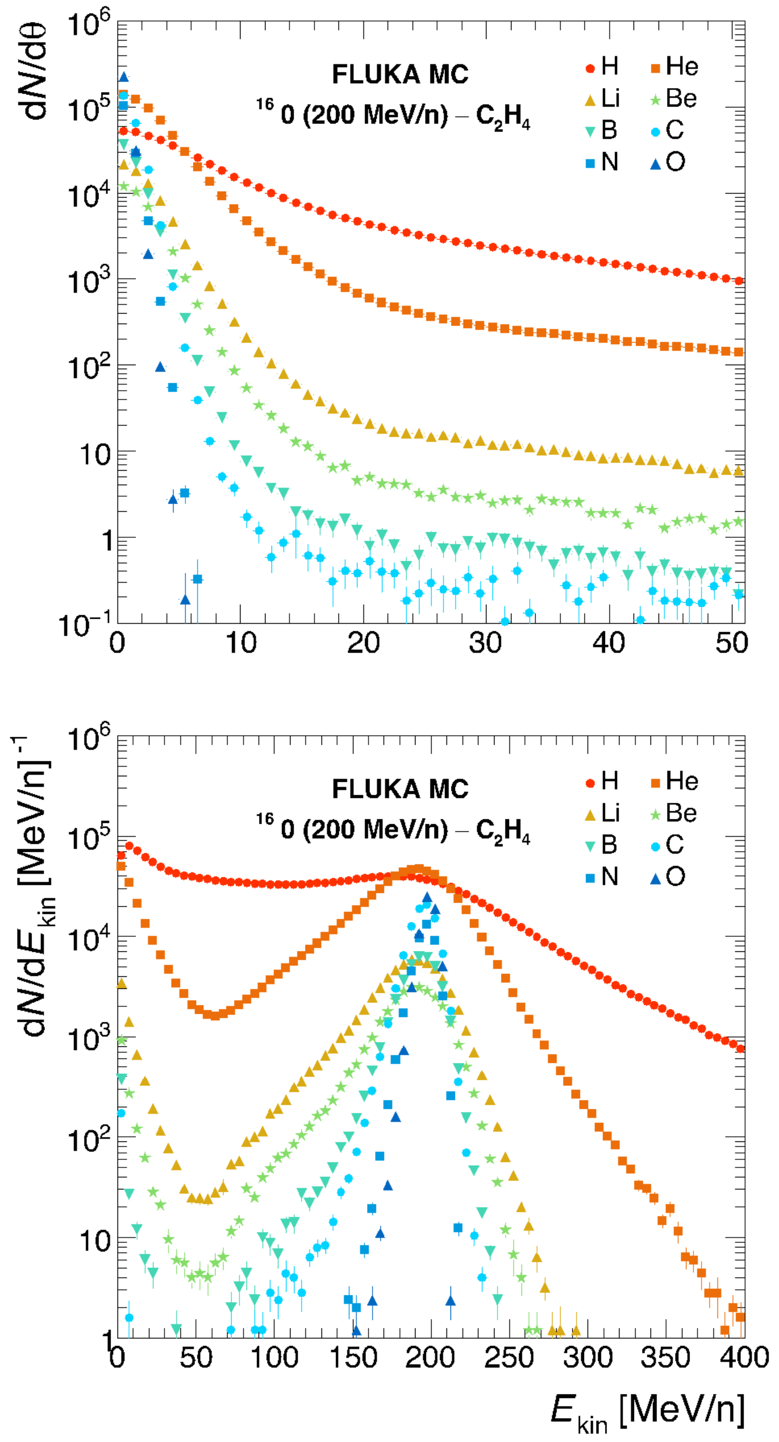

Radiobiological desiderata in PT:

- ✓ dσ/dE for target fragm. in PT ~ 10%
- ✓ d²σ/dΩdE for projectile fragm. in PT ~ 5%
- ✓ ΔZ ~ 2-3% ; ΔA ~ 5%

Emulsion spectrometer with high angular acceptance (<70°) optimized for fragments with Z<3:

- **Vertexing region**: emulsion films alternated with target layers to identify the interaction vertices
- **Charge id. region**: only emulsion films exploited for the charge id. with a refreshing procedure
- **Absorbing region**: emulsion and absorber layers for the momentum and mass id., exploiting the track length and the Multiple Coulomb Scattering effect

Data acquisition at GSI

- Preliminary data taking @ GSI with a partial FOOT experimental set-up composed of Start Counter, Beam Monitor and Tof-Wall detector with a beam of ^{16}O at 400 MeV/u meant for calibration

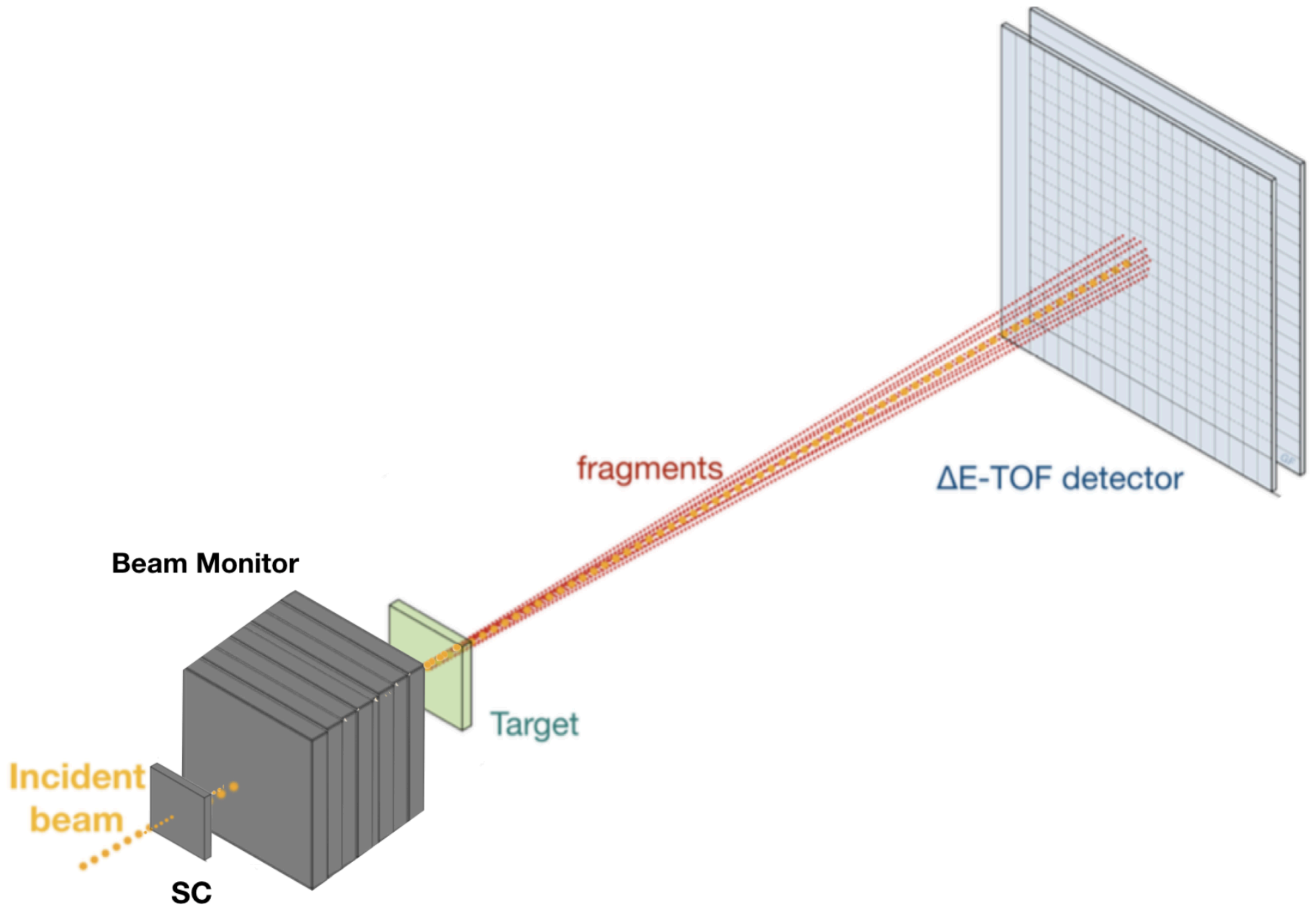

Run	Type	Target	Events
2210	calibration	no	20463
2211	calibration	no	62782
2212	calibration	no	116349
2242	calibration	no	202728
2239	physics	C	20821
2240	physics	C	20004
2241	physics	C	20041
2251	physics	C	6863

- Very few statistics (~67k events) collected for physics runs with fragmentation of the ^{16}O beam of 400 MeV/u on a C target
- Preliminary charge-changing cross sections integrated over the angular TW acceptance for the process ^{16}O (400 MeV/u)+C

Start Counter and Beam monitor

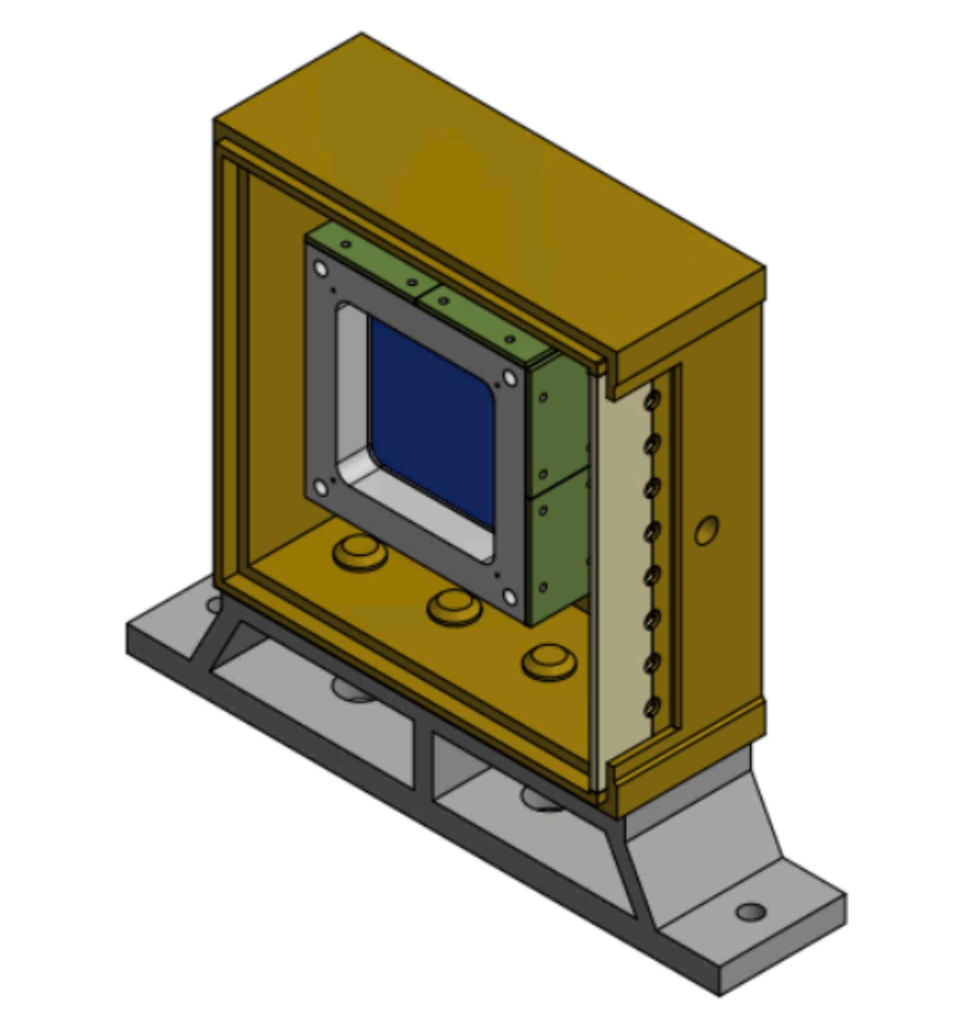

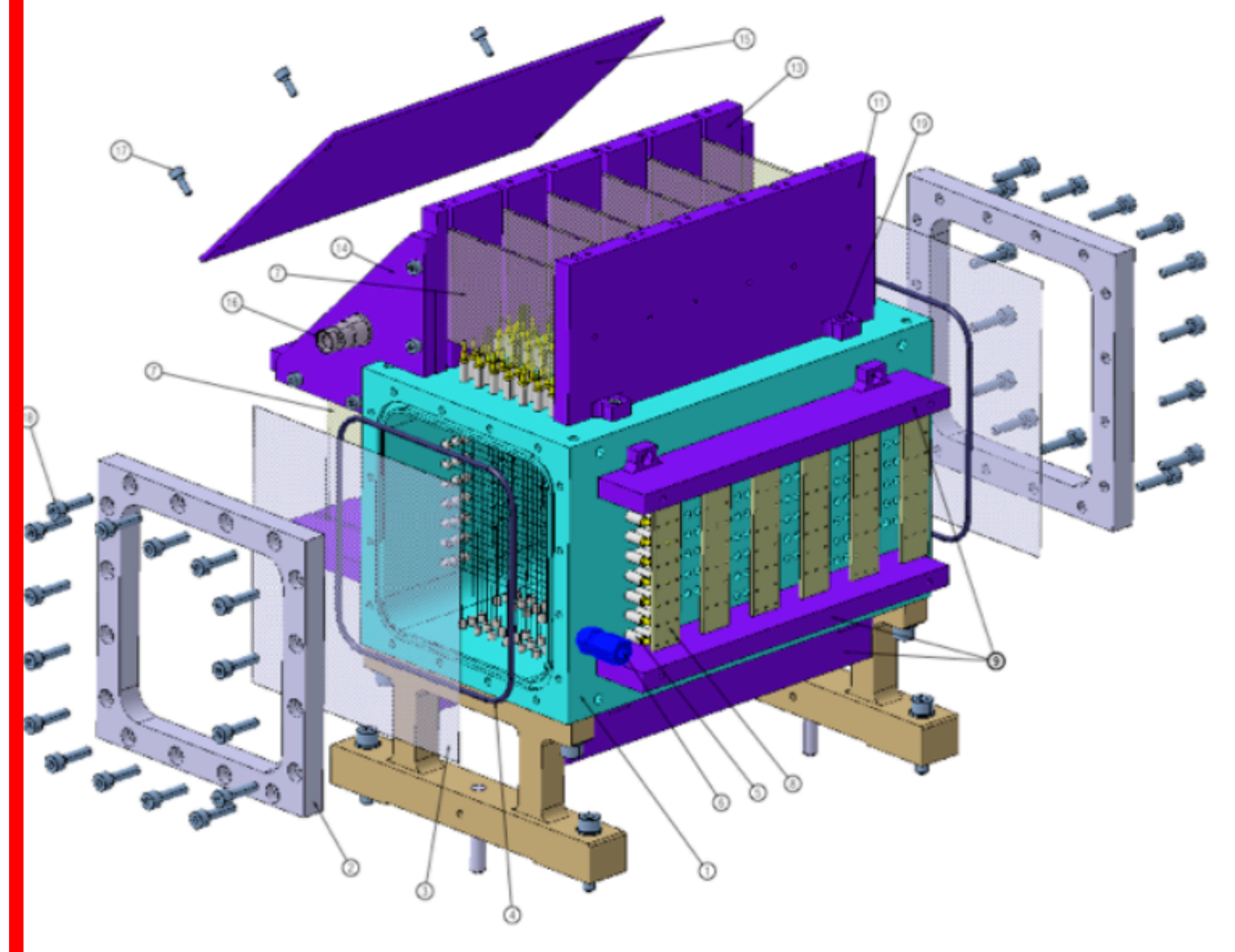

- The Start Counter (SC) is a **thin plastic scintillator layer** (EJ-228 – [250 μm, 1mm] thick) placed about 30 cm before the target with an active surface of $5 \ x \ 5 \ cm^2$
- Coupled to **48 SiPM** (8 channel readout)
- Layout optimized to **maximize the light collection**, minimizing the out of target fragmentation probability

It provides:

1. The **start of the TOF** masurements
2. The **trigger signal**
3. The measurement of the incoming **ion flux**

- The Beam Monitor (BM) is a drift chamber consisting of twelve wire layers, with three drift cells per layer
- Planes with wires oriented along the x and y axes are alternated allowing the beam profile reconstruction in both views
- The cell shape is rectangular (16 mm × 10 mm)
- The BM operates at ≃ 0.9 bar with a 80/20% gas mixture of Ar/CO2

- The BM detector will be placed between the SC and the target and will be used to measure the direction and impinging point of the beam ions on the target

Tof-Wall detector: charge ID of the fragments

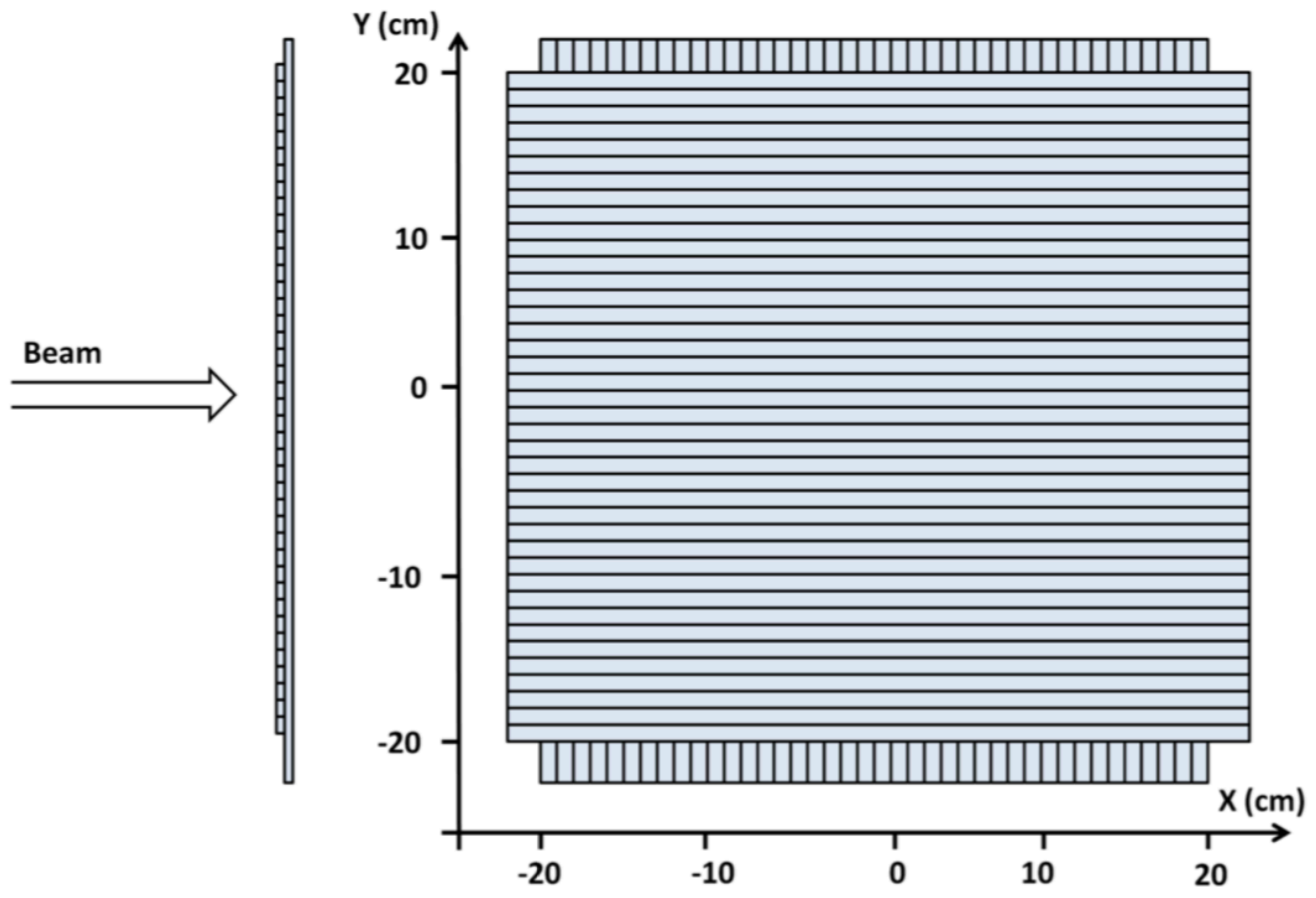

TW provides:

1. Deposited energy ΔE
2. Time of flight **TOF** (using the t_0 provides by ST)
3. Hit **positions**

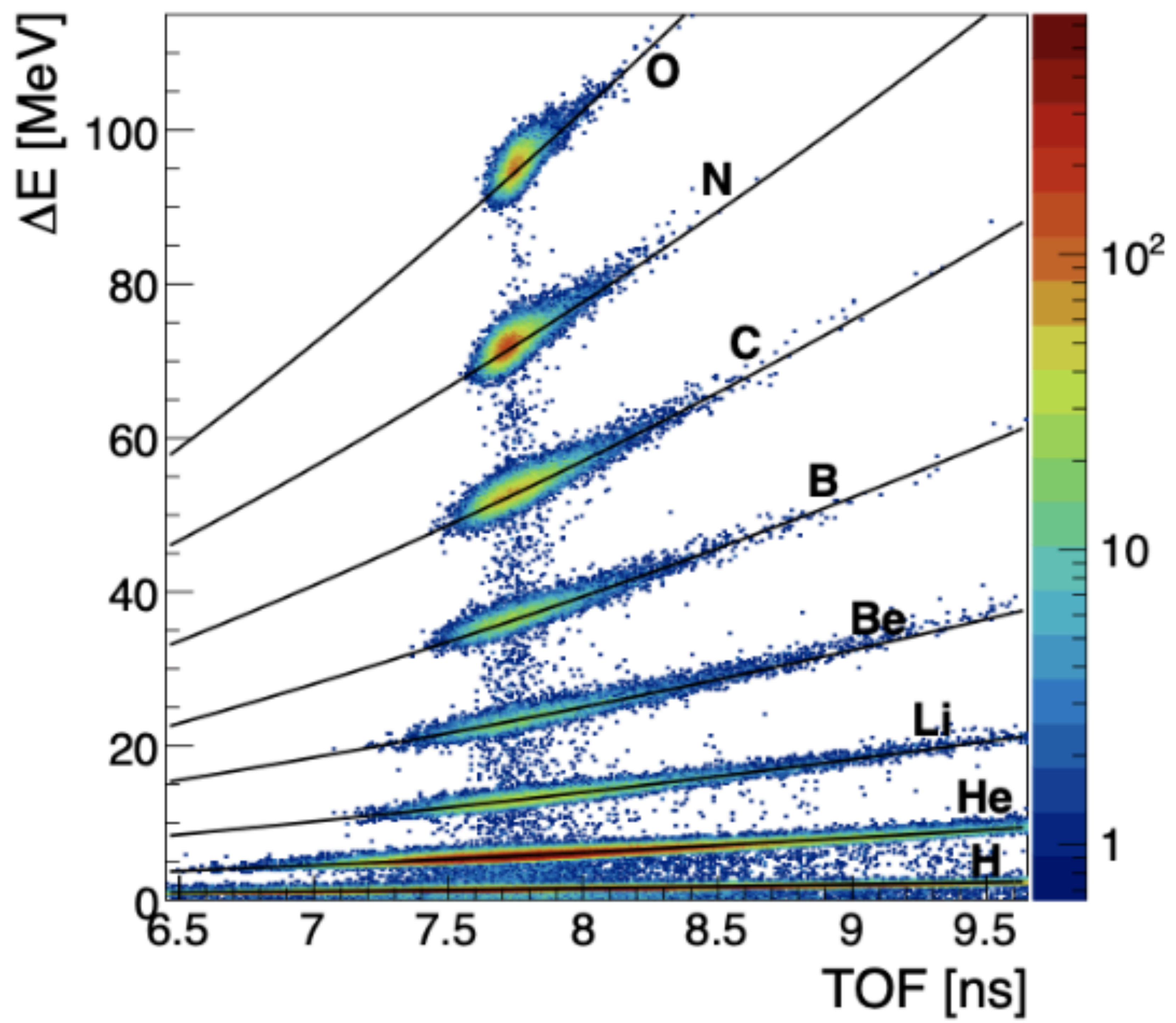

- The **Tof-Wall** detector (TW) is composed of **two layers of 20 scintillator bars** (0.3 cm thick, 2 cm wide, 44 cm long) arranged orthogonally with a $40\ x\ 40\ cm^2$ active area
- Each of two edges of the TW bars is coupled to **4 SiPM** with a $3\ x\ 3\ cm^2$ active area and 25 μm microcell pitch.

Fragment charge Z identification performed using a Bethe-Bloch parametrization as a function of TOF for each Z

Cross section measurement strategy

^{16}O beam @ 400 MeV/nucleon on a 5 mm Carbon TG

$$\sigma(Z) = \int_{E_{min}}^{E_{max}} \int_0^{\Delta\theta} (\frac{\partial^2 \sigma}{\partial\theta \partial E_{kin}})\, d\theta dE_{kin} = \frac{N_{frag}(Z)}{N_{prim} \cdot N_{TG} \cdot \epsilon(Z)}$$

$$N_{TG} = \frac{\rho \cdot dx \cdot N_A}{A}$$

$$\begin{cases} \rho = 1.83\ g/cm^3 \\ dx = 0.5\ cm \\ A = 12.0107 \end{cases}$$

Run	Type	Target	Events
2210	calibration	no	20463
2211	calibration	no	62782
2212	calibration	no	116349
2242	calibration	no	202728
2239	physics	C	20821
2240	physics	C	20004
2241	physics	C	20041
2251	physics	C	6863

1. **Align FOOT detector** at GSI and select angular acceptance for cross section integration;
2. Compute **MC efficiencies** for each fragment;
3. Estimate **fragmentation out of target** for background subtraction;
4. Extract the **fragments yields** from Z identification TW algorithms;
5. **Systematics** study.

Very low statistics and no detectors for mass identification → cross section integrated in angular and kinetic energy interval is feasible

MC studies: efficiencies and background rejection

Developed a detailed FLUKA simulation with the geometry of the set-up used at GSI data taking

$$\epsilon(Z) = \frac{N(Z)_{TW}}{N(Z)_{prod}}$$

Numerator: asking for a reconstructed and Z identified fragment with TW matched to primary fragments with origin in target with production angle < 5.7° and E_{kin} production in the range [100, 800] MeV/u

Denominator: asking for primary fragments produced in target with an angle < 5.7° and E_{kin} production in the range [100, 800] MeV/u

Element	Efficiency(%)
He	91.92 ± 0.05
Li	85.38 ± 0.20
Be	88.32 ± 0.26
B	88.75 ± 0.24
C	91.13 ± 0.15
N	95.88 ± 0.09

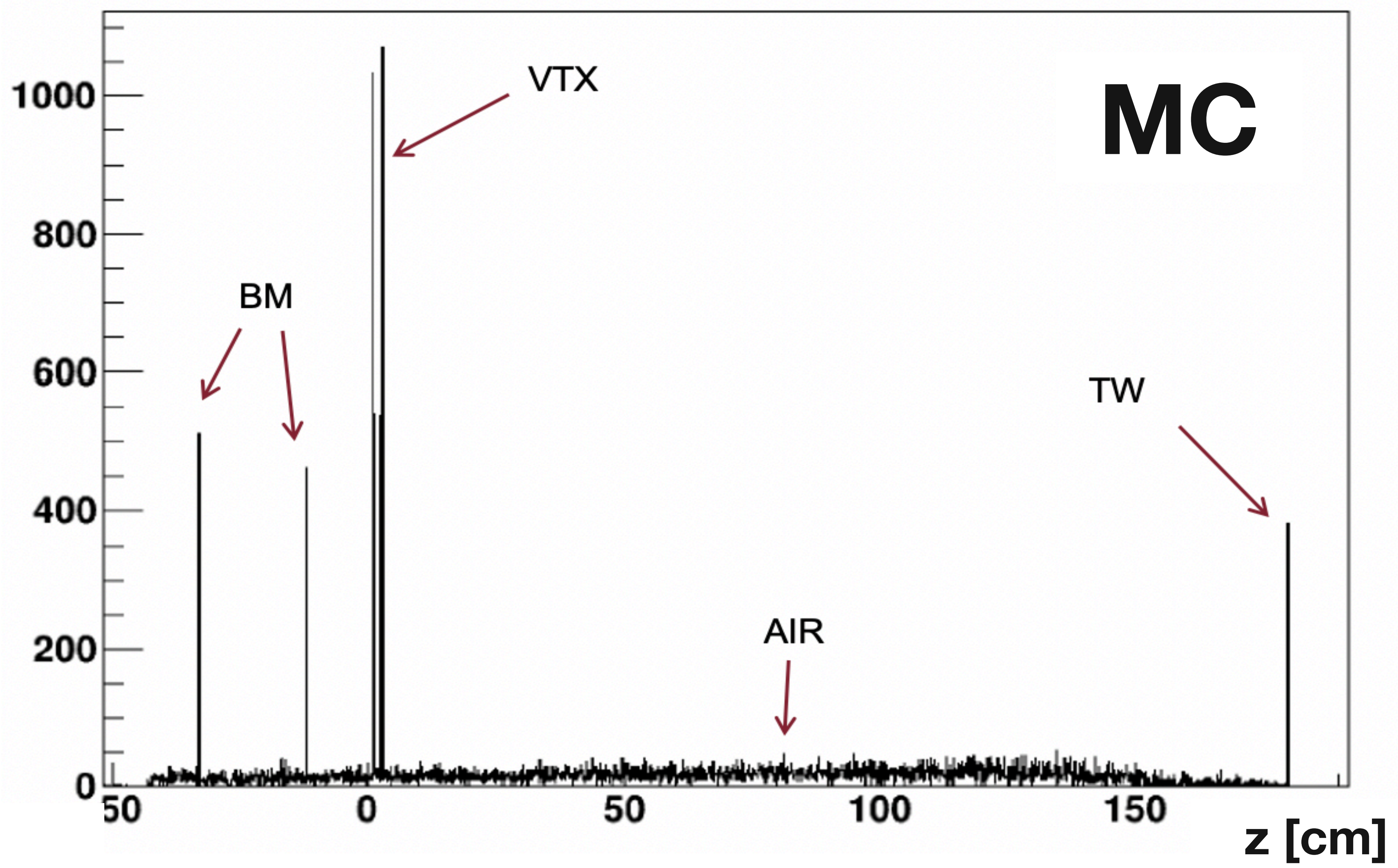

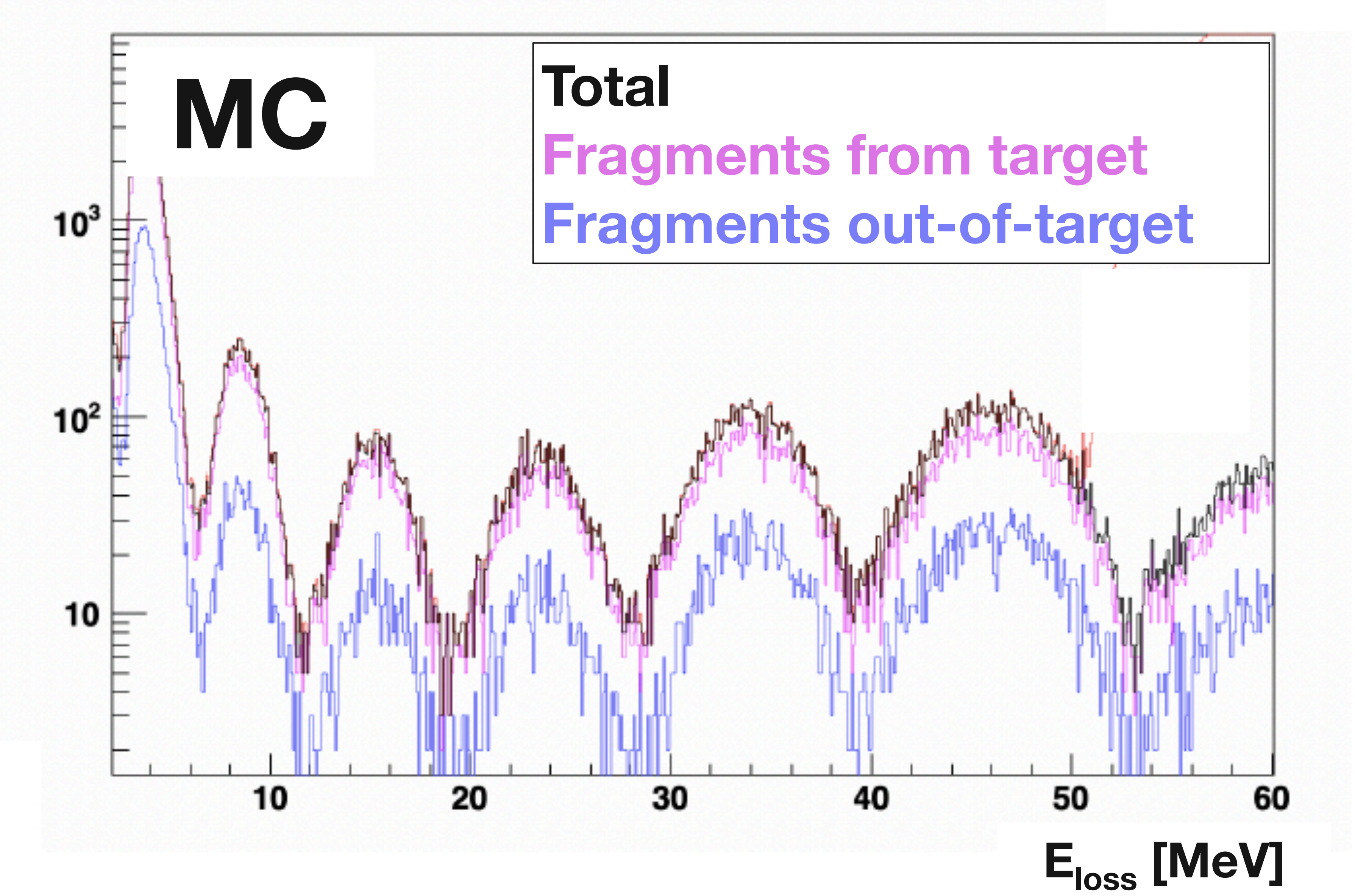

Out of target primary fragmentation is a not negligible background to be subtracted (~30% of the signal from MC studies). Most of it coming from air

Data: fragment yields and background subtraction

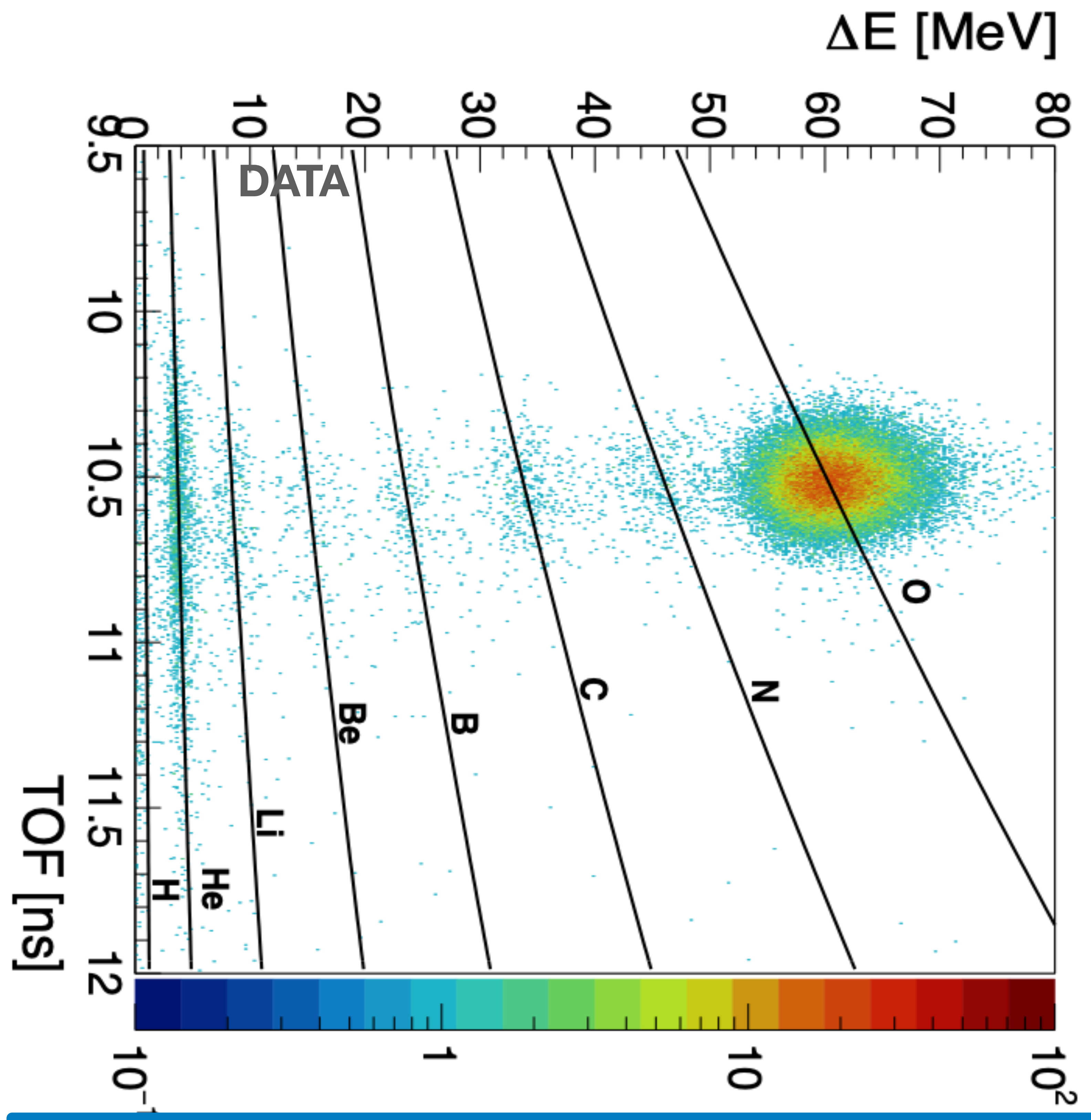

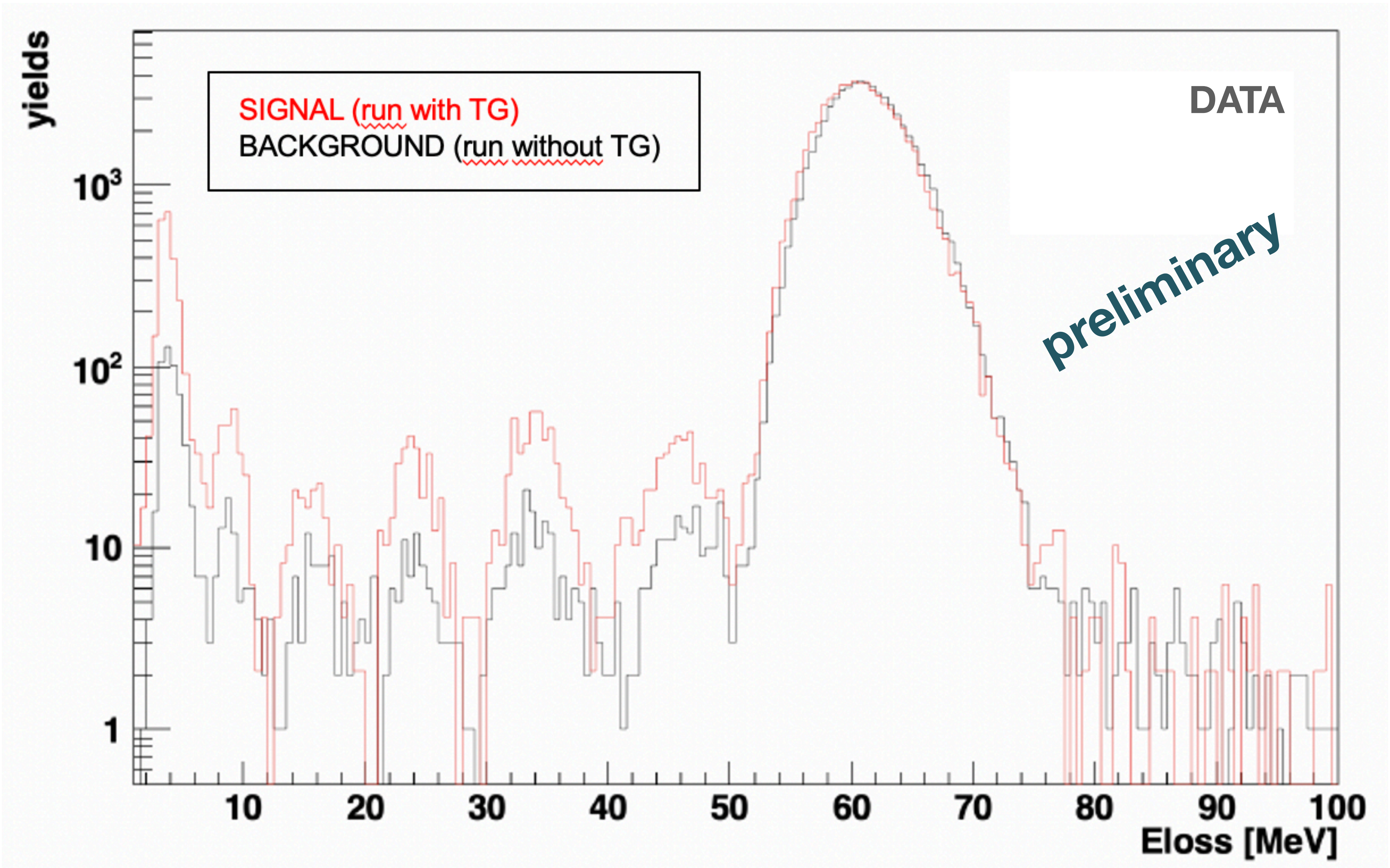

$$\sigma(Z) = \frac{1}{N_{TG} \cdot \epsilon(Z)} \left[\frac{N_{TG}(Z)}{N_{TG}^{prim}} - \frac{N_{noTG}(Z)}{N_{noTG}^{prim}} \right]$$

$$N_{TG} = \frac{\rho \cdot dx \cdot N_A}{A}$$

$\rho = 1.83$ g/cm^3
dx = 0.5 cm
A = 12.0107

Element	$Yields_{bkg}$	$Yields_{signal}$
N_{prim}	31660	61516
He	484 ± 22	1087 ± 33
Li	89 ± 9	152 ± 12
Be	73 ± 9	77 ± 9
B	88 ± 9	136 ± 12
C	156 ± 13	231 ± 16
N	207 ± 14	248 ± 16

The **count of the primary ions** of the beam interacting with the target is provided by the **Start Counter**

Nuclear Emulsion Detector

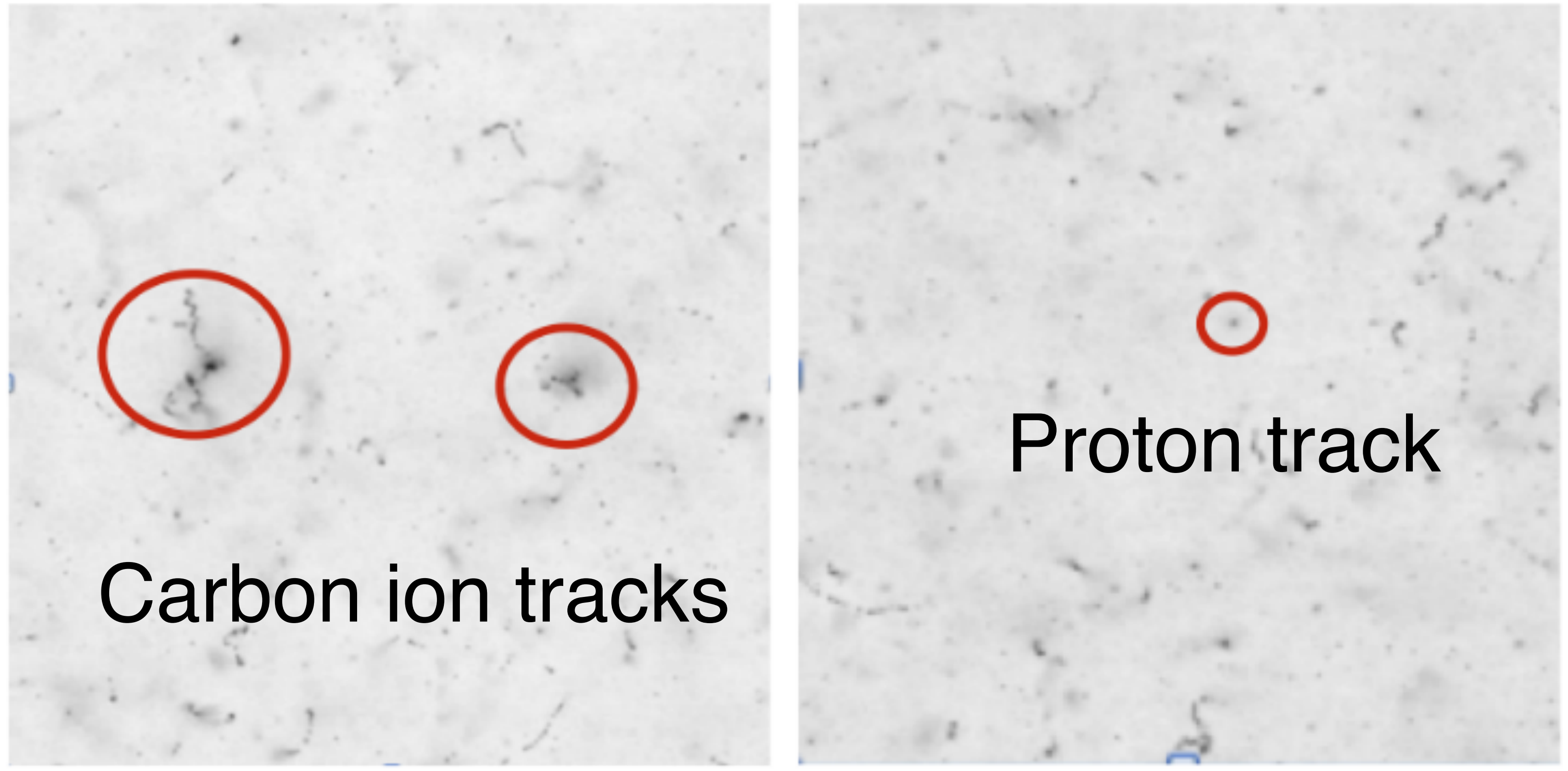

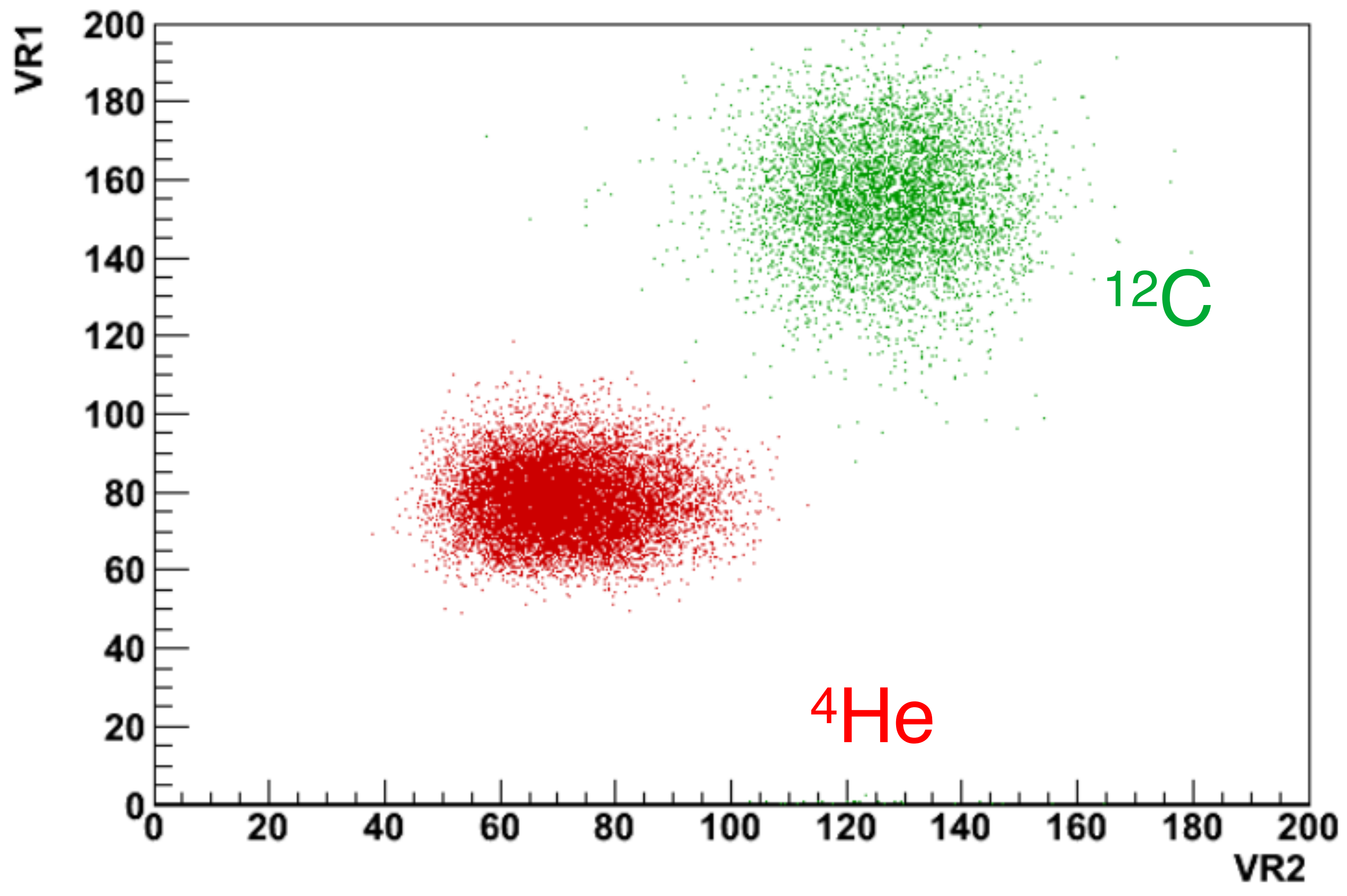

M.C. Montesi et al. Ion charge separation with new generation of nuclear emulsion films. *Open Physics*, 17(1):233–240, 2019.

Emulsion Cloud Chamber (ECC) detector to measure the fragments with Z≤3 and θ<70°

Nuclear emulsion films:

- Same technology of the OPERA exp. Emulsions
- Charged particles ionize the medium leaving a latent image of the track (dE/dx ∝ track volume)
- Refreshing: keep emulsions at different temperature and humidity conditions to progressively erase the less ionizing tracks and to perform the charge identification
- General workflow: exposure, refreshing, microscope scan, track reconstruction, data analysis

Emulsion Spectrometer data taking

^{16}O @ 200 MeV/u on C_2H_4 targets:

Fragments angular distributions:

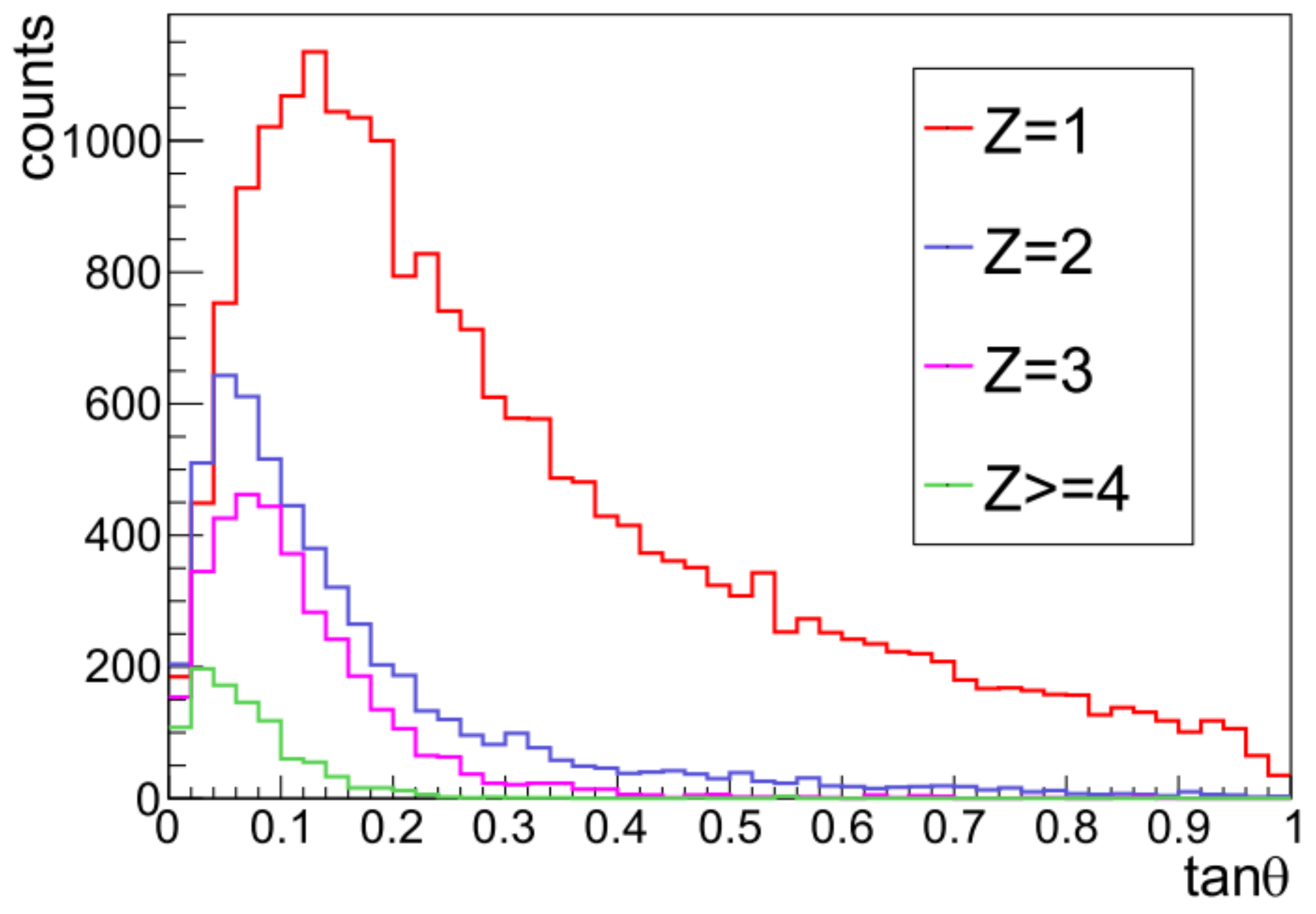

Angular differential cross section:

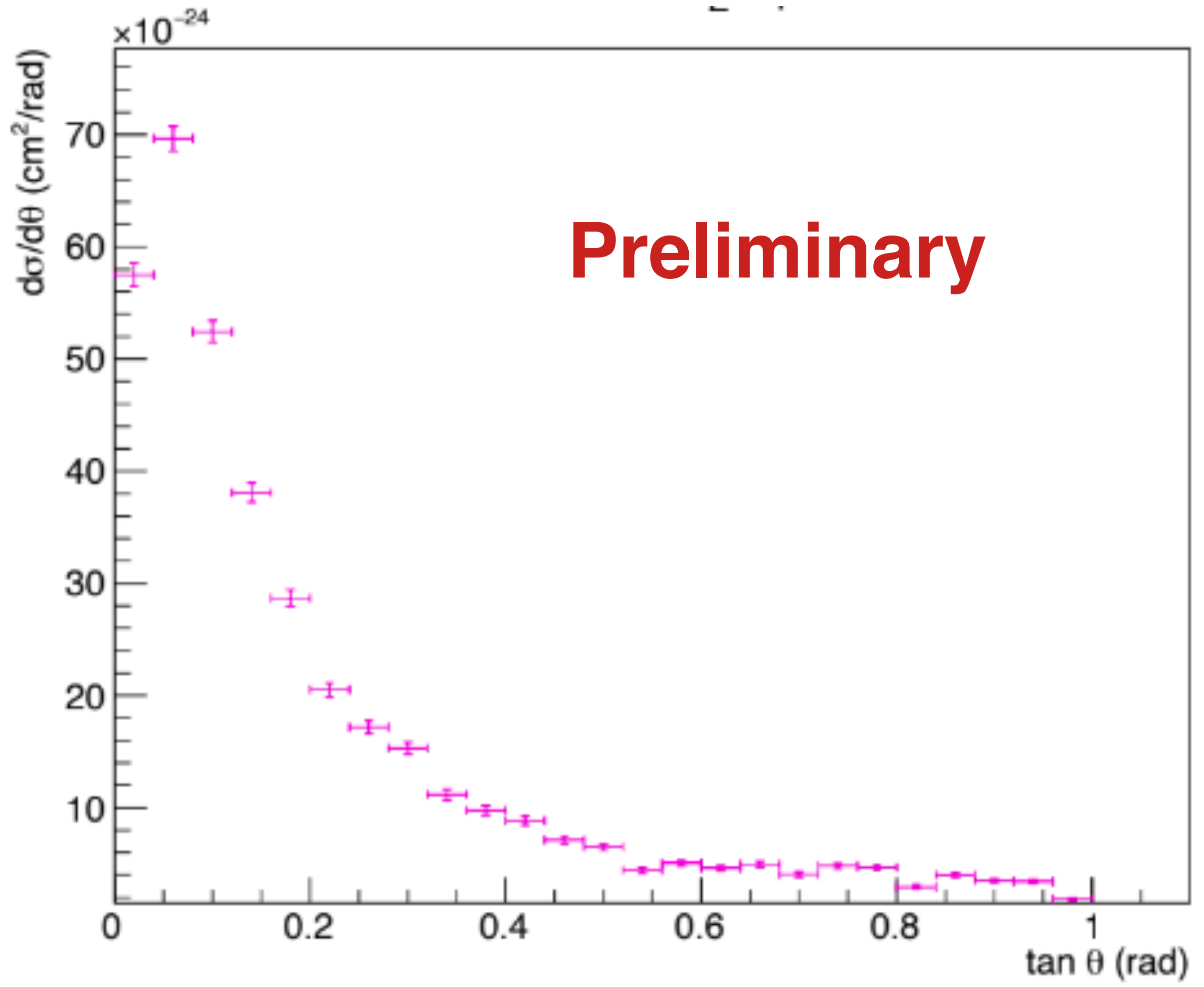

Concluded campaigns:

- Characterization with P, ^{4}He and ^{12}C at 80 Mev/u

M.C. Montesi et al. Ion charge separation with new generation of nuclear emulsion films. *Open Physics*, 17(1):233–240, 2019.

- ^{16}O @ 200 - 400 MeV/u and ^{12}C @ 700 MeV/u on C and C_2H_4 targets (data analysis ongoing)

G. Galati et al. Charge identification of fragments with the emulsion spectrometer of the foot experiment. *Open Physics*, 19(1):383–394, 2021.

Next measurements:

- ^{12}C @ 200 and 400 MeV/u on C and C_2H_4 targets at CNAO in 2023
- Study of a novel kind of emulsions to measure the target fragmentation process with direct kinematics

Mechanical checks

- Total weight: 74 kg
- Repulsion forces between M1 and M2: 2.2-2.4 kN
- Mechanics checked with 4-6 kN repulsive forces

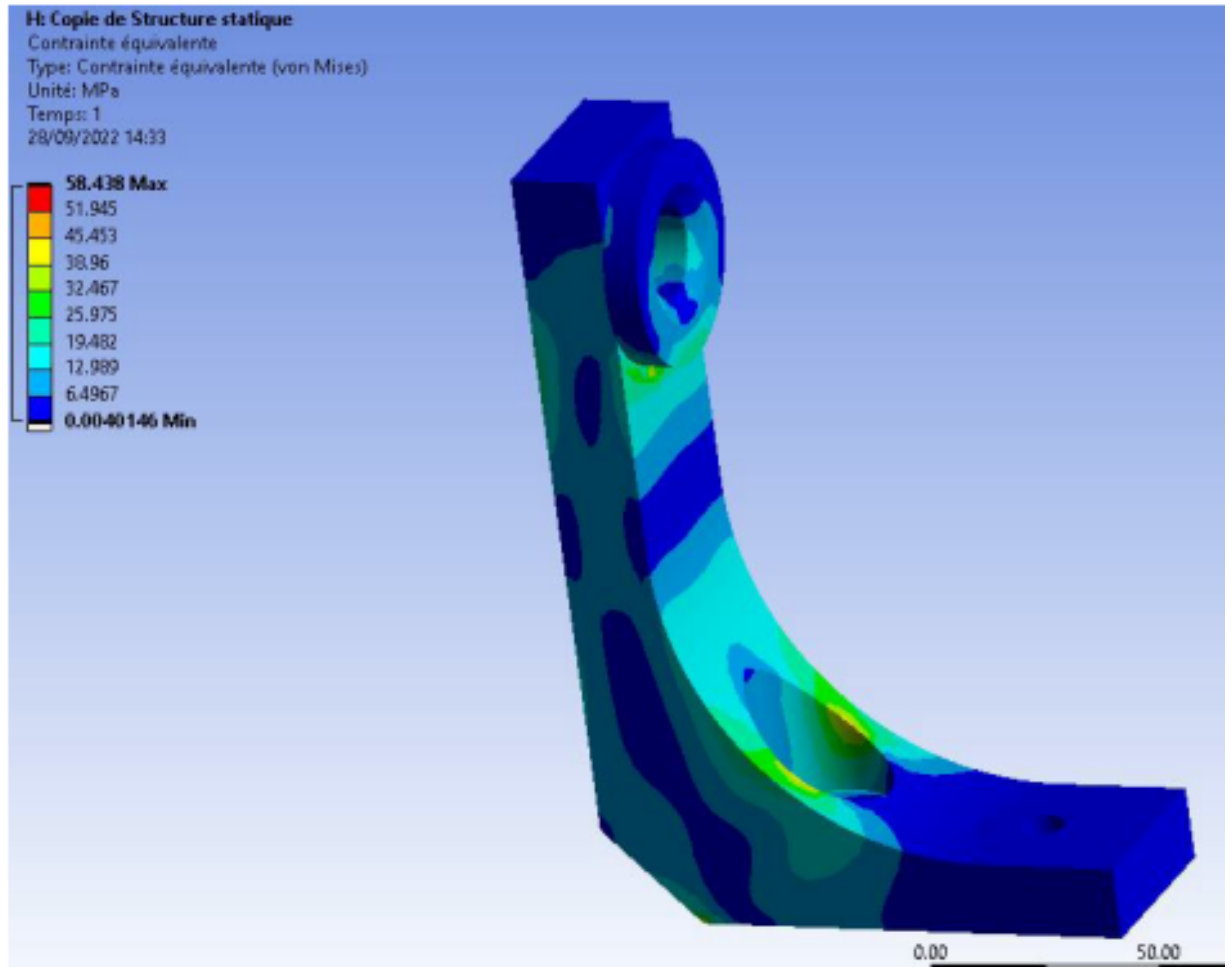

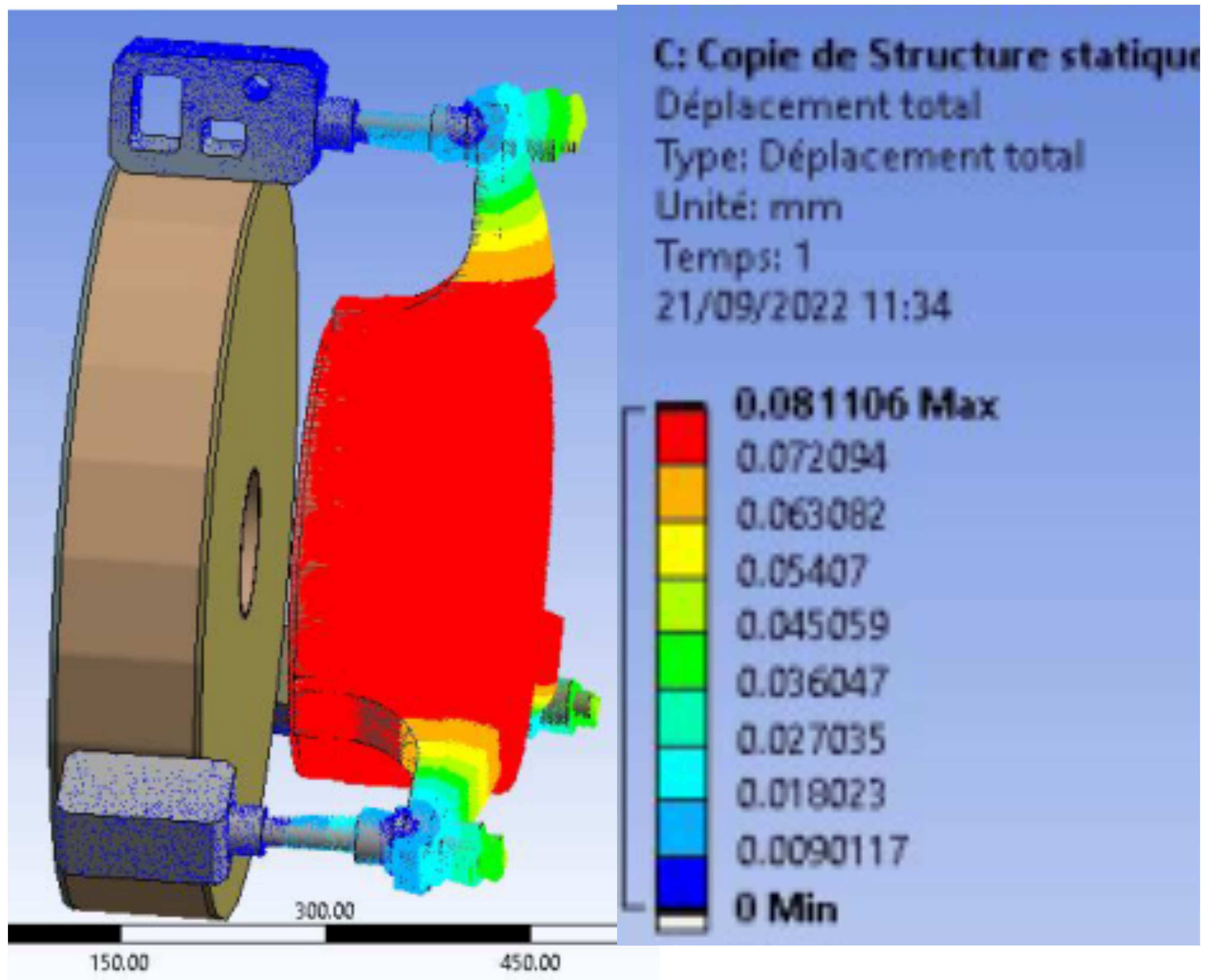

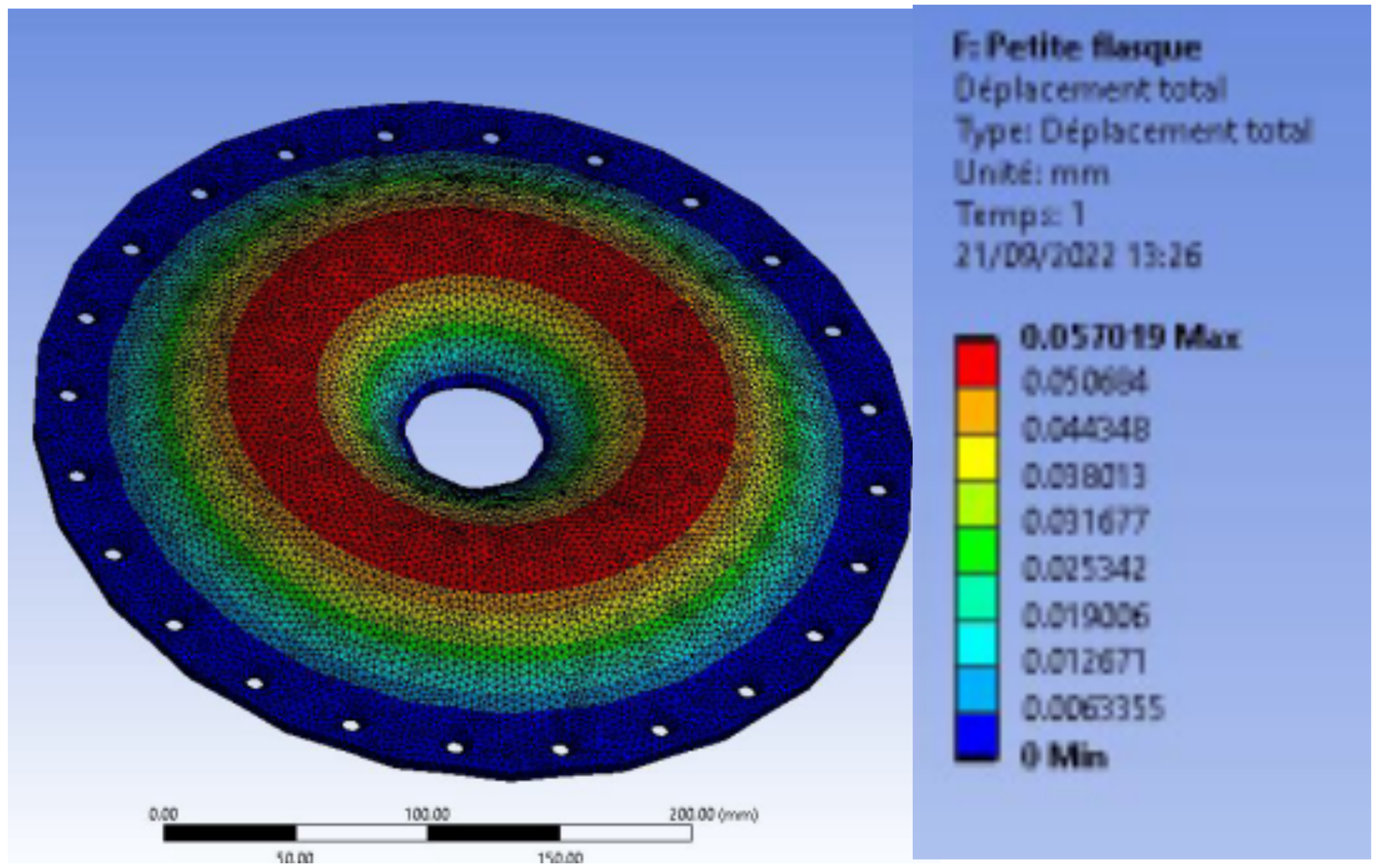

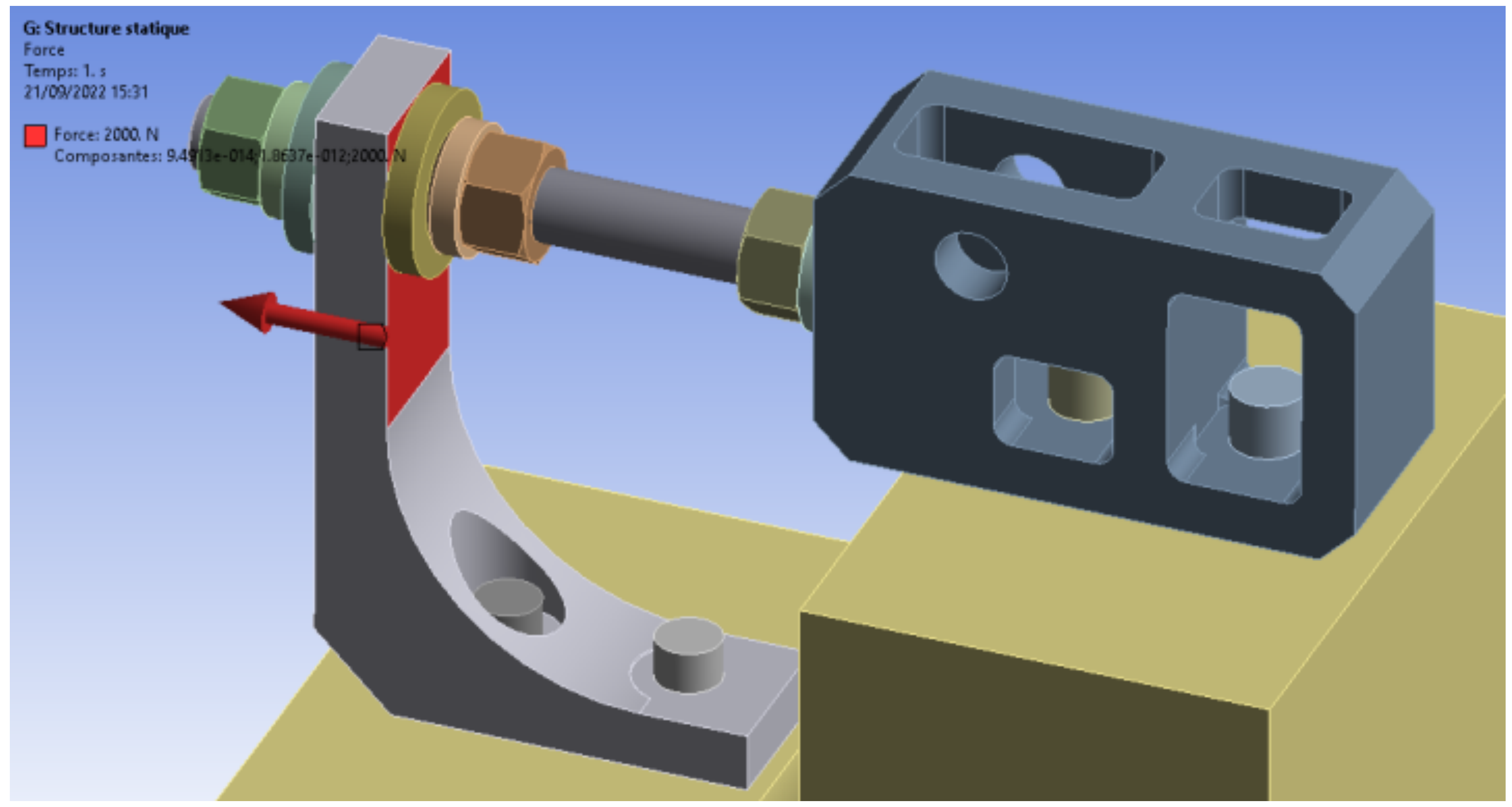

0.1 mm max displacement

0.06 mm max displacement

Survival fraction

An estimation of the RBE is based on the **Survival curves**. To compare the different biological effects for different radiations, the cell survival curves show the relationship between the fraction of cells preserving their reproductive integrity and the absorbed dose. The ratio between survivor cells and seed cells defines the **Survival Fraction** (**SF**).

$$SF = \exp(-\alpha D - \beta D^2)$$

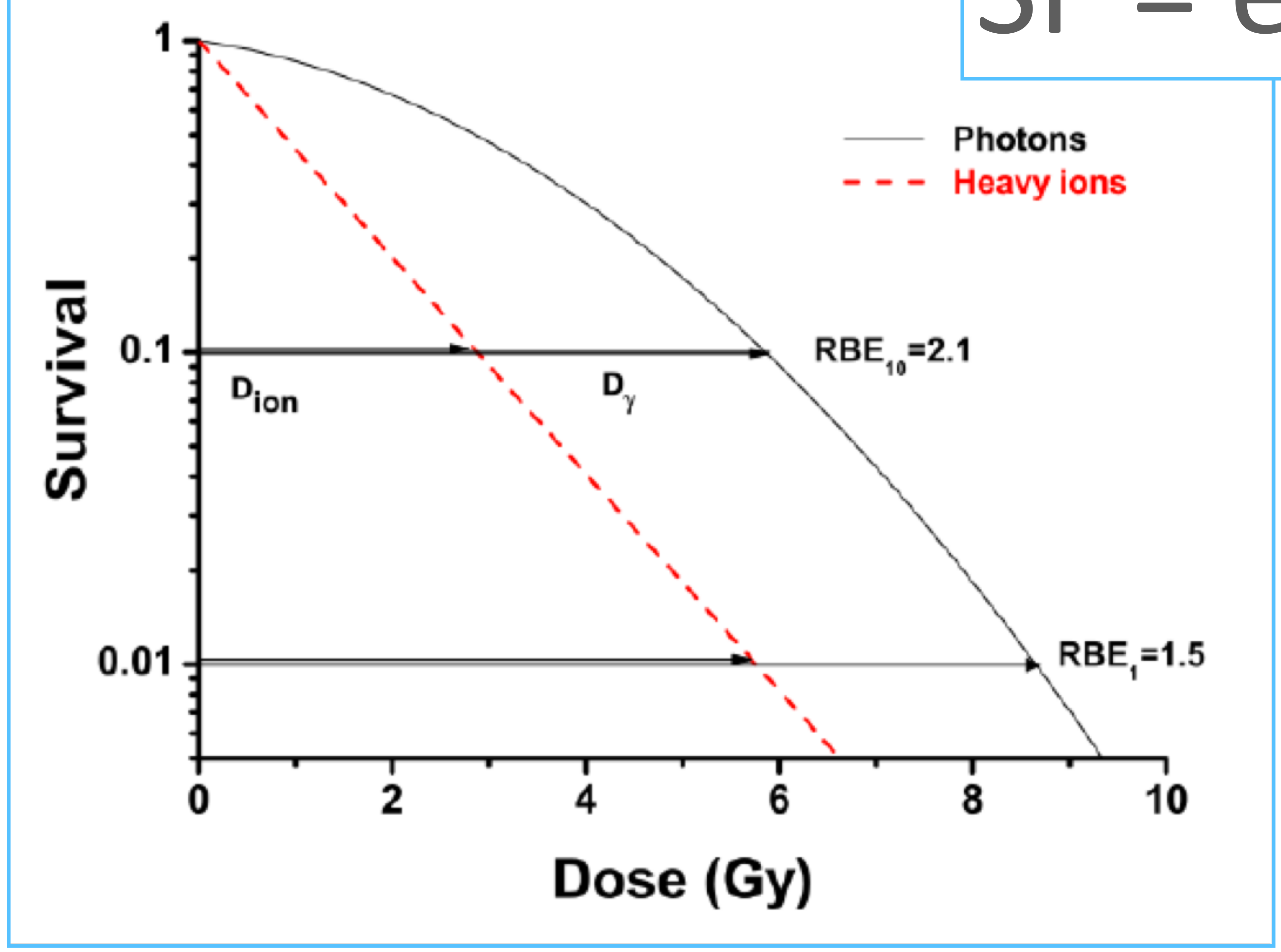

$$RBE = \frac{D_\gamma}{D_{ion}}\Big|_{iso}$$

RBE vs LET

- The RBE increases with LET up to an ion-dependent maximum value, then decreases for higher LET values.
- Indeed, at a certain LET value, a single-particle traversal is sufficient to reduce cell survival probability, making further ionisations unnecessary

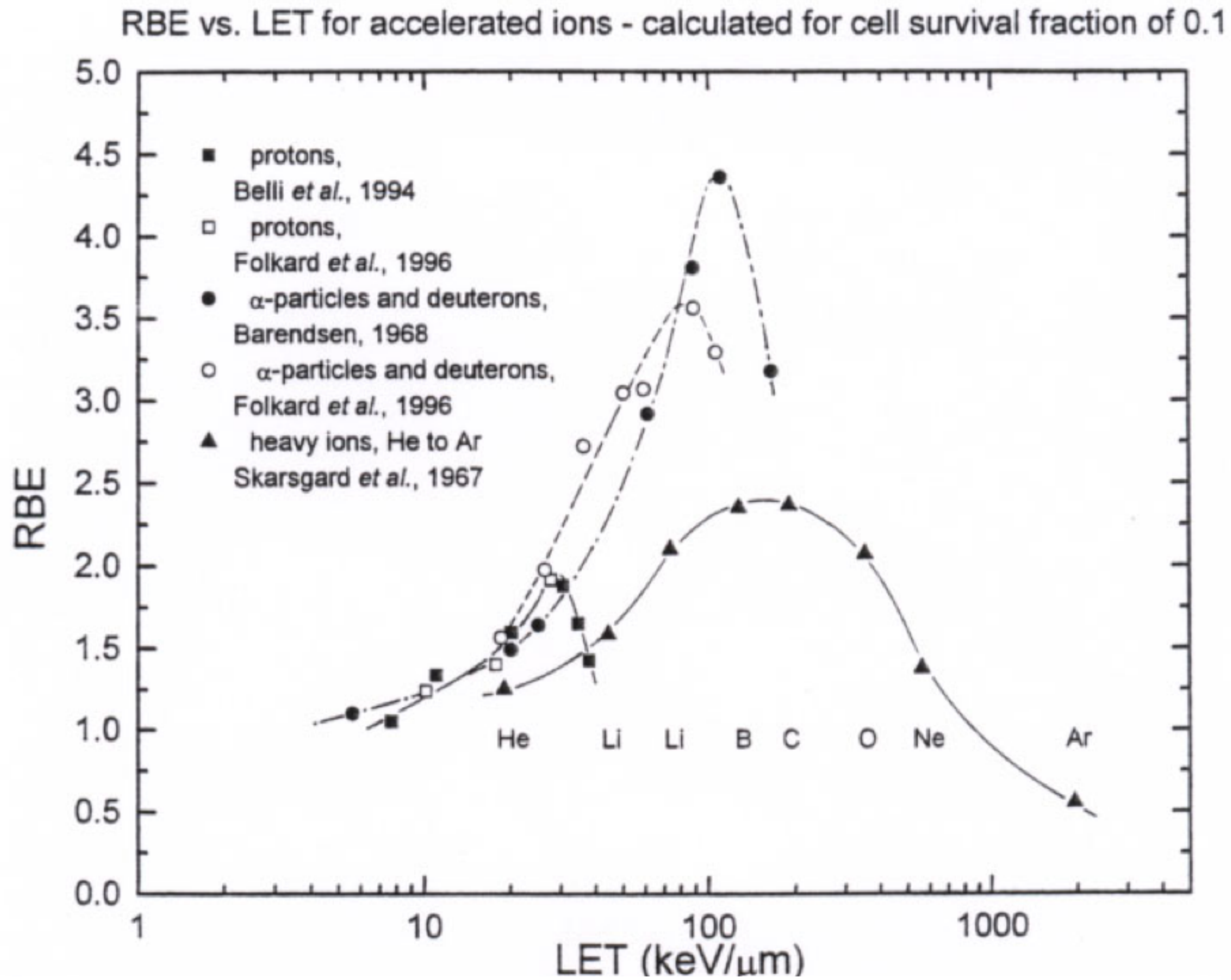

- Moreover, the RBE decreases due to the lower hitting probability, since the number of ions required for the same dose deposition is lower for particles with a higher LET

SPREAD OUT BRAGG PEAK (SOBP)

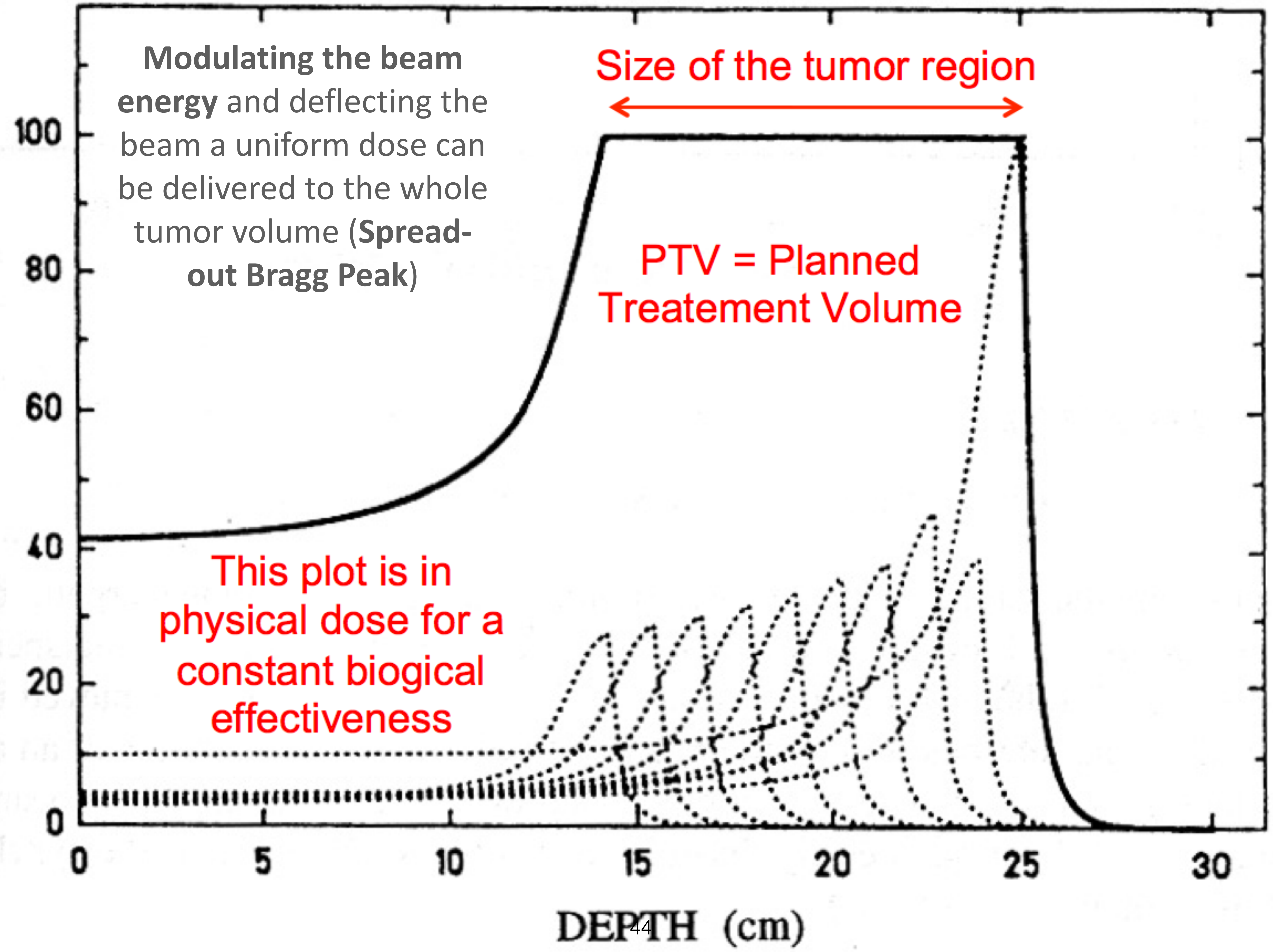

Beam Delivery System in PT

Active Scanning